

Hyperspectral sounding for severe storm forecasting

Testbeds to assess the potential and practical requirements in Europe

EUMETSAT contract EUM/CO/18/4600002214/TA

ESSL Report 2020–01



European Severe Storms Laboratory

Authors: Tomáš Púčik, Pieter Groenemeijer
European Severe Storms Laboratory – Science & Training

European Severe Storms Laboratory – Science & Training
Reg. No. 052480132, Bundespolizeidirektion Wiener Neustadt

Bräunlichgasse 6a / 6
2700 Wiener Neustadt
AUSTRIA

E-Mail: eb@essl.org

Web: <http://www.essl.org>

Telephone: + 43 2622 23622 / +49 151 5903 1839

Fax: +49 8151 9659 999 11

Contents

Executive Summary.....	5
1 Introduction	6
2 IASI Data integration into Testbed Platform	8
2.1 Sounder data implementation.....	8
2.2 The choice of the parcel.....	12
3 Evaluation at the ESSL Testbed.....	14
3.1 The ESSL Testbed 2019.....	14
3.2 Questionnaires and responses.....	14
4 Case studies	18
4.1 Case selection.....	18
4.2 1 August 2017: Convective initiation failure over Northeast Germany; severe storms in Poland 19	
4.3 11 August 2017: Damaging convective windstorm over Poland.....	24
4.4 17 September 2017: Damaging convective windstorm in Serbia and Romania.....	28
4.5 13 June 2018: Severe storms over the Balkans occurring further south than expected.....	32
4.6 26 January 2019: Strong tornadoes over southern Turkey.....	35
4.7 5 June 2019: Severe thunderstorms with unexpected severe wind gusts over Holland.....	38
4.8 11 June 2019: Giant hail over Poland and Slovenia; initiation failure over Czech Republic.....	41
4.9 10 July 2019: Extremely severe storms over central Italy and northern Greece.....	47
5 An evening overpass sampled the environment just after the intense phase of the Chalkidiki	51
5.1 9 August 2019: Severe wind and tornadoes across France, the Benelux and Germany	52
5.2 11–12 September 2019: Heavy rainfall over Spain in weak CAPE environment.....	56
6 Case catalogue.....	61
6.1 9 June 2014: Severe weather over Germany instead of the Benelux.....	61
6.2 1 June 2016: Deadly flash flood in southeast Germany.....	62
6.3 20 June 2016: Giant hail over Serbia, Romania and Hungary	63
6.4 23 June 2016: Damaging hailstorms over Netherlands and Germany	64
6.5 10 August 2017: Damaging convective windstorm occurs more east than forecast.....	65
6.6 8 June 2018: Severe storms over Croatia and Slovenia with surprisingly large hail.....	66
6.7 9 October 2018: Deadly flash floods over Mallorca.....	67
6.8 13 October 2018: Landfalling tropical storm Leslie in Portugal with severe wind gusts.....	68
6.9 29 October 2018: Widespread severe weather over the Mediterranean.....	69
6.10 28 May 2019: Damaging hailstorm over Northwest Romania.....	70
6.11 4 June 2019: Severe thunderstorms across north-western Europe.....	71
6.12 10 June 2019: Severe hailstorm hit Munich area.....	72
6.13 13 June 2019: Widespread severe storms over Czechia, Poland and Baltic states.....	73

6.14	15 June 2019: Severe storms in central Europe; French storms more severe than expected..	74
6.15	18 June 2019: Large hail in northern France and uncertain initiation across the Benelux.....	75
6.16	19 June 2019: Unexpected severe storm over Toulouse.....	76
6.17	27 June 2019: Storms across Slovakia, Hungary and Romania; few storms over Germany.....	77
6.18	1 July 2019: Widespread severe storms across Europe: storms occurred further east than forecast.....	78
6.19	6 July 2019: Severe storms over France and Italy: coverage underestimated by models.....	79
6.20	7 July 2019: Widespread severe storms: model underestimation of extent of convection.....	80
6.21	8 July 2019: Severe storms over Spain and Italy: Initiation failure over eastern Spain.....	81
6.22	9 July 2019: Severe convective system over the Adriatic Sea further south than expected.....	82
6.23	20 July 2019: Severe storms across the Benelux and Germany.....	83
6.24	27 July 2019: Severe weather in Italy and central Europe; a night-time tornado near Rome.	84
6.25	7 August 2019: Severe storms in Italy, central Europe; storms in Czechia weaker than forecast	85
6.26	11 August 2019: Unexpected damaging hailstorm over Piemonte, Italy	86
6.27	12 August 2019: Severe storms over Central Europe and Italy.....	87
6.28	22 August 2019: Deadly lightning strikes in Poland and Slovakia with low CAPE.....	88
6.29	26 August 2019: Severe weather over Spain, Czechia and Poland	89
6.30	13 September 2019: Giant hail over Algeria.....	90
7	Conclusions and recommendations.....	91
	Appendix A: Usage instructions of Python programme for the computation of convective indices.....	93
	Appendix B: Responses to IASI evaluation at the ESSL Testbed 2019.....	94

Executive Summary

As part of the Meteosat Third Generation (MTG) mission, EUMETSAT will employ two geostationary sounding satellites (MTG-S) each carrying an Infrared Sounder (IRS) instrument. Similar data is already available from the Infrared Atmospheric Sounding Interferometer (IASI) instrument on the polar-orbiting Metop satellites. IRS and IASI sounder data can be used to generate vertical profiles of temperature and humidity throughout the troposphere. ESSL has assessed if these profiles can be used to support forecasting severe convective storms without first assimilating them into a numerical weather prediction (NWP) model. To that aim, ten severe weather case-studies were performed. Additionally, ESSL exposed 40 forecasters from European weather services to IASI data by integrating it into the ESSL Testbed programme of 2019. The data were to facilitate a direct comparison with NWP predictions: as coloured dots overlaid on shaded NWP fields, and in an interactive display of vertical soundings showing NWP and IASI data alongside each other.

Almost all forecasters who used the IASI profiles at the Testbed found this type of product useful. They also indicated that a higher spatiotemporal availability would be helpful and for some this was even a requirement. This is important given the future availability of similar, but more frequent, data from the MTG-IRS. There was a high level of agreement among forecasters that the IASI data should stay completely independent of NWP model forecasts, so that it is an independent source of information that forecasters can use to instantly verify NWP models. The most popular derived quantities from the data were CAPE (preferably mean-layer CAPE), lapse rate of temperature, and total precipitable water. This information can guide the definition of L2 products at EUMETSAT.

During the testbed sessions and the case studies several characteristics of the IASI data were discovered. The detected temperature was typically found to be close to the NWP forecast valid at the same time and location. Exceptions are sharp inversions that cannot be fully resolved. Deviations of IASI from the modelled temperature close to the surface are usually confirmed by surface observations, i.e. they indicate an NWP model error, which is valuable information to forecasters. The humidity retrieved from IASI was often found to be less accurate than temperature, in the lowest troposphere, where underestimations often occurred in thunderstorm situations. Since thunderstorms are very dependent on low-level humidity, this limits the extent to which IASI can be used to anticipate them. Finally, it was noted that both temperature and humidity can differ substantially between two overpasses occurring soon after each other.

Since the data was received positively by forecasters, and the case studies have confirmed that the data can contribute to a better anticipation of thunderstorm development (or lack thereof), it is recommended to continue to explore the use of IASI data. More precisely, it is recommended to assess whether the retrieval algorithms can be further optimized to infer low-level humidity more accurately. Furthermore, IASI data can be combined with other observations such as *in situ* measurements, LIDAR data and AMDARs, in order to obtain an improved observation-based data set. In order to simplify the comparison between IASI data and NWP models, difference fields of key parameters can be computed and visualized. Additionally, it is recommended that error estimates of the measurements are presented to forecasters throughout the retrieved vertical profile.

1 Introduction

As part of the Meteosat Third Generation (MTG) mission, EUMETSAT will employ two geostationary sounding satellites (MTG-S) each carrying an Infrared Sounder (IRS) instrument. The IRS will enable the analysis of the atmosphere, of the tropospheric temperature and humidity, at unprecedented spatial and temporal sampling. Since severe convective storms are strongly controlled by the stability and moisture distribution in the troposphere, it is expected that these new data will aid the forecasting of such weather systems. This can be done both by assimilating the observations into Numerical Weather Prediction (NWP) models, and by presenting retrieved profiles directly to forecasters.

Today similar sounder data is already available from the Infrared Atmospheric Sounding Interferometer (IASI) instrument on the polar-orbiting Metop satellites. The EUMETSAT Advanced Retransmission Service EARS-IASI was recently extended to include regional Level 2 products providing sounding profiles for regional applications. These products are available to forecasters within 30 minutes from sensing and include data from the Advanced Microwave Sounding Unit (AMSU) and Microwave Humidity Sounders (MHS).

Since (severe) convective storms are strongly controlled by the stability and moisture distribution in the troposphere, it is expected that these new data will aid the forecasting of such weather systems, both by assimilating the data into Numerical Weather Prediction (NWP) models, and by the direct use of the retrieved profiles by forecasters.

EUMETSAT has requested ESSL to investigate the potential and practical aspects of directly using hyperspectral sounding products in severe storm forecasting, and to gain practical experience using these products with users and their collect their feedback. Specifically, the aims of the work are to user awareness and preparedness, especially in view of MTG-IRS, to investigate the potential and practical aspects of directly using hyperspectral sounding products in severe storm forecasting, and to contribute to the consolidation of products requirements in that perspective. The work has been performed with operational sounding products from the Metop satellites to evaluate what could be exploited already from the Polar missions. The collected feedback from forecasters, provided in the quasi-operational environment of the ESL Testbed, can be used by EUMETSAT in the definition of MTG-IRS Level 2 products and the preparation of the associated processing algorithms.

To allow the comparison between IASI observations and NWP data, the Testbed data platform was extended to display parameters relevant to convective storm prediction such as CAPE, CIN and humidity at various levels. Moreover, a direct visual comparison between the satellite-derived and NWP-modelled profiles of temperature and humidity was made possible. Chapter 2 describes the development of the visualizations of IASI data and the software that was developed to that aim.

At the ESSL Testbed 2019, the use of IASI-retrieved temperature and humidity profiles for storm forecasting have been evaluated as part of this study procured by EUMETSAT. At the Testbed, forecasters of European weather services, researchers and the ESSL team have jointly used experimental products to make convection forecasts. At the Testbed, feedback from forecasters was requested. Chapter 3 details the procedure and the outcome of the Testbed evaluation.

In addition, ESSL researchers have performed an in-depth study of 10 past cases in which (severe) convective storms developed, or the evolution of storm development differed from forecasts. For these cases that occurred in 2017, 2018 and 2019 IASI data was retrieved from the archive where necessary and visualized in the Testbed data display. The various cases are described in Chapter 4.

ESSL furthermore compiled a list of 30 potential past cases for further study, of which the main characteristics in relation impact and meteorology are described. This list is contained in Chapter 5.

Finally, Chapter 6, summarizes the work and presents several suggestions relevant to further work on the use of sounder data in forecasting severe weather.

2 IASI Data integration into Testbed Platform

2.1 Sounder data implementation

Two ways to visualize the sounder data in the Testbed platform were implemented. They are:

1. Plotting the data of derived parameters with a relevance to forecasting convective storms as coloured circles on a background map.
2. Integration of the profiles into the interactive "roaming sounding" tool, alongside NWP-predicted profiles

The plotting of the circles required the prior computation of several parameters from the profile data. The original data that was received in HDF5 format through the EUMETCast service and subsequently the data files containing data across Europe were read in by the Python program *sounder.py*. This program calculates the values of several convective forecast parameters for each sounding location, and, additionally, produces text files with horizontally gridded temperature and humidity data that are read in by the roaming sounding tool. In order to compare the exact same parameters from the sounder and the NWP model, scripts to calculate the parameters from ECMWF IFS model level data were constructed in collaboration with ECMWF and operationally run on a Linux cluster provided for this purpose.

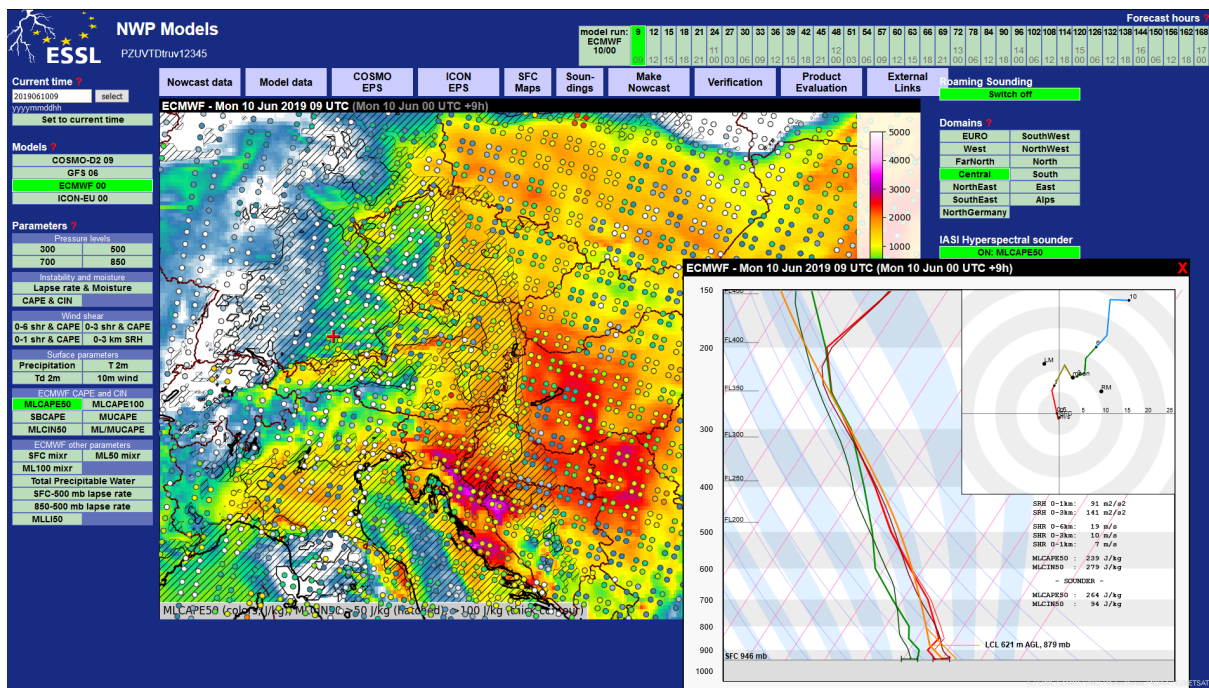


Fig. 2.1. NWP Model page of the Testbed Platform with IASI data included in the map and the roaming sounding tool (right bottom inset).

Fig. 2.1 shows the NWP Model page of the Testbed platform with the measured IASI values of the parameter MLCAPE50 displayed as filled coloured circles onto the forecast of the same parameter according to the ECMWF IFS model. The Skew-T diagram at the right bottom of Fig. 2.1 has been magnified in Fig 2.2. and shows the temperature and humidity profiles from

the model (thick bright red and green, respectively) and of the IASI measurements (thin dark red and dark green). The roaming sounding tool is roaming in the sense that it is interactive and, by moving the mouse pointer across the map, the curves in the diagram evolve to always display the data at the mouse pointer location. It has been extended to display the IASI profiles alongside the NWP-based profiles. In addition, the sounding tool's readability has been improved, the hodograph display improved, and the values of selection of interactively changing parameters are displayed. The uncertainty of the measurement is indicated by an error bar at the bottom of the diagram. The convective parameters that were selected for displaying are listed in Table 2.1:

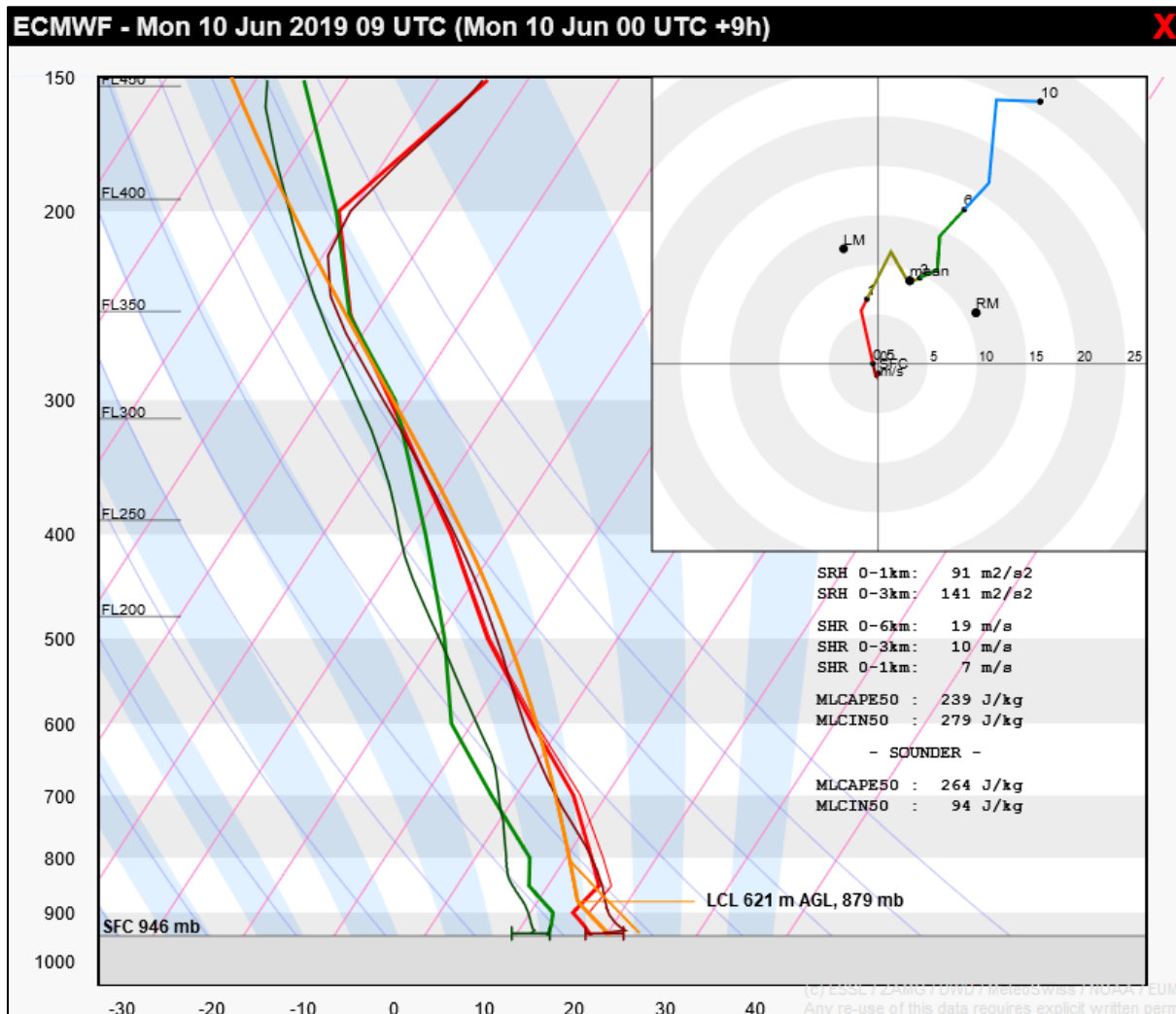


Fig. 2.2. Magnification of the 'roaming sounding' in Fig. 2.1.

Table 2.1.

Parameter	Description	Unit
MLCAPE50	CAPE for a mixed-layer parcel from the lowest 50 mb above the surface (in J/kg)	J/kg or m ² /s ²
MLCAPE100	CAPE for a mixed-layer parcel from the lowest 100 mb above the surface (in J/kg)	J/kg or m ² /s ²
SBCAPE	CAPE for a parcel lifted from the lowest available model or IASI level (in J/kg)	J/kg or m ² /s ²
MUCAPE	CAPE for a parcel lifted from the lowest available model or IASI level (in J/kg)	J/kg or m ² /s ²
MLCIN50	CIN for a mixed-layer parcel from the lowest 50 mb above the surface (in J/kg)	J/kg or m ² /s ²
SFC mixr	mixing ratio at the lowest available model or IASI level (in g/kg)	J/kg or m ² /s ²
ML50 mixr	mixing ratio for a mixed-layer parcel from the lowest 50 mb above the surface (in g/kg)	g/kg or 10 ⁻³
ML100 mixr	mixing ratio for a mixed-layer parcel from the lowest 100 mb above the surface (in g/kg)	g/kg or 10 ⁻³
Total Precipitable Water	vertically integrated water content (in mm)	mm
SFC-500 mb lapse rate	vertical temperature gradient between the lowest available model or IASI level and the 500 mb level (in 10 ⁻³ K/m, or K/km)	K/km or 10 ⁻³ K/m
850-500 mb lapse rate	vertical temperature gradient between the 850 and the 500 mb level (in 10 ⁻³ K/m, or K/km)	K/km or 10 ⁻³ K/m
MLLI50	Lifted Index for a mixed-layer parcel from the lowest 50 mb above the surface (in K, or °C)	K or °C

CAPE and CIN are two parameters that can be derived from vertical profiles of temperature and humidity throughout the troposphere. They are widely used in the prediction of convective storms, as they describe, respectively, the specific potential energy of air in the lower troposphere that is potentially released in convective storms, and which must be overcome before the energy release takes place. They are quantities with a direct physical interpretation, which sets them apart from the plethora of convective indices that only relate to the physics of convection in an indirect or convoluted way (see, e.g., Haklander and Van Delden, 2003; or Kunz, 2007).

CAPE and CIN are both vertical integrals of the thermal buoyancy B^1 of a hypothetical air parcel that is lifted from its original vertical position. The computation can be visualized on a thermodynamic diagram, for instance a Skew-T-log-p diagram (Fig 1.). They can be expressed as (e.g., Markowski and Richardson, 2010):

¹ Thermal buoyancy is buoyancy purely due to density differences, and we will hereafter refer to it as *buoyancy*. A more complete definition of buoyancy that includes the effects of pressure perturbations is given by Doswell and Markowski (2004).

$$CAPE = \int_{LFC}^{EL} B \, dz \approx \int_{LFC}^{EL} \frac{T_{v,parcel} - T_{v,env}}{\bar{T}_v} g \, dz$$

and

$$CIN = - \int_{surface}^{LFC} B \, dz \approx - \int_{surface}^{LFC} \frac{T_{v,parcel} - T_{v,env}}{\bar{T}_v} g \, dz$$

The CAPE integration starts at the Level of Free Convection (LFC), the first level above the Lifted Condensation Level (LCL), where a parcel obtains positive buoyancy and continues until the level where it ceases to be buoyant, the Equilibrium Level (EL), (or Level of Neutral Buoyancy, LNB). The CIN integration starts at the surface and continues until the LFC. The Lifted Index is defined as the temperature difference of the ascending parcel at the 500 mb level.

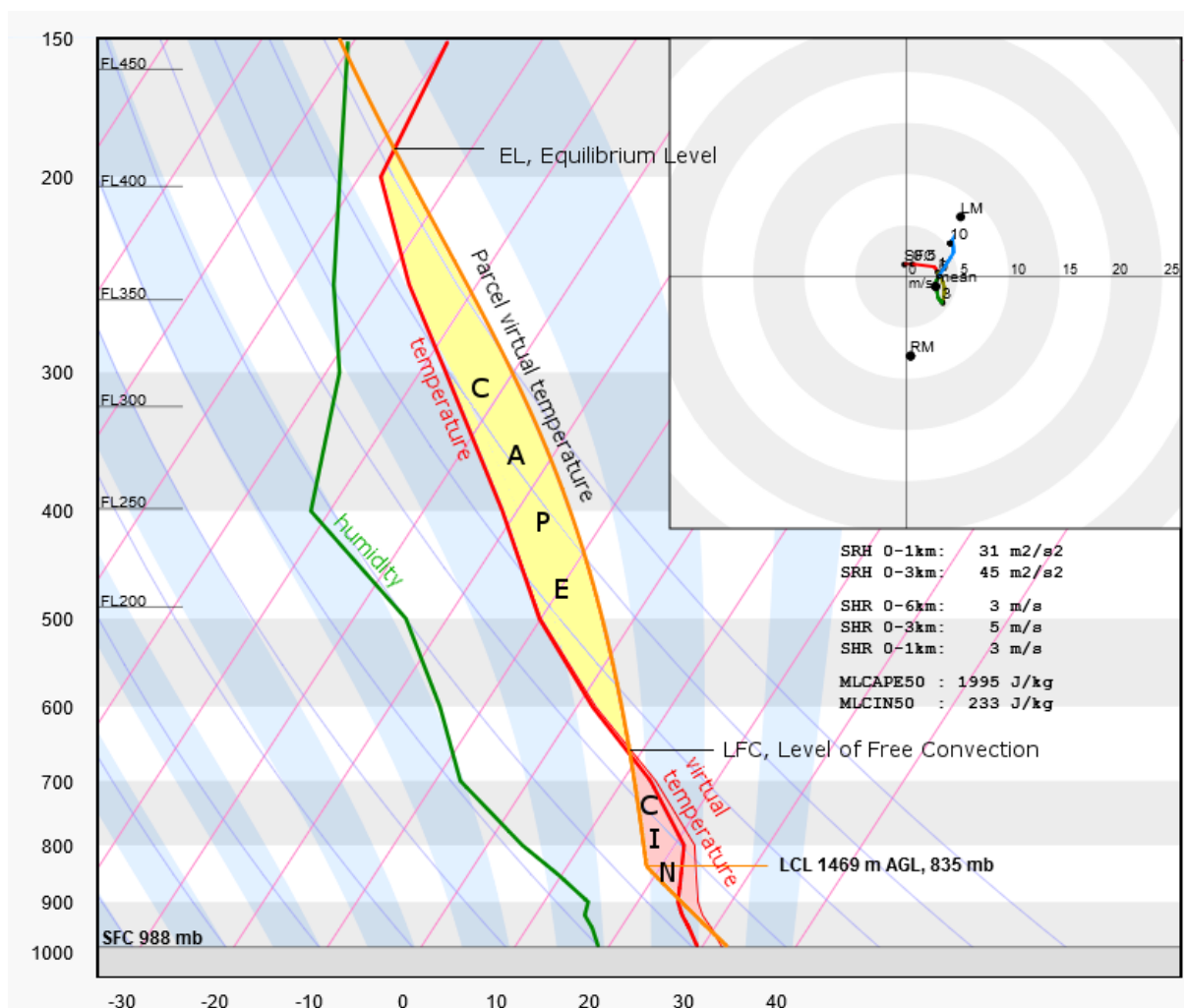


Figure 2.3. Skew-T-log-p diagram illustrating several key parameters for forecasting (severe) convective storms. From: ECMWF Newsletter, 2019.

2.2 The choice of the parcel

The magnitude of CAPE, CIN and the Lifted Index depend on the choice of the parcel that is lifted. Common choices for the parcel are:

1. a 50 mb mixed-layer parcel, which is lifted from the surface, having the potential temperature and the water vapor mixing ratio of the air in the lowest 50 mb above the surface. CAPE, CIN and other parameters calculated for this parcel are called 50 mb mixed-layer CAPE, -CIN, etc., abbreviated: MLCAPE50, MLCIN50, etc.
2. a 100 mb mixed-layer parcel, as for the 50 mb parcel, for which the parameters get the prefix "ML" and the suffix "100".
3. The parcel that yields the highest CAPE, i.e. the most unstable CAPE, -CIN, or another parameter, abbreviated with the prefix "MU".
4. A surface-based parcel, i.e. the parcel that starts at the earth's surface with the temperature and humidity measured or forecast at 2 m AGL or lifted from the lowest level available in the data set for which it is calculated. The resulting CAPE, CIN and other parameters for this parcel are called surface-based CAPE, surface-based CIN, etc., abbreviated with the prefix "SB".

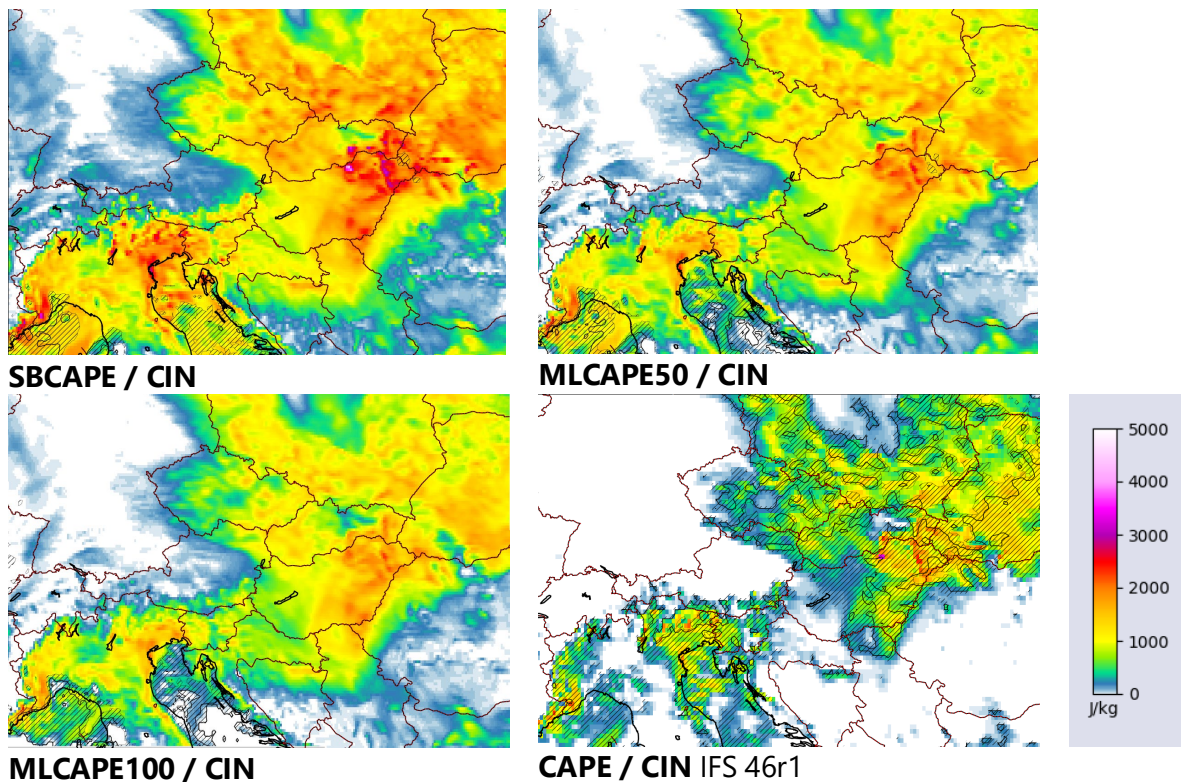


Figure 1.4. CAPE (colour scale) and CIN (hatched areas where $CIN > 50$ J/kg, contour at $CIN = 100$ J/kg) forecast for 30 July 2019 15 UTC (+39 h), calculated for a surface based parcel (left top), 50 mb mixed-layer parcel (right top), 100 mb mixed-layer parcel (left bottom), and as implemented in the ECMWF IFS cycle 46r1 (right bottom). From ECMWF, 2019.

For forecasting convective storms, it is reasonable to aim for the parcel that most representative of the mixture of air entering the base of a convective updraught. Craven et al. (2002) have demonstrated that the observed condensation level of convective clouds is corresponds best to that of a mixed-layer parcel. Moreover, it would be difficult to assume that the air flowing into a storm originates exclusively from the lowest few meters of the boundary layer. Fig. 2.4 shows that the differences between the parameters can be substantial, dependent on the choice for the parcel. For more details about this, we refer to a study ESSL has performed for ECMWF (ECMWF, 2019).

3 Evaluation at the ESSL Testbed

3.1 The ESSL Testbed 2019

Key facts

The ESSL Testbed 2019 took place during the weeks of 3–7 June, 24–28 June, 1–5 July and 15–19 July 2019 at the ESSL Research and Training Centre in Wiener Neustadt. During these four weeks, 41 participants took part in the Testbed in addition to 4 ESSL staff members. The participants came from 14 different countries: Austria, Germany, the Netherlands, Slovakia, Croatia, Portugal, Latvia, Bulgaria, Italy, Czechia, Poland, Cyprus, Slovenia, and the United Kingdom. The Testbed week of 15–19 July 2019 was a special "Expert week", meaning that ESSL invited those who had already visited the Testbed or an ESSL course before. This allowed the team to focus even more on product evaluation instead of training that week. From EUMETSAT, Thomas August took part in person during this week. In the other weeks, Thomas August was able to provide a remote presentation on IASI to the participants.

Resources

The following online resources contain further information about the Testbed:

The Testbed Data Interface showing all products and all data, is available online after the end of the Testbed at: <http://weather.essl.org/>

Login credentials can be obtained from Pieter Groenemeijer.

A Blog describing the daily activities at the Testbed can be found at: <http://www.essl.org/testbed/blog>

Background information and all presentations given at the Testbed can be accessed at: <http://www.essl.org/testbed/info>

Passwords will likely be changed early in 2020.

Feedback on the products was collected throughout the Testbed, partly **i) in direct discussions with the on-site R&D participants**, and in part **ii) through the documentation of answers to questionnaires** that were filled out jointly by participants, who typically worked in groups of 2–4 persons in dedicated sessions during the afternoons. The feedback from participants has been attached to this report.

3.2 Questionnaires and responses

Five specific questions were posed to the Testbed participants in a questionnaire. The participants were requested to form groups of 2–4 persons and answer the questions together after and during the investigation of the IASI products for a specific severe weather case, often a case that happened earlier the same week. These questions focus on several aspects of the IASI product. In addition, participants were queried for any other feedback.

The full questionnaire responses are given in Appendix B. Here, we will summarize the results.

Question 1

Could atmospheric soundings such as those provided from Metop/IASI (available within 30 minutes from sensing) be useful for your forecasting work? In what way?

The first question asked for a very general assessment of the usefulness of the type of information IASI can deliver. Out of 15 groups of respondents, 12 thought it was useful in principle or in theory, two had a more nuanced response, and one responded that it was not useful in an experiment of assimilating the data at the Italian Weather Service –but that was not the question that was asked.

Nine responses mentioned the benefit of validating NWP model output against the retrieved IASI profiles. Even though we did not ask about limitations of the IASI product in the question yet, three groups mentioned that the IASI data must have high enough accuracy to do so, and two of them mentioned that a higher spatial and/or temporal resolution would be required.

Question 2

Which of the provided parameters based on the sounder data do you find most useful? Please mention the 3 to 5 most useful ones.

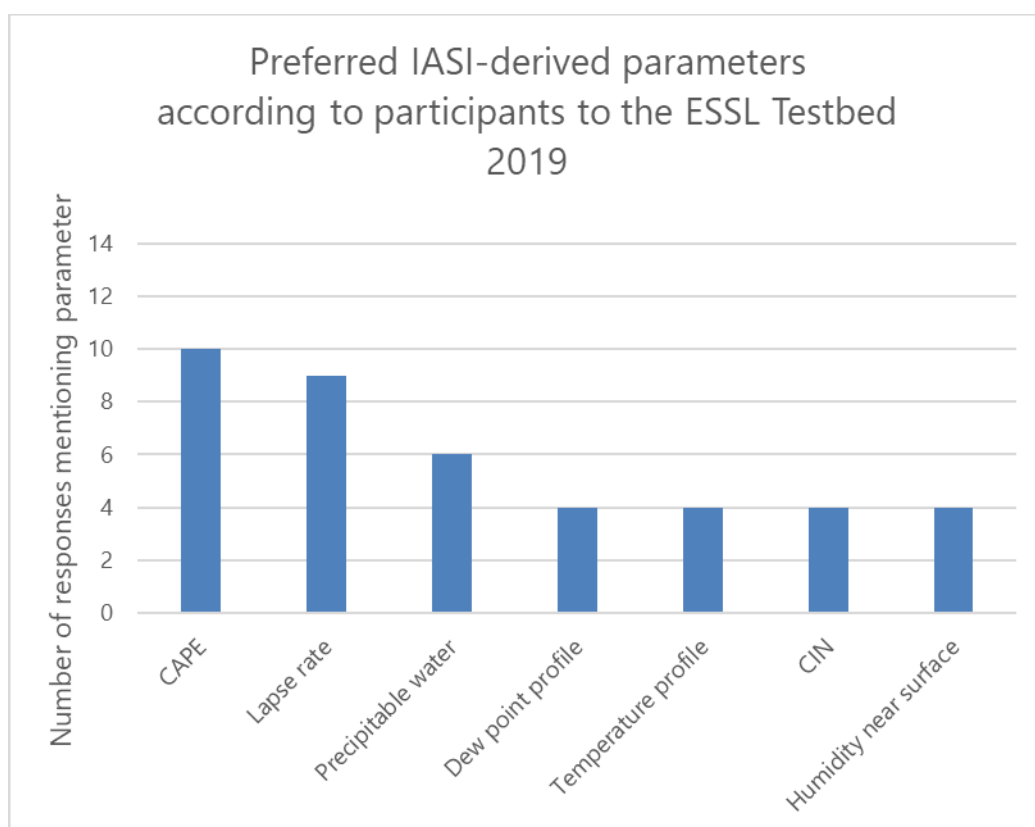


Fig. 3.1. Participant preference of IASI-derived parameters.

Among the participant teams, who were asked to mention 3–5 parameters, variants of CAPE and of the temperature lapse rate were mentioned the most frequently, followed by Total Precipitable Water (Fig 3.1). Although not strictly parameters, 4 out of 15 responses mentioned the vertical profiles of temperature and dew point. Probably, many more teams found these data of interest, but did not consider them to be a parameter.

Question 3

We would like to know how interesting you think the current products are for operational forecasting, considering the limited spatial and temporal resolution in comparison to the planned Meteosat Third Generation - Infrared Sounder (MTG-IRS), that will deliver data every 30 minutes with contiguous pixels sampled at about 7 km over Europe. Please select the statement that best describes what you think:

A. I think the IASI products with their limited temporal availability (twice a day) already provide important additional information that makes the data interesting to use.

B. I think the IASI products could be useful for forecasting, but first it is necessary that more observations become available throughout the day.

C. I think the IASI products as they are now having limited value for forecasting but are interesting to prepare for the MTG-IRS data, that will have better resolution.

Of the 15 participant groups, 11 have chosen option B (Fig. 3.2). This indicates that most participants think that getting IASI-like data is important and necessary for IASI-like data to be of high value for forecasting. This is interesting in the light of the MTG-IRS data that will become available in the near future. Minorities of 2 out of 15 expressed their satisfaction with the present sounder product or expressed the requirement for better resolution before finding it useful.

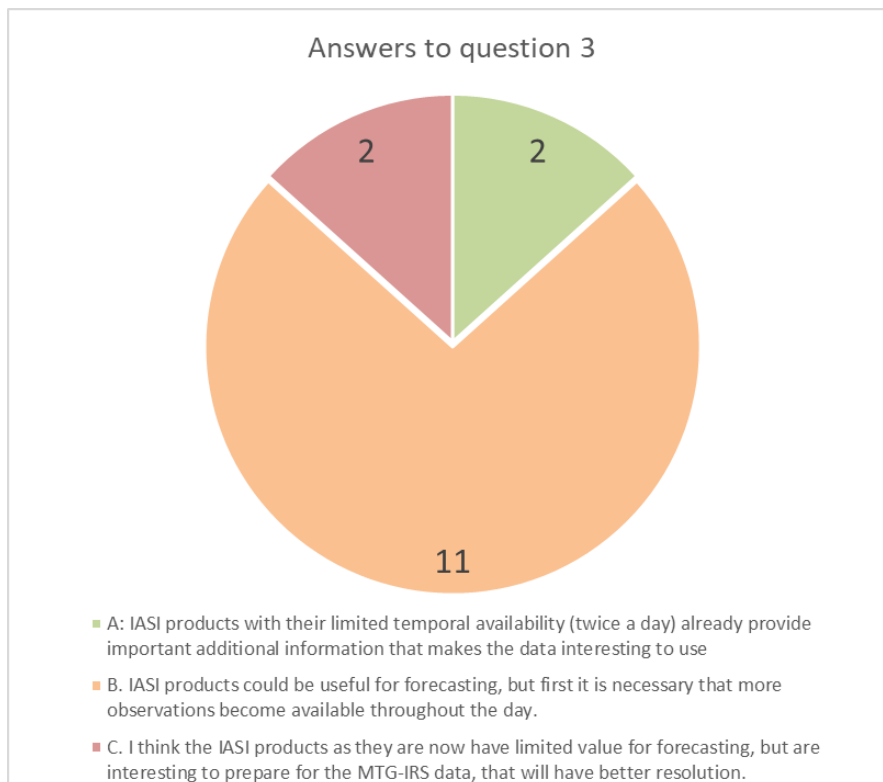


Fig. 3.2. Answers to question 3.

Question 4

In principle, NWP (forecast model) data could be used to improve the limited vertical resolution of hyperspectral sounder products, but this would introduce a dependence on them. In their

present form the data are available in the form of smoother/less resolved profiles (than e.g. sondes) and as integrated-/lapse-/instability quantities, but they are fully independent of any NWP model. How important is it to your work that the products are independent of any NWP model?

Almost all participant groups (14 out of 15) clearly stated that it was important or very important to have an IASI dataset that is independent from numerical model output. One group who agreed with this, also pointed out the use of IASI data for initializing NWP models: *"We think that it should be independent, so that observations are closer to reality and then we could compare them with model data. But of course, it is a good thing that the IASI data are assimilated into the model to improve the performance of the model."*

Question 5

The vertical profiles are currently provided with a single error estimate, displayed with an error bar at the bottom of the profile. In principle, it is possible to display errors for any given level. How useful do you think this would be for your work? In practice, how would you use this quality-control information?

12 out of 15 participant groups responded that they would find such information useful. 3 out of 15 thought it would not be useful, the main objection being the risk of overloading the user with information. This concern was shared by some groups that thought the added information would be useful. The participants gave suggestions to avoid the display from becoming too cluttered, which included plotting shaded semi-transparent areas of uncertainty around the existing curves and an option to turn the display of uncertainty on or off, or to provide this information only for a limited number of levels.

Question 6

Do you have any additional comments or suggestions regarding the data? Did something in particular catch your attention?

Participants replied to this question with a large number of suggestions and observations. Seven groups of participants mentioned in one way or another that low-level humidity differences between the IASI data and NWP model, or between IASI and surface observations was large. Three of them mentioned explicitly that they noted an underestimation of the humidity. It was also mentioned by one group, but this was discussed more widely, to try to improve the low-level humidity estimates from IASI by combining it with surface observations of humidity. Two groups mentioned that the temperature profile seems to be (much) better. Other comments included these suggestions regarding data visualization:

1. enable a 3D (i.e. cross-section) view of sounder data
2. display low-level dew point temperature
3. indicate the time difference between time of sounder and the NWP model
4. highlight CAPE area in sounding profile by shading it

4 Case studies

4.1 Case selection

Date	Description	Location
1 Aug 2017	Convective initiation failure in high CAPE and high shear setup	Germany
11 Aug 2017	Destructive convective windstorm	Western Poland
17 Sep 2017	Damaging convective windstorm in low CAPE environment	Northern Balkans
13 Jun 2018	Damaging hailstorm. Low storm activity further north	Serbia, Hungary
26 Jan 2019	Strong tornadoes	South Turkey
5 Jun 2019	Severe wind gusts with elevated CAPE	Netherlands, Belgium
11 Jun 2019	Giant hail	Slovenia, Croatia
10 Jul 2019	Extremely severe storms	Italy and Greece
9 Aug 2019	Severe storms with tornadoes and hail	Luxembourg, France, Netherlands
11–12 Sep 2019	Deadly flash floods	Spain

4.2 1 August 2017: Convective initiation failure over Northeast Germany; severe storms in Poland

On this day, strong south-westerly flow exceeding 25 m/s was simulated on the forward flank of a cyclone centred over the British Isles. At the same time, a wavy frontal boundary stretched from France into Germany and northern Poland. Along and ahead of the boundary, abundant lower tropospheric moisture combined with steep lapse rates. NWP models unanimously predicted an overlap of CAPE exceeding 2000 J/kg and strong vertical wind shear (exceeding 20 m/s in the 0–6 km layer), as well as widespread initiation of convective storms over parts of northern and eastern Germany. Thus, forecasts were calling for a major outbreak of severe thunderstorms capable of all kinds of severe weather.

In contrast to the anticipation, north-eastern Germany was spared from severe weather and most of the area did not even experience any thunderstorms. Soundings and weather station observations revealed high values of convective inhibition and the negative influence of an early frontal boundary passage. In the wake of the boundary, the airmass was stabilizing as the temperature dropped. Over this region, storms initiated only close to the Ore mountains on the border with north-western Czech Republic in the late evening after 18 UTC. Further severe weather occurred over the Alpine region in the afternoon and between 20 and 24 UTC over western Poland (Fig. 4.1).

This case presents a good opportunity to investigate the usefulness of the sounder data to forecaster decision-making. This day proved to be a scenario with a potentially high risk to the public, but also one where the model predictions were wrong. In this type of situation other sources of data than NWP models may prove important and can improve the short-term forecast. We will discuss both the morning and evening overpass data. The morning overpass will be discussed in the context of the anticipation of the afternoon evolution and evening overpass in the context of the ongoing severe storms over Poland.

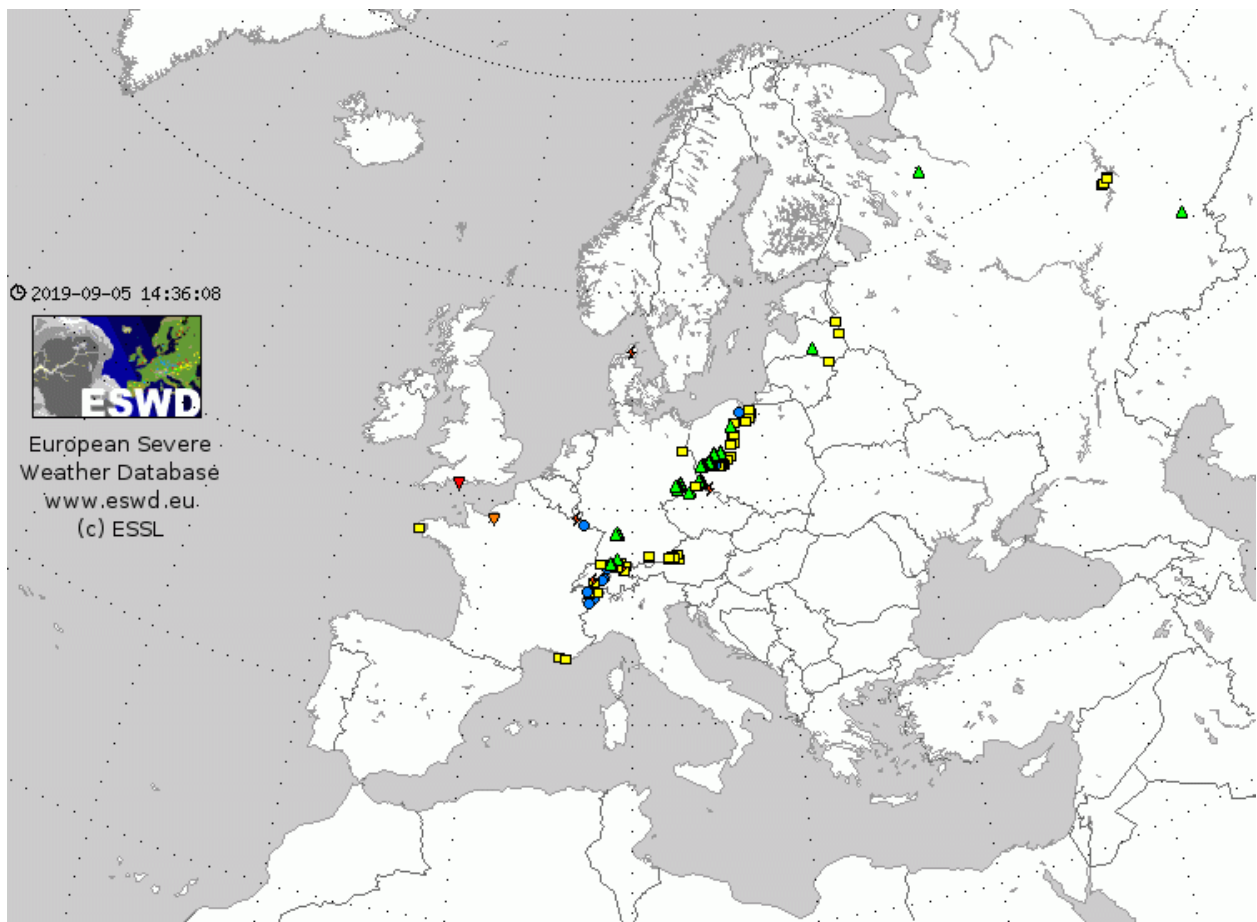


Fig. 4.4.1. Plot of ESWD reports for period of 1 August 2019 00–24 UTC. Green triangles represent large hail, yellow squares severe wind gusts, blue circles heavy rainfall and red triangles tornadoes.

Morning overpass

IASI sampled the environment at around 10 UTC, which is several hours before the NWP models simulated the first severe storms. The highest severe weather threat over north-eastern Germany was anticipated to occur within the 15–21 UTC time frame. Thus, the 10 UTC overpass data do not represent the immediate pre-convective environment of late afternoon storms. Nevertheless, we can compare the data to the NWP forecast and to the 12 UTC soundings and discuss the morning evolution of the pre-convective environment.

IASI data, similarly to the ECMWF model, show CAPE that generally increases from north to south. There are some differences between the sounder and the model in terms of the absolute values (Fig. 4.4.2). The model has higher CAPE over western and northern part of the displayed area, whereas sounder has higher values over south-eastern Germany and the south-western Czech Republic. These discrepancies have different reasons, over western Germany it is because the sounder has less lower-tropospheric moisture than the model, whereas over Czechia IASI sampled a warmer temperature near the surface. While the sounder underestimated the moisture over western Germany (16–18 °C dewpoints vs 18–20 °C in reality), it was accurate with the 29–30 °C temperature over the south-western Czech Republic, compared to 26–27 °C in the model). It must be noted though that the sounder overpass sampled the atmosphere between 9 and 10 UTC, whereas the model data is valid at 9 UTC and temperature increased on average by around 1 °C over Czechia between 9 and 10 UTC.

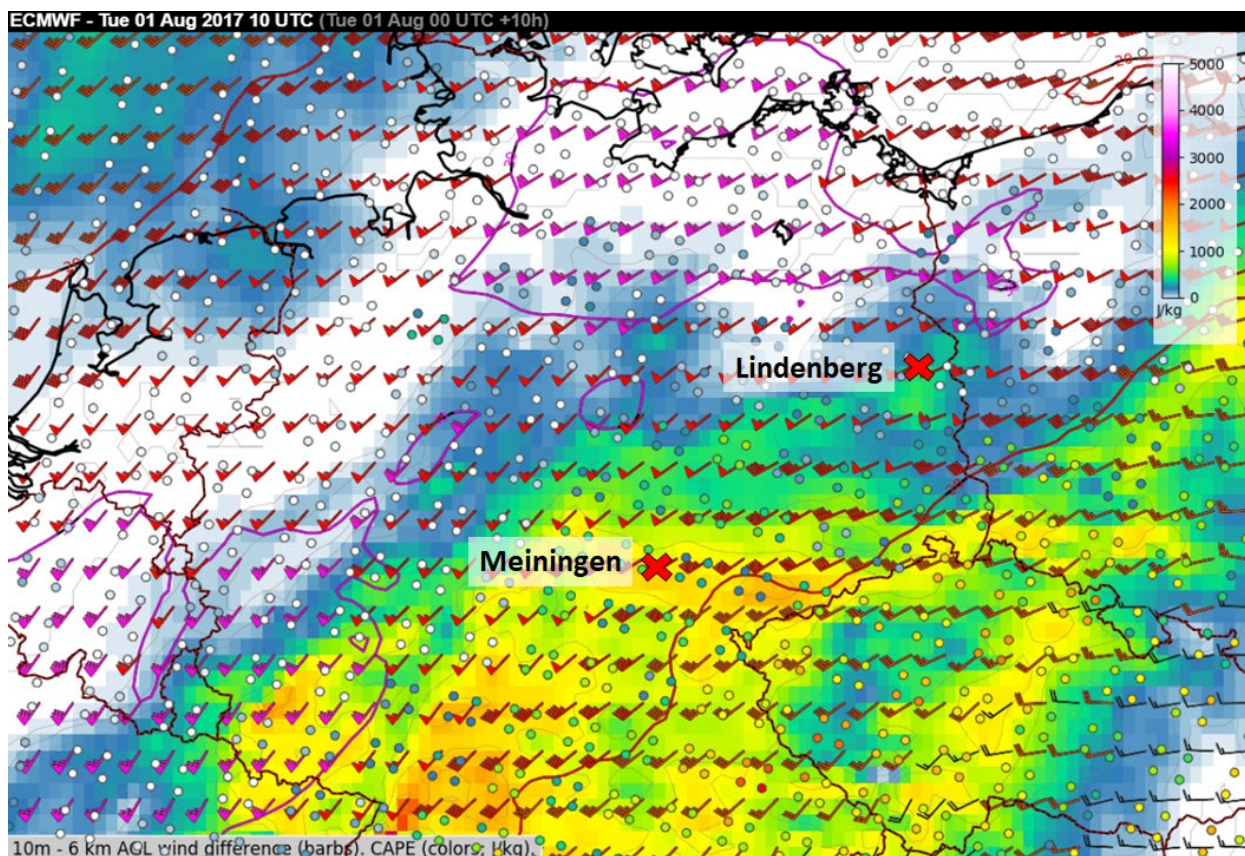


Fig. 4.4.2. ECMWF forecast of 1 August 2017 10 UTC CAPE (filled contours) compared to CAPE derived from the IASI measurements (coloured dots). Wind barbs represent the 0–6 km bulk vertical wind shear. Red crosses indicate the location of profiles discussed below.

One of the main concerns regarding the evolution of the forecast scenario stemmed from the presence of convective inhibition (CIN), preventing the initiation of convective storms until the late afternoon. Two sample profiles, which coincide with the location of the soundings show that the IASI did not sample the stable layer near 900 mb, which was present in the model simulations for both locations (Fig. 4.4.3). Thus, the IASI-derived profiles had lower CIN than the model. IASI also sampled the presence of steep mid-tropospheric lapse rates between 850 and 600 mb in the southern profile (Meiningen), but not for northern one (Lindenberg). 12 UTC soundings from these locations show that both the model and the sounder underestimated the CIN and that the stable layer was much sharper in reality. IASI represented the stable layer better over the southern parts of the studied area. While there is no stable layer in the profile derived from Lindenberg, it is discernible over Meiningen. This could be because the stable layer for the latter is located higher, where the sounder has better vertical resolution.

For example, over the western Czech Republic, the sounder-derived temperature profile matches the temperature profile measured by 12 UTC Prague sounding, with both showing pronounced stable layer around 800 mb.

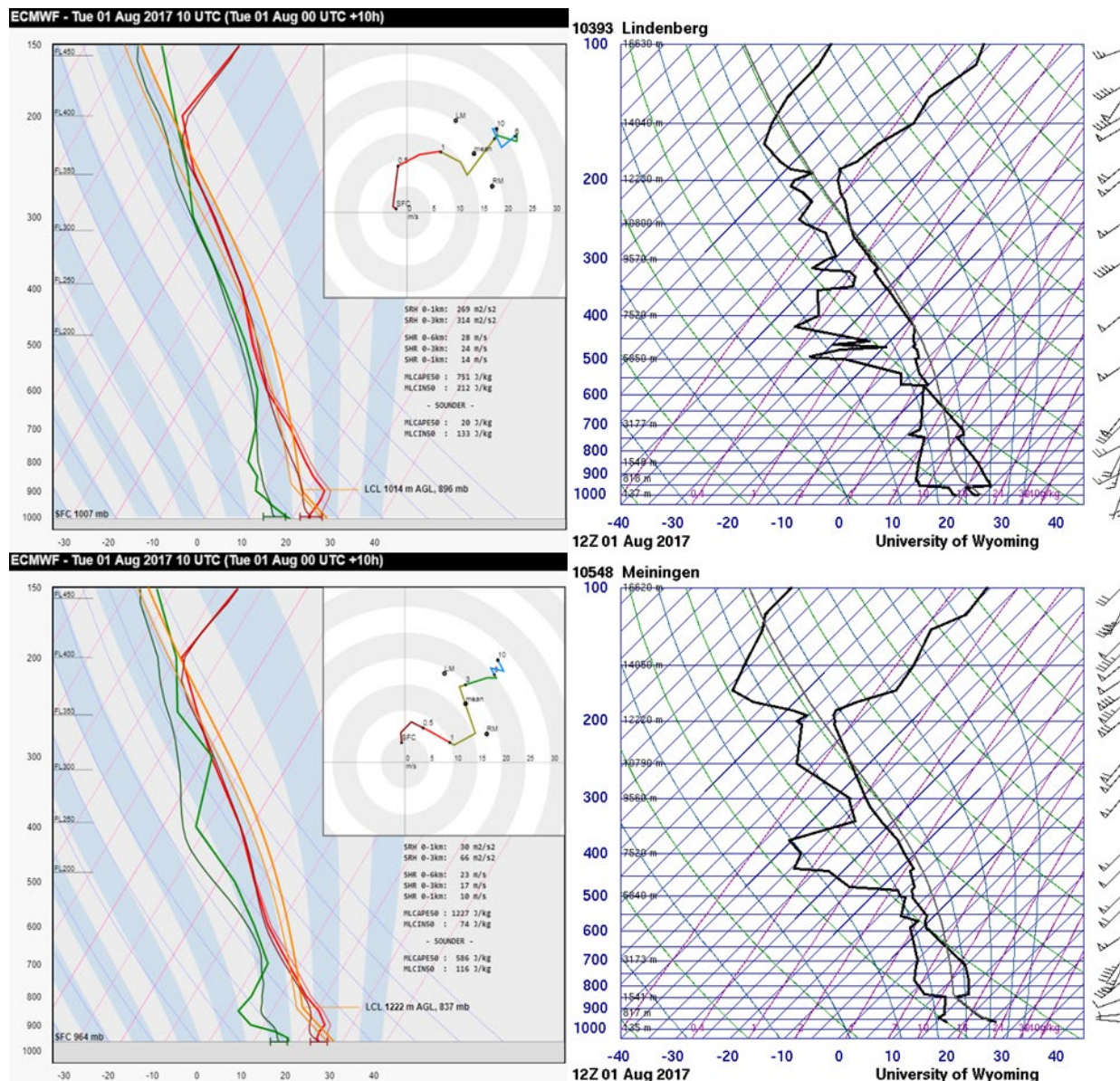


Fig. 4.4.3. Vertical profiles over Lindenberg (upper row) and Meiningen (bottom row). Profiles derived from the model and the IASI are shown on the left, whereas profiles derived from the 12 UTC radiosounding measurements are shown on the right. For the model and IASI profiles, vertical profile of temperature (red line), dewpoint (green line) and the calculated parcel curve (orange line). Thick lines represent the model simulation and thin lines are based on the IASI profile. Error bars are shown at the bottom of the dewpoint and temperature curve for IASI profile. For the radiosounding measurements, both temperature and dewpoint are plotted using thick black line, thin grey line represents the parcel curve. Source of radiosounding plots: University of Wyoming.

Evening overpass

As of 20 UTC, numerous severe storms initiated over western Poland, producing reports of large hail up to 5 cm in diameter. IASI sampled the environment ahead of the storms, as they continued producing reports of large hail and severe wind gusts. Both the model and sounder show ample CAPE over western and northern Poland, although there are some differences between the two (Fig. 4.4.4). Plotting a sample profile shows that IASI sampled less moisture than the model simulation, but it had substantially warmer lower troposphere. Surface

observations from Poland at 20 UTC near the location of selected profile show a temperature of 27 °C and a dewpoint of almost 20 °C. Thus, the model was closer to reality regarding the moisture, but the sounder represented the temperature better. Both datasets show similar CAPE (around 800 J/kg), but if we calculate CAPE using the temperature profile from IASI and humidity profile of the model, we arrive at much higher values (over 2000 J/kg), which could be closer to reality given the severity of the ongoing storms.

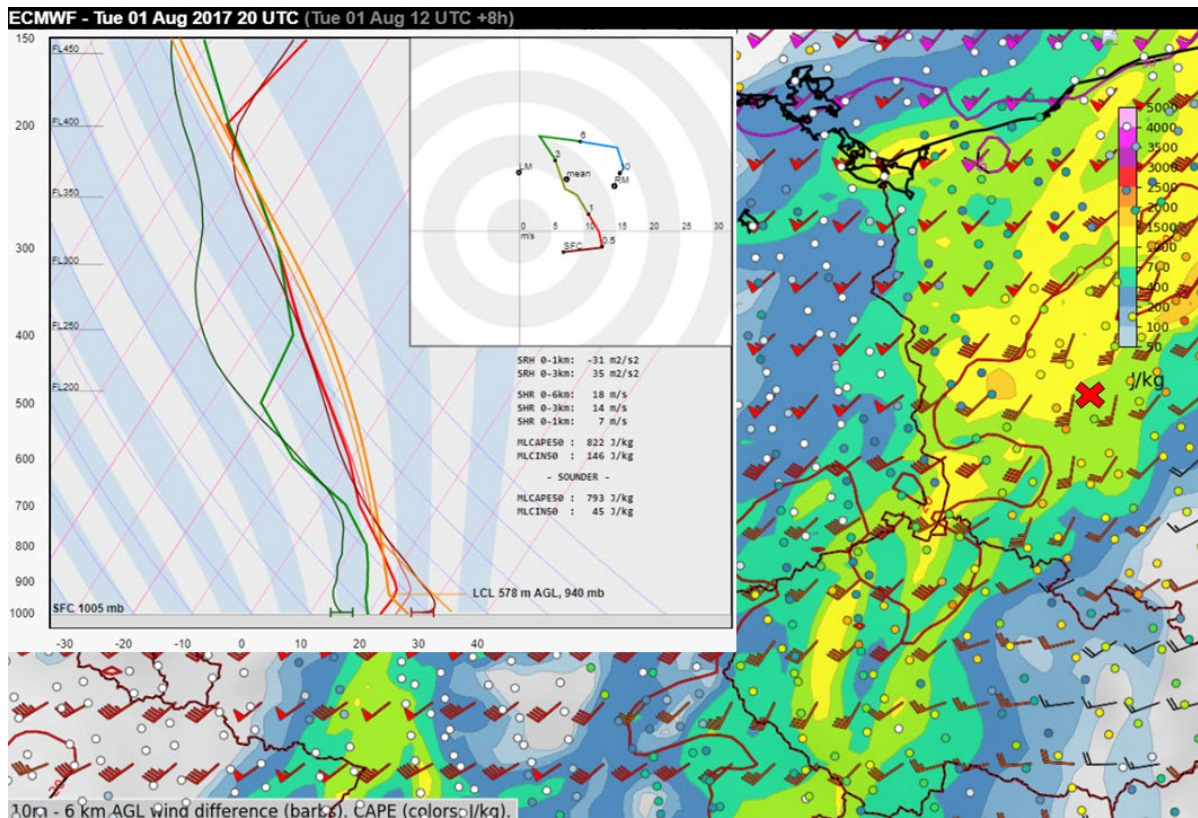


Fig. 4.4.4. As in Fig. 4.4.2 but for 1 August 2017 20 UTC. Red cross represents the location of the profile displayed on the left.

Summary

This case highlights a type of situation in which the environment is clearly supportive of extremely severe storms, but it is uncertain whether convective storms can initiate. Morning overpass data from this day show that sounder was able to detect the stable layer resulting in high CIN where that stable layer was not too close to the ground. Generally, the sounder was able to represent the vertical profile of temperature better than the humidity profile. While the humidity was underestimated in most of the studied profiles, IASI data were able to detect when the lower troposphere was warmer than anticipated by the model.

4.3 11 August 2017: Damaging convective windstorm over Poland

11 August was part of a multi-day outbreak of severe weather, that started on 9 August and ended on 12 August. From 10 to 12 August, several long-lived convective windstorms were observed in a belt from northern Italy to northern Poland and from the Baltic states to southern Finland. The situation was characterized by a deep cyclonic vortex at 500 mb, which moved from France to southern Germany on 11 August with a short-wave trough on its periphery moving rapidly from Austria towards Czechia and southern Poland. In conjunction with the eastward movement of the vortex, the wavy frontal boundary also moved eastwards. Widespread severe storms were forecast from the northern Czech Republic to northern Poland, in an environment characterized by abundant lower-tropospheric moisture, CAPE up to 3000 J/kg and strong vertical wind shear, as the southerly flow increased to over 20 m/s at 700 to 500 mb level.

In the morning, a large convective system formed over Czechia and continued towards southern Poland, where it gained strength and formed a bow-echo. During its fast movement to the north, a swath of damaging wind gusts was observed all the way to the Baltic Sea (Fig. 4.4.5) with the highest measured gust of 42 m/s. The first severe wind gusts were observed after 14 UTC and the most severe phase of the storm lasted between 18 and 22 UTC. The windstorm claimed 6 lives and became the worst disaster to Polish national forestry, destroying more trees than the Kyrill windstorm of 2007 over an area of 790 km². Both the environment and the structure of the convective system were analyzed in detail by Taszarek et al. (2019).

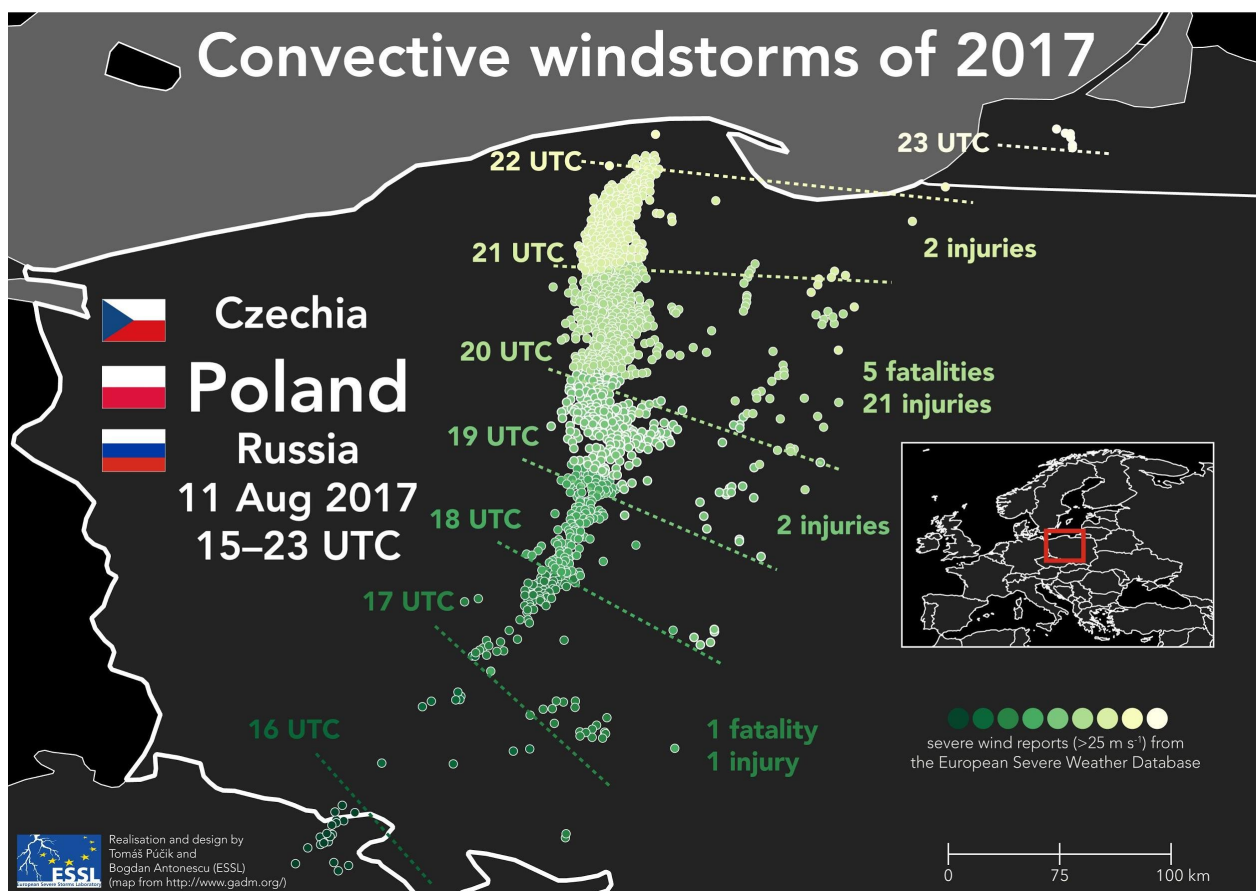


Fig. 4.4.5. A map of the wind damage reports collected for 11 August 2017.

800 mb which could serve as a source layer for the “elevated” instability. The presence of no “surface-based” and only “elevated” instability likely limited the ongoing storms in producing severe wind gusts. The sounder was able to replicate the transition from a stable to an unstable boundary layer between the northern Czech Republic and Poland. This was important for the future evolution of the storms—the severe wind gust production started exactly with the transformation of the elevated to surface-based storms in the afternoon.

Both the model and the sounder show a large area of CAPE around and above 1000 J/kg over eastern Czechia, Slovakia and the eastern half of Poland. The sounder generally showed lower CAPE due to the lower moisture content in the lower troposphere compared to the model. The largest differences were observed over eastern Poland, where the moist layer near the surface was shallow and thus harder to detect for the IASI instrument.

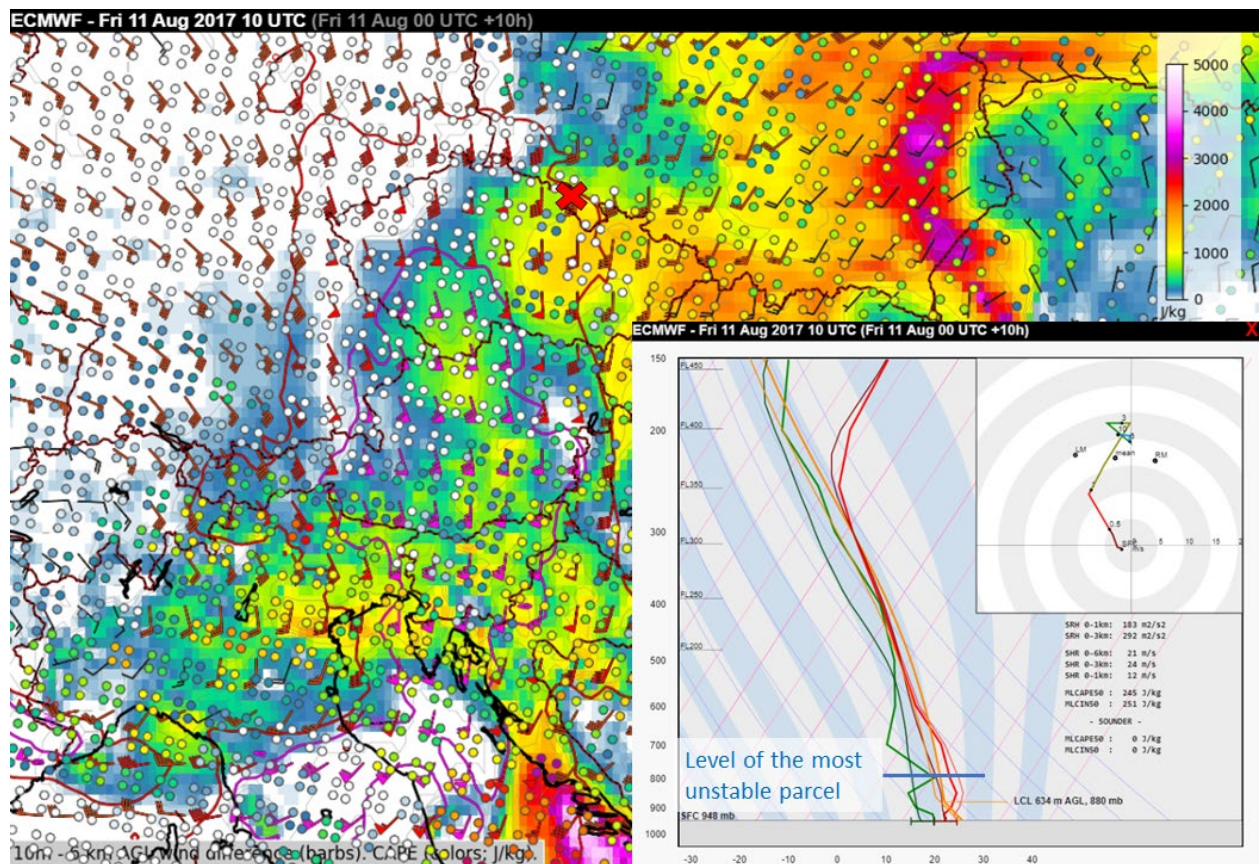


Fig. 4.7. As in Fig. 4.2, but for 11 August 2017 10 UTC. Red cross marks the location of the profile shown on the lower left.

Evening overpass

During the 20 UTC evening overpass, the convective windstorm had just reached peak intensity, forming a classic “bow-echo” shape in radar reflectivity (Fig. 4.8). The storm was moving rapidly northward and IASI sampled the environment ahead of it. Compared to the model expectation, the sounder sampled a warmer lower troposphere (26 vs 22 °C). A weather station that was impacted by the storm a few minutes before 20 UTC measured 25 °C, which means that the sounder was closer to reality. This difference could have notified forecasters of higher chances of severe wind gusts compared to the model, as steeper lapse rates in the boundary layer are more favourable for generation of strong downdrafts. Like the morning

overpass, the evening overpass also underestimated the lower tropospheric moisture with widespread measured values of 20 °C across Poland, compared to the 15–16 °C sampled by IASI. Combining the IASI temperature profile with surface dewpoint measurement would likely yield CAPE approaching 3000 J/kg, not surprising given the intensity of the ongoing storm.

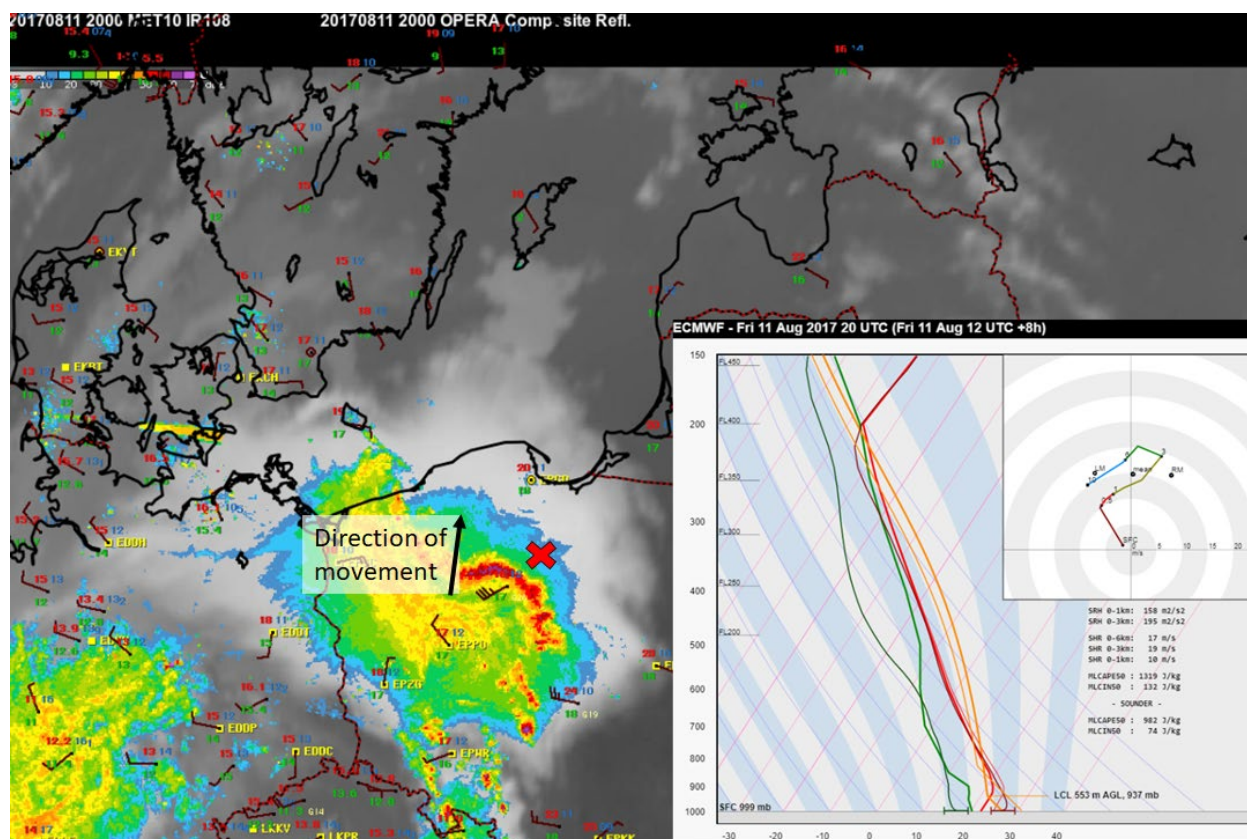


Fig. 4.8. An infrared satellite imagery on 11 August 2017 20 UTC overlaid with OPERA radar reflectivity composite and the surface station measurements. Vertical profile of temperature and dewpoint is shown for the location indicated by the red cross.

Summary

IASI sampled the morning evolution of the situation that led to one of the most destructive convective windstorms of the last decade over Europe. The sounder correctly identified the build-up of CAPE over Poland but was not able to capture the presence of elevated instability over Czechia. Both in the morning and evening, IASI data generally underestimated the lower tropospheric moisture. On the other hand, it was able to detect the warm lower troposphere ahead of the advancing convective system, which could have been helpful to forecasters in need of forecasting the intensity of the severe wind gusts with the storm.

4.4 17 September 2017: Damaging convective windstorm in Serbia and Romania

After a series of hot days and a drought, a change in the weather pattern was occurring across Balkans. In an unseasonably strong south-westerly flow, reaching 40 and 35 m/s at 500 and 700 mb respectively, a fast-moving short-wave trough moved from Italy towards Hungary and Slovakia. In the lower troposphere, a cold front with precipitation was forecast to cross the area. While NWP models were clear about the strong flow in the mid troposphere and the associated strong vertical wind shear, they showed only low, if any, CAPE. Thus, it was unclear whether deep moist convection would develop along the front.

In the morning, first storms developed near the Croatian coastline that turned into a powerful convective windstorm that crossed Bosnia, Serbia, western Romania and southern Ukraine between 11 and 17 UTC (Fig. 4.9). A 35 m/s wind gust was measured in Romania and the storm claimed 8 fatalities and 89 injuries in Serbia and Romania. Besides severe wind gusts, a dust storm with significantly reduced visibility was observed on the leading edge of the windstorm. So, despite the uncertain model forecast owing to the low CAPE, this situation resulted in an extremely severe storm. For a successful forecast or warning, forecasters would have had to recognise that enough CAPE is present in the environment to support the convective storms, which could quickly turn severe under the influence of unseasonably strong vertical wind shear.

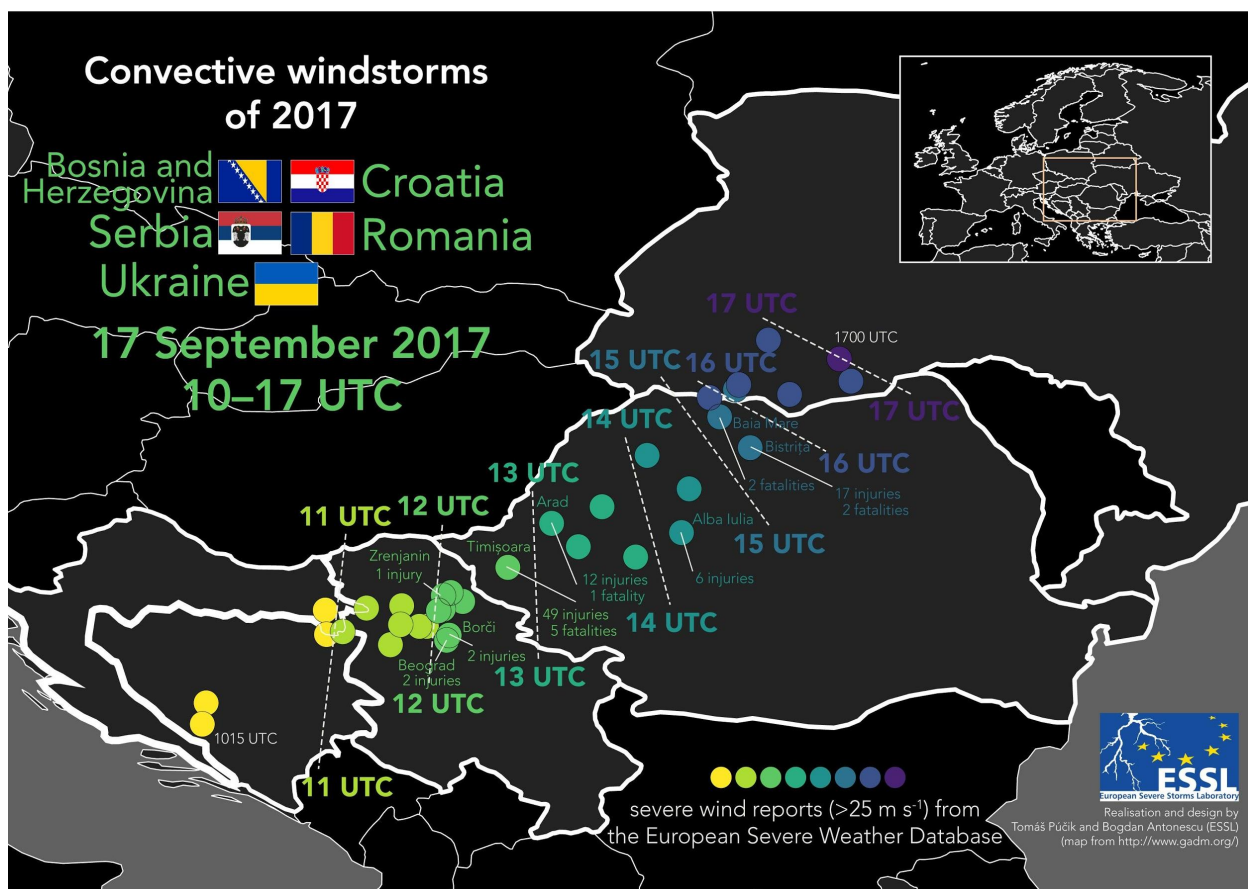


Fig. 4.9. A map of the wind damage reports from the ESWD for 17 September 2017.

Morning overpass

The 09 UTC overpass data were available just as the first storms moved from Croatia into Bosnia (Fig. 4.10). They were intensifying with several overshooting tops visible in the infrared imagery. At this time, the first severe wind gusts were reported over Bosnia, but the storm system had not yet reached its peak intensity. Ahead of it, IASI sampled non-zero CAPE over eastern Bosnia and western Serbia in the areas where model simulated no CAPE (Fig. 4.11). This coincides with the path that the storm system took in the following hour. The CAPE discrepancy can be attributed to the higher dew point samples by the sounder compared to the model. Surface stations measured dewpoints between 11–15 °C ahead of the storm, the highest values still above the sounder measurement and thus there was locally even more CAPE in the environment.

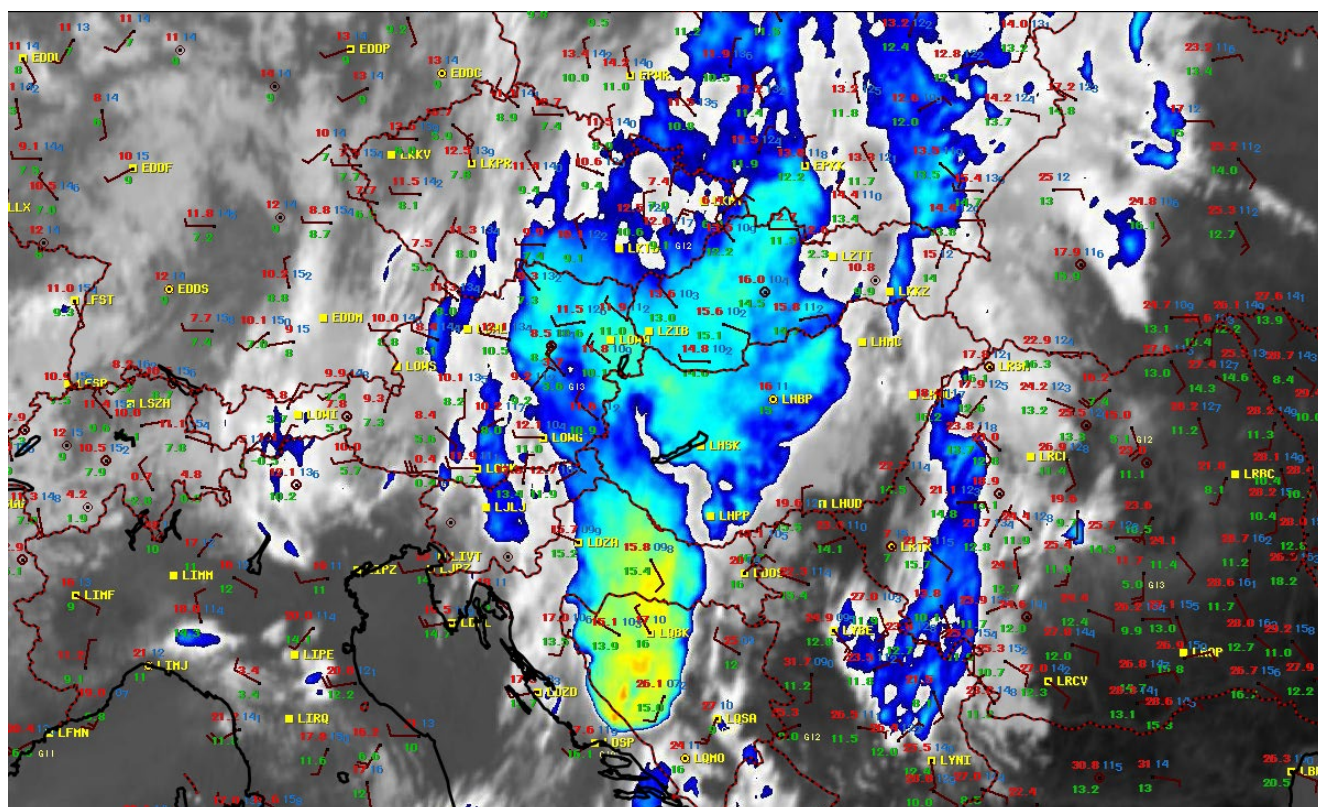


Fig. 4.10. An infrared brightness temperature enhanced imagery on 17 September 2019 09 UTC overlaid with surface station data (red numbers correspond to temperature and green to dewpoint temperature).

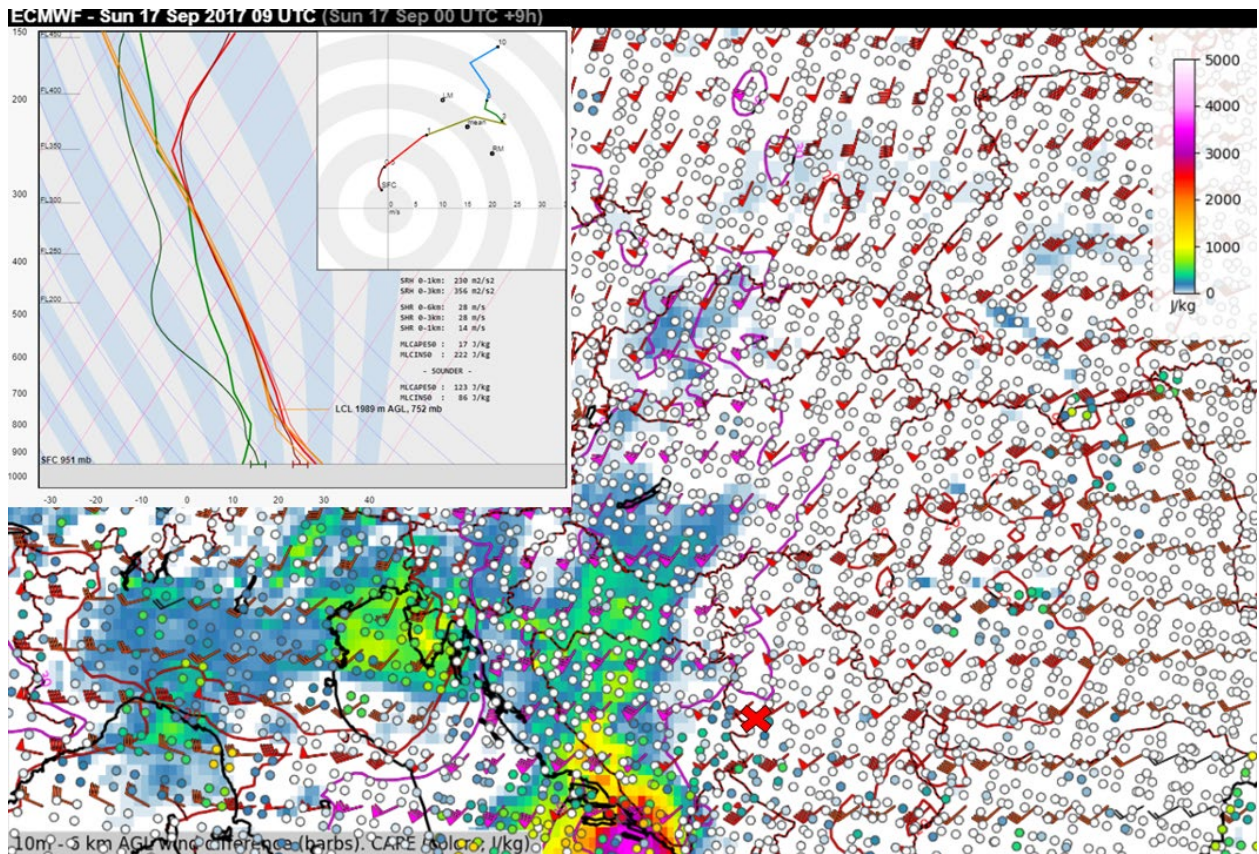


Fig. 4.11. As in Fig. 4.2. but for 17 September 2017 09 UTC. Red cross marks the location of profile displayed on upper left.

There were two reasons for the extremely severe wind gusts in the storm. One was the presence of strong vertical wind shear, which allowed a well organised convective system to develop. Another was the presence of a deep and dry boundary layer, which resulted in high cloud bases and efficient evaporative cooling of precipitation underneath the bases, supporting strong downdrafts. IASI sampled such an environment already at 9 UTC with large differences between temperature and dewpoint near the surface (Fig. 4.12). Observations of the 12 UTC Belgrade radiosounding show an almost dry-adiabatic stratification in the layer from the surface to 600 mb, a condition more typically observed over arid areas. The severe wind gust production in the storm rapidly picked up around 12 UTC as the storm passed this area. At 9 UTC, the sounder did not sample such steep-lapse rates, but this is not surprising given the large amount of heating and mixing that took place in the subsequent three hours. Nevertheless, compared to model and surface observations, the sounder underestimated the surface temperature and, therefore, the lapse rates in the lower troposphere.

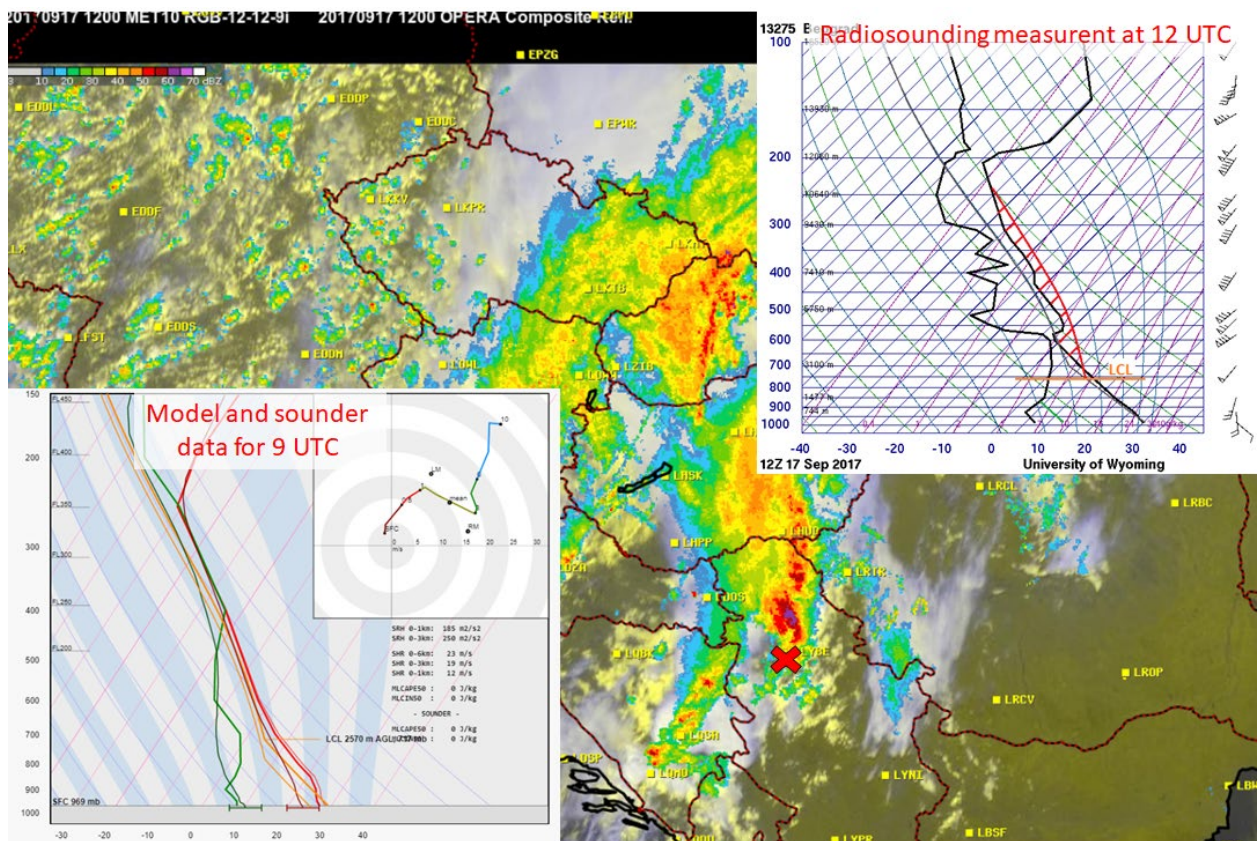


Fig. 4.12. Visible imagery overlaid with the OPERA radar composite on 17 September 2019 at 12 UTC. The red cross corresponds to the location of the sounder and model profile from 9 UTC and the radiosounding measurement at 12 UTC. The 12 UTC radiosounding measurement was adjusted using the surface dewpoint observations ahead of the storm (green line) with modified CAPE area indicated by red hatching.

Summary

On 17 September 2017, a long-lived convective windstorm crossed northern Serbia and western Romania with numerous injuries and fatalities. The convective storm formed in an environment of strong vertical wind shear and a marginal CAPE, which was underestimated by the model predictions. This made a forecast of this event difficult. Morning sounder data indicated more moisture in the lower troposphere than forecast by model ahead of the storm, which would be relevant information for the forecaster. The sounder also sampled deep boundary layer over Serbia although it underestimated the lapse rates in the lower troposphere. Subsequent overpasses, if available, would likely reveal destabilising and deepening boundary layer as the storm was approaching northern Serbia. In this type of rapidly evolving and difficult situations, 30-minute resolution sounder data may become an asset for a forecaster on duty.

4.5 13 June 2018: Severe storms over the Balkans occurring further south than expected

On this day, widespread thunderstorms were anticipated over a large area spanning eastern Austria, Slovakia, Hungary, northern Serbia and Romania. The situation was characterised by a mid-tropospheric trough stretching from north-western Germany to Corsica, with winds reaching 10 to 15 m/s at its forward flank. In the lower troposphere, a warm airmass was present across much of the Balkans with a frontal zone stretching from the Alps across south-eastern Austria and Hungary to Slovakia. The model simulated CAPE around and above 1000 J/kg across much of the Balkans all the way into southern Slovakia. The most severe activity was forecast across Hungary, where NWP models simulated the most storms and where the strongest vertical wind shear was forecast.

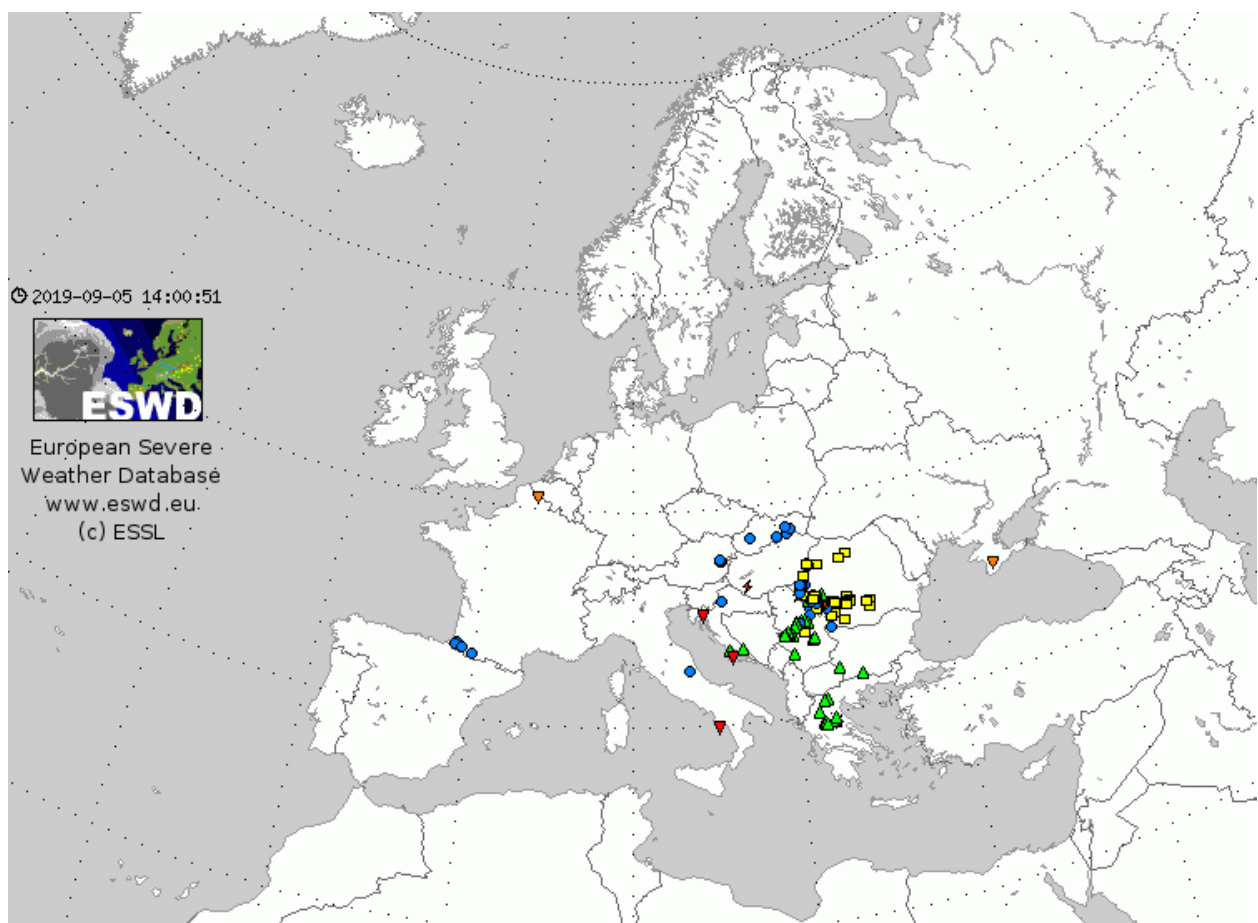


Fig. 4.13. As in Fig. 4.1 but for 13 June 2018 00–24 UTC.

In the end, little severe weather occurred over Hungary (although 16 people were injured by lightning, but this does not require a severe storm). The low storm activity was due to the cloudiness left over by early morning convective activity. Most severe storms were confined to south-eastern and central Serbia, and western Romania (Fig. 4.13). Over Serbia, severe damage to crops and buildings occurred between 12 and 14 UTC as large hail fell in combination with severe wind gusts of up to 33 m/s. Further severe weather was observed in Romania as the storms moved eastward with numerous reports of severe wind gusts and local flash flooding. The highest measured wind gust reached 28 m/s here, and the severe weather continued into late evening. Morning overpass data is used to discuss the lack of severe weather over Hungary

up to 22 °C, which is higher than the maxima both in the model (18 °C) and in the sounder data (19 °C). Thus, it is likely that early afternoon storms had even more CAPE available, perhaps close to 4000 J/kg, which is a reason for their extreme severity despite the presence of only marginal vertical wind shear.

Over northern Hungary and Slovakia, IASI indicated higher CAPE than in the model, owing to the higher moisture content in the lower troposphere. Surface observations from the area confirm this, for example Budapest measured a dewpoint of 19 °C, in contrast to 15 °C simulated by the ECMWF model. Numerous thunderstorms developed over the area in the afternoon and resulted in several flash flood reports.

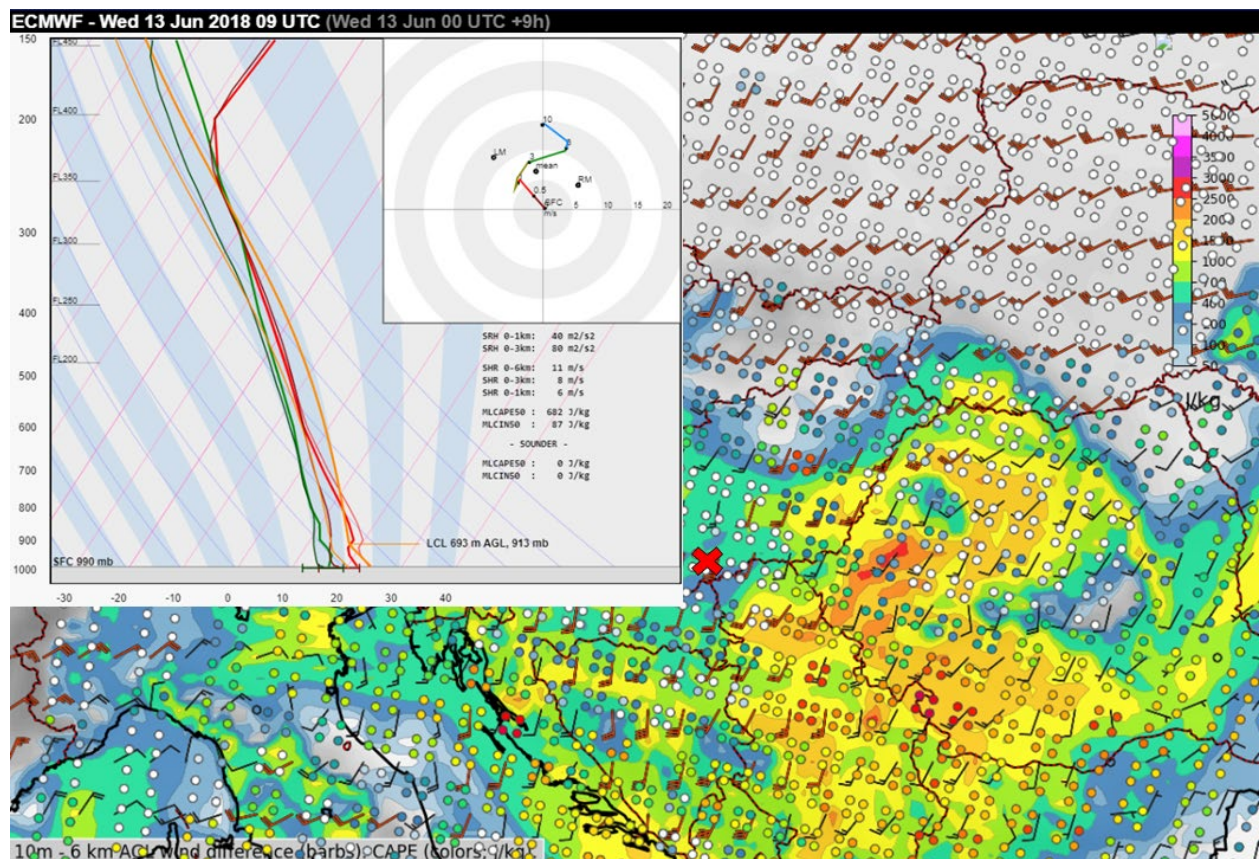


Fig. 4.15. As in Fig. 4.2, but for 13 June 2018 09 UTC. Red cross represents the location of the profile shown on the upper left.

Summary

Extremely severe thunderstorms were observed over Serbia and Romania, producing large hail and damaging wind gusts. Relative to the NWP model forecast, severe weather occurred further south than predicted, and little severe weather occurred further north over Hungary. This was because early morning convective activity stabilized and cooled the environment. This adjustment of the environment was sampled by IASI, which showed a reduction in CAPE over the southern part of Hungary. The sounder also sampled more moisture than forecast over northern Hungary, Serbia and Romania, coinciding with elevated CAPE.

4.6 26 January 2019: Strong tornadoes over southern Turkey

On this day a deep cyclonic vortex was centred over the Aegean Sea, with a jet-streak at its forward flank covering much of the eastern Mediterranean area. Closer to the surface, a cold front was crossing the Mediterranean Sea towards east. Ahead of it, strong southerly flow was observed with 850 mb winds reaching 20 m/s in the morning. Models simulated an overlap of marginal CAPE (100 to 400 J/kg) with strong vertical wind shear along the coastline of southern Turkey with CAPE rapidly diminishing further inland. Much of the vertical wind shear was confined to the lower troposphere with high values of Storm Relative Helicity, suggesting a risk of tornadoes.

Numerous storms developed over the sea in the early morning and tracked inland during the day, producing a local outbreak of tornadoes (Fig. 4.16). In total, 15 tornadoes were reported, causing 16 injuries. Two of the tornadoes were rated as F2. One of them struck Antalya airport, overturning bus with passengers, which resulted in 11 injuries. Two of the tornadoes was rated as F2. Besides tornadoes, storms also produced hail up to 4 cm in diameter over the land, damaging crops and cars, which suggests that CAPE could have been underestimated by models.



Fig. 4.16. As in Fig. 4.1 but for 26 January 2019 00–24 UTC.

A morning overpass sampled the environment of a band of convective storms (Fig. 4.17) in the Antalya area. The data were available for 8 UTC, while the Antalya airport was struck by the tornado precisely at 7:58 UTC. Thus, we can consider the overpass to be in a good temporal proximity to the tornado-producing storm. Due to the strong southerly flow in the lower

troposphere, measurements taken just south of the ongoing storms were likely the best representation of the conditions in their inflow.

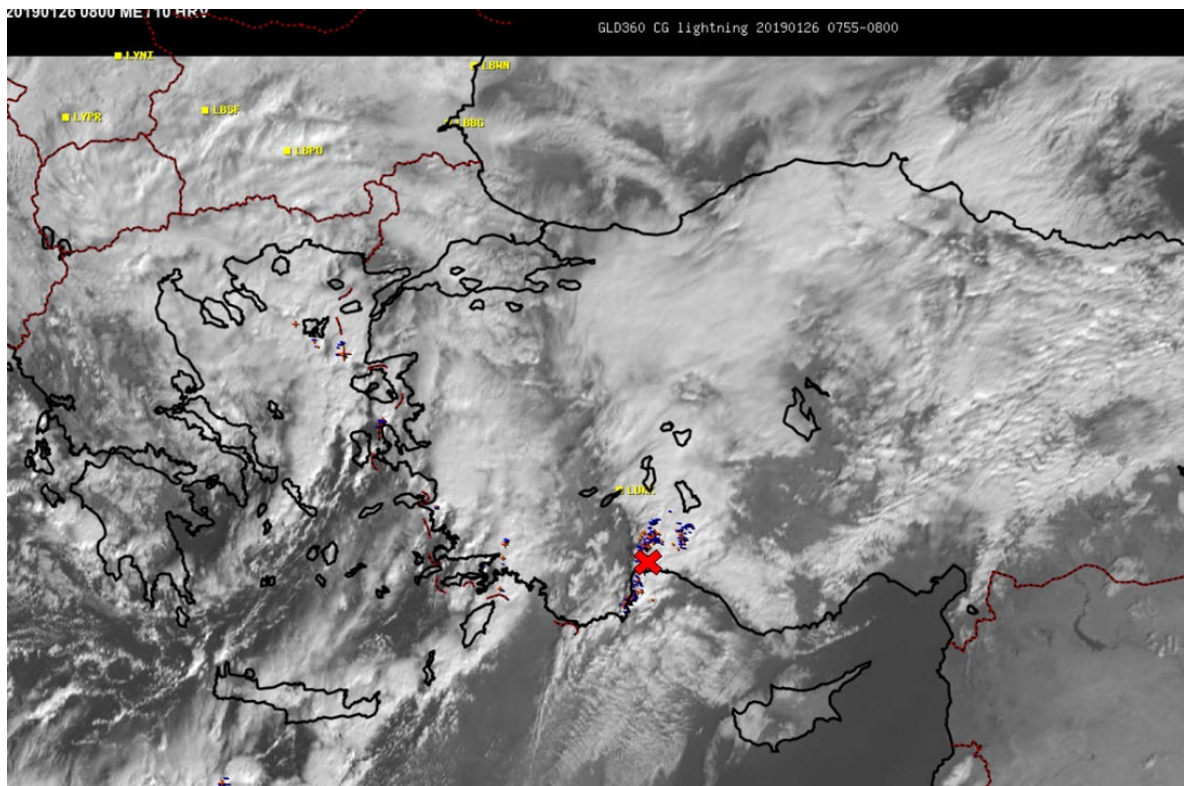


Fig. 4.17. High resolution visible satellite imagery on 26 January 2019 08:00 UTC, overlaid with the lightning strikes between 07:55 and 08:00 UTC based on the GLD lightning detection network. Red cross represents the location of Antalya airport.

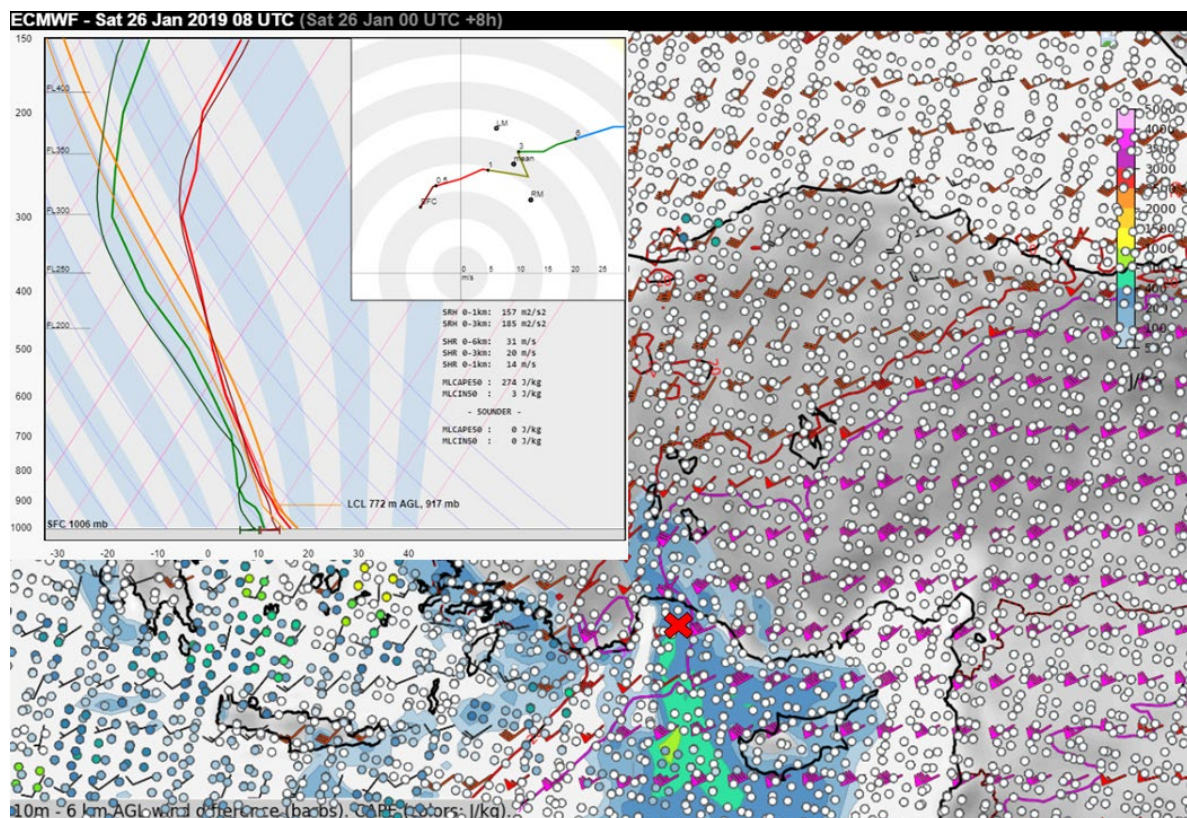


Fig. 4.18. As in Fig. 4.2 but for 26 January 2019 08 UTC. Red cross represents the location of the profile shown on the upper right.

While the model showed at least marginal CAPE near the coastline, increasing towards the south, the sounder data showed zero CAPE over the entire coastline of southern Turkey (Fig. 4.18). The sounder sampled both lower temperature and lower dewpoints over the area compared to the model. Antalya airport measured temperature of 14 °C and a dewpoint of 10 °C at 8 UTC. Just south of the coastline, the sounder measured 12 / 8 °C respectively. Thus, the sounder underestimated both the temperature and the dewpoint near the surface, which resulted in an underestimation of CAPE.

Summary

A local tornado outbreak, involving 15 tornadoes in a span of several hours, occurred over southern Turkey on 26 January 2019. The pre-convective environment featured strong vertical wind shear and marginal CAPE. IASI sampled the environment just after one of the tornadoes struck Antalya airport, but showed zero CAPE for the whole area. This can be attributed to an underestimation of both temperature and the moisture near the surface. While an error in moisture seems to be common in numerous investigated cases, the underestimation of temperature is not typical.

4.7 5 June 2019: Severe thunderstorms with unexpected severe wind gusts over Holland

The synoptic scale situation was dominated by two synoptic scale features: A fast-moving shortwave trough ejecting from northern Spain towards France and the Benelux, and a slowly moving cyclone over Romania. Two foci for severe convection were forecast during this day. The first was along a cold front over the Benelux and western Germany in an environment of strong vertical wind shear and forecast CAPE around 2000 J/kg. The other one was over the Ukraine in an environment of modest vertical wind shear and CAPE locally up to 3000 J/kg. A greater threat of severe storms was anticipated over the Benelux and Germany than over Ukraine.

Both areas experienced severe weather: Severe wind gusts up to 37 m/s were measured over Netherlands (Fig. 4.19). However, this was in an area where convection was expected to be elevated and, hence, with a reduced risk of severe wind gusts. A higher risk was anticipated more to the east on the border of the Benelux and Germany, where surface-based convection was forecast by NWP models. Here, convection was less severe. Crimea also experienced severe weather with large hail up to 9 cm in diameter, exceeding expectations given rather weak shear over the area. Because Crimea was not within region sampled by the overpasses, further discussion concentrates on the Benelux / western Germany.

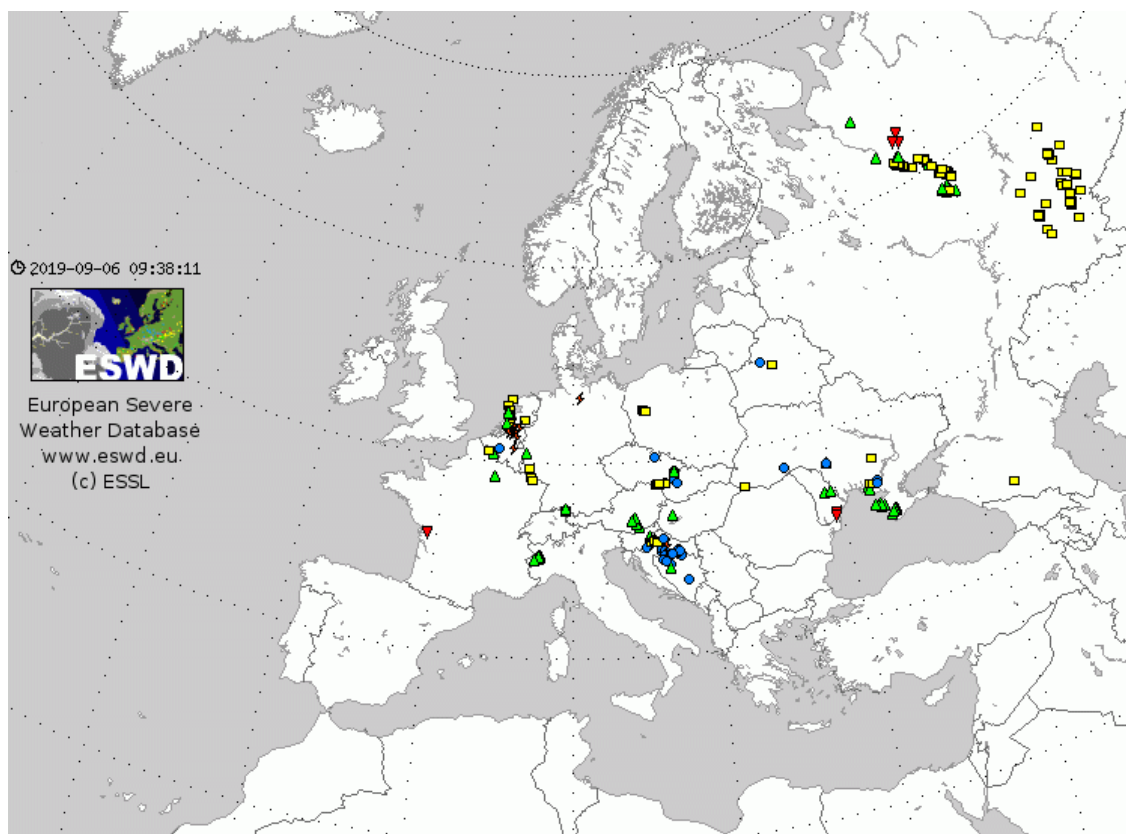


Fig. 4.19. As in Fig. 4.1, but for 5 June 2019 00–24 UTC.

Conditions ahead and behind of the convective system

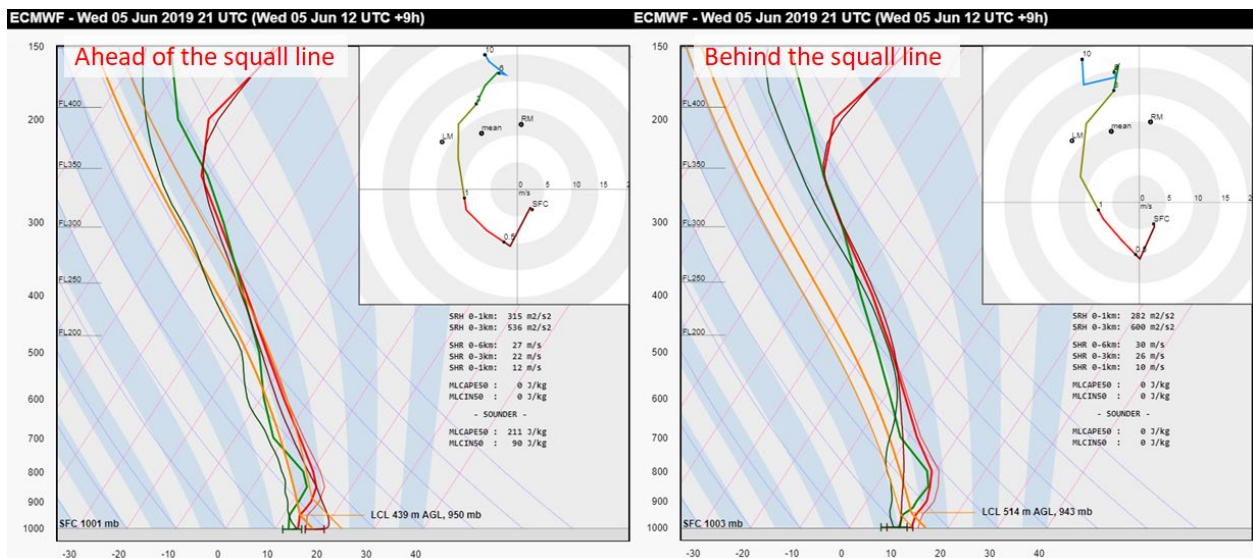


Fig. 4.21. As in Fig. 4.3. But for left/ southern Holland, ahead of the squall line and right/ northern Belgium, behind the line on 5 June 2019 21 UTC.

Elevated instability

Although IASI-based profiles detected warmer boundary layer than simulated by the model output, IASI was not able to capture a layer of warm and humid air between 850 and 800 mb that had been advected over cool at the surface over much of the Netherlands. Such a configuration is clearly visible in all the shown modelled profiles in Figs. 4.21 and 4.22 but is not apparent in the sounder-based profiles. The IASI-based profile (Fig. 4.22) would yield zero CAPE if any parcel in the bottom 300 mb is lifted, whereas model-based profile yields substantial CAPE, over 1000 J/kg, if a parcel from around 850 mb is lifted. In this specific case, calculating CAPE using the surface parcel or the mixed layer of bottom 50 mb yields values close to 0 J/kg, but calculating the highest CAPE for all possible parcels in the bottom 300 mb (most-unstable CAPE) suggests that the environment was capable of thunderstorms (Fig. 4.4). For correct anticipation of such cases of “elevated” (i.e. not based on the surface parcels) convection, the humid and moist layer of air must be reproduced correctly.

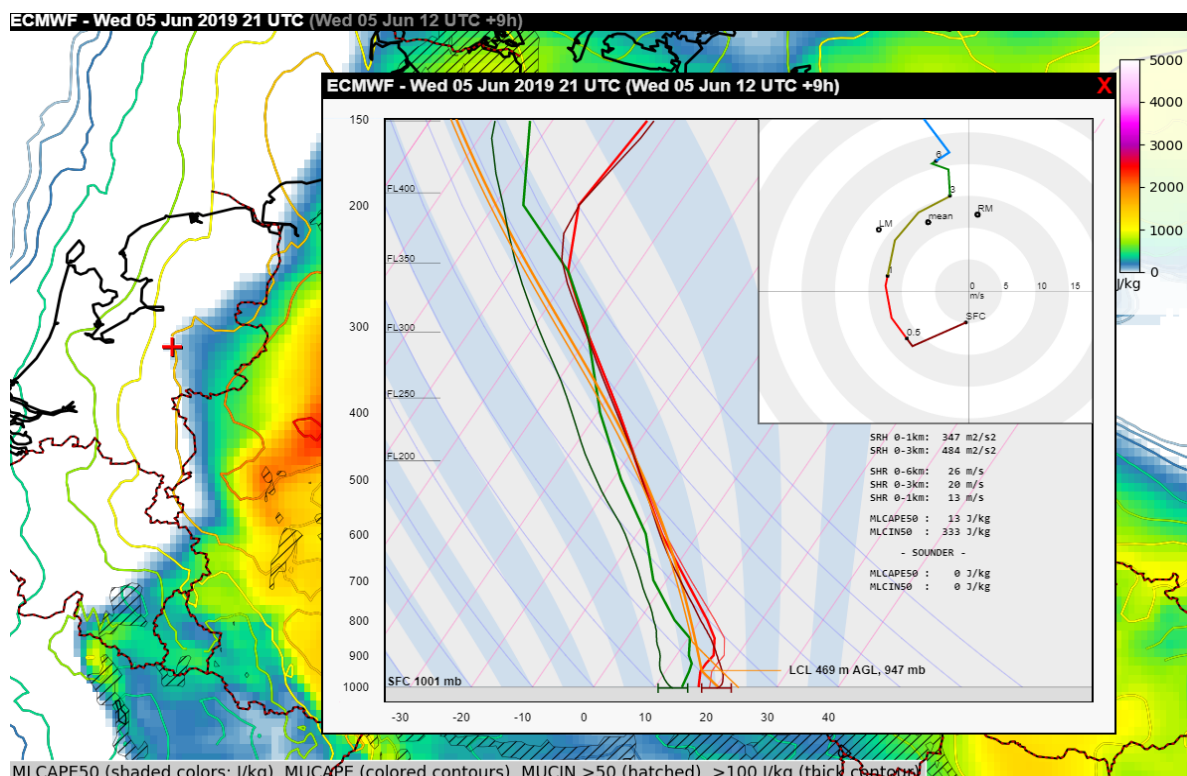


Fig. 4.22. ECMWF forecast of 21 UTC most-unstable (coloured contours) and mixed-layer CAPE (shaded colours). Hatched areas correspond to the CIN (> 50 J/kg for light and >100 J/kg for thick hatching). Profile as in Fig. 4.X, but for the location marked by red cross.

Summary

In the evening of 5 June 2019, a linearly-oriented convective system was progressing across the Benelux and western Germany. The main question was whether the system would be capable of severe wind gusts, given the anticipated stable stratification in the boundary layer. IASI sampled the environment both ahead and behind the convective line. IASI showed that the boundary layer was less stable than forecast ahead of the system, pointing to a higher risk of severe gusts. IASI also showed a decrease of lapse rates behind the system and reduction in the likelihood of further storms in its wake. IASI data did not capture the layer of warm, humid air with elevated CAPE > 1000 J/g, which probably contributed most to the strength of the convective system.

4.8 11 June 2019: Giant hail over Poland and Slovenia; initiation failure over Czech Republic

On 11 June 2019, a deep cyclonic vortex was centred over western France, with a southerly flow at its forward flank. Ahead of a cold front stretching across Germany, warm air with abundant lower tropospheric moisture was advected towards northern Germany and northern Poland. Due to the abundant moisture, high CAPE was forecast by NWP models across a large area, including eastern Germany, Czechia, Poland, Austria, northern Italy, Slovenia and Croatia. At the same time, strong vertical wind shear was forecast over the western parts of the high CAPE area, resulting in a situation with high potential for an outbreak of severe thunderstorms.

In the afternoon and evening, extremely severe storms formed over eastern Germany and western Poland, that produced giant hail with diameters of up to 12 cm and severe wind gusts (Fig. 4.23). By 12 UTC, severe storms also formed over Slovenia and started moving south towards Croatia, producing giant hail up to 11 cm in diameter on the border between the countries. The severity of storms over this region exceeded expectations as models showed only modest vertical wind shear, which was thought to preclude supercellular convection. At the same time, severe storms were predicted over the western Czech Republic, but storms failed to initiate there due to the presence of a stable layer with high values of CIN. All three areas, Slovenia and Croatia, the western Czech Republic and eastern Germany to western Poland are discussed separately below in the context of the IASI data.

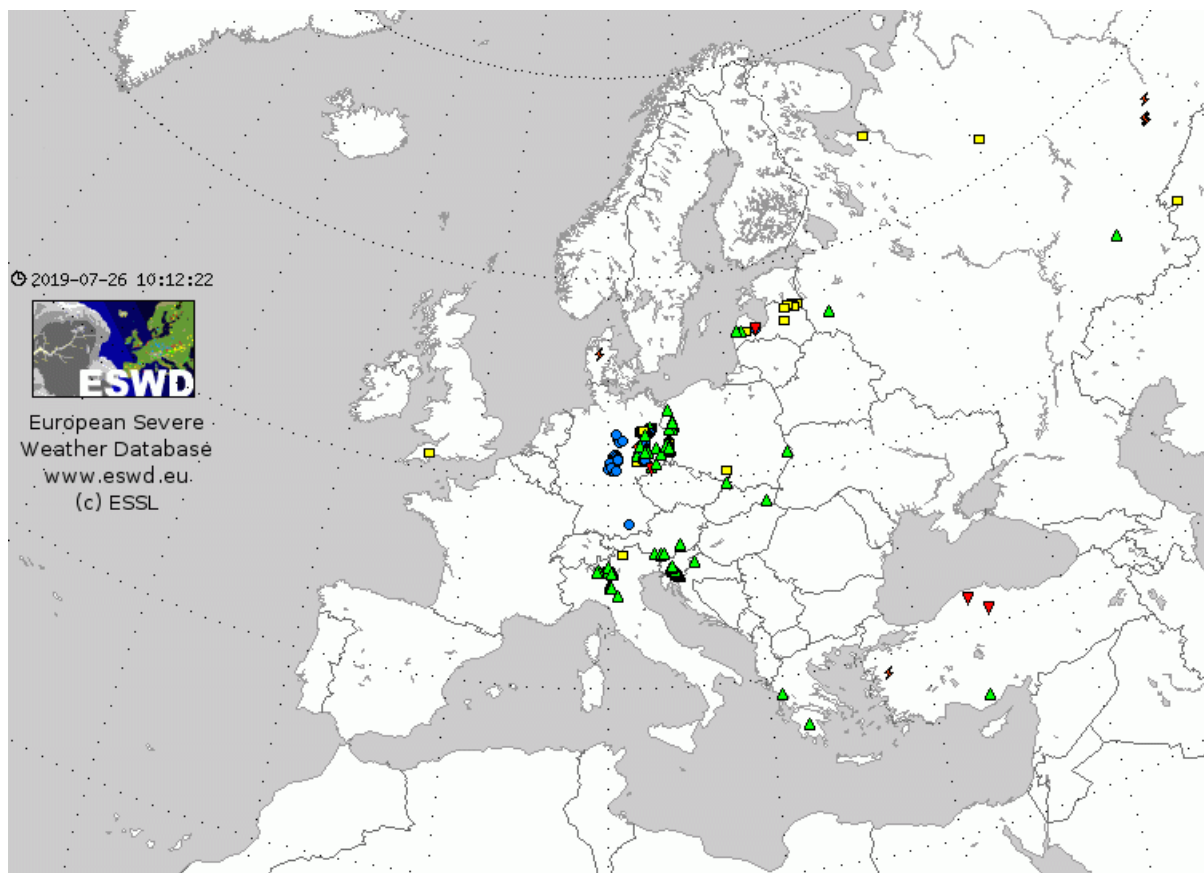


Fig. 4.23. As in Fig. 4.1, but for 11 June 2019 00–24 UTC.

Slovenia / Croatia

The ECMWF and ICON models initialized at 00 UTC predicted the surface dewpoint to reach 18 to 21 °C over the area by 9 UTC, whereas the temperature gradient between 800 to 600 mb was forecast to exceed on average 7 K/km. Due to the presence of abundant lower tropospheric moisture and steep mid-tropospheric lapse rates, numerical models forecasted high CAPE over southern Slovenia and north-eastern Croatia, ranging from 2500 to 4000 J/kg (Fig. 4.24). Such high CAPE is climatologically rare over central Europe.

IASI sampled the environment at around 10 UTC. The vertical temperature profile was similar to the modelled profile with a stable layer near 850 mb and a layer of steep mid-tropospheric lapse rates between 850 and 600 mb (Fig. 4.25). At the same time, there was a large difference between the model and the sounder regarding the lower tropospheric moisture. In a sample profile in Fig. 4.25, the sounder shows a dewpoint of 13 °C, with the error bars suggesting possible range of 11 to 15 °C, whereas model the dewpoint reached 18 °C. At 10 UTC, weather stations reported dewpoints of 18 to 21 °C over Slovenia and northern Croatia. Thus, model simulations were closer to the reality than the sounder. The vertical profile of dewpoint suggests that the sounder was not able to detect a 50 mb deep layer of high moisture close to the surface.

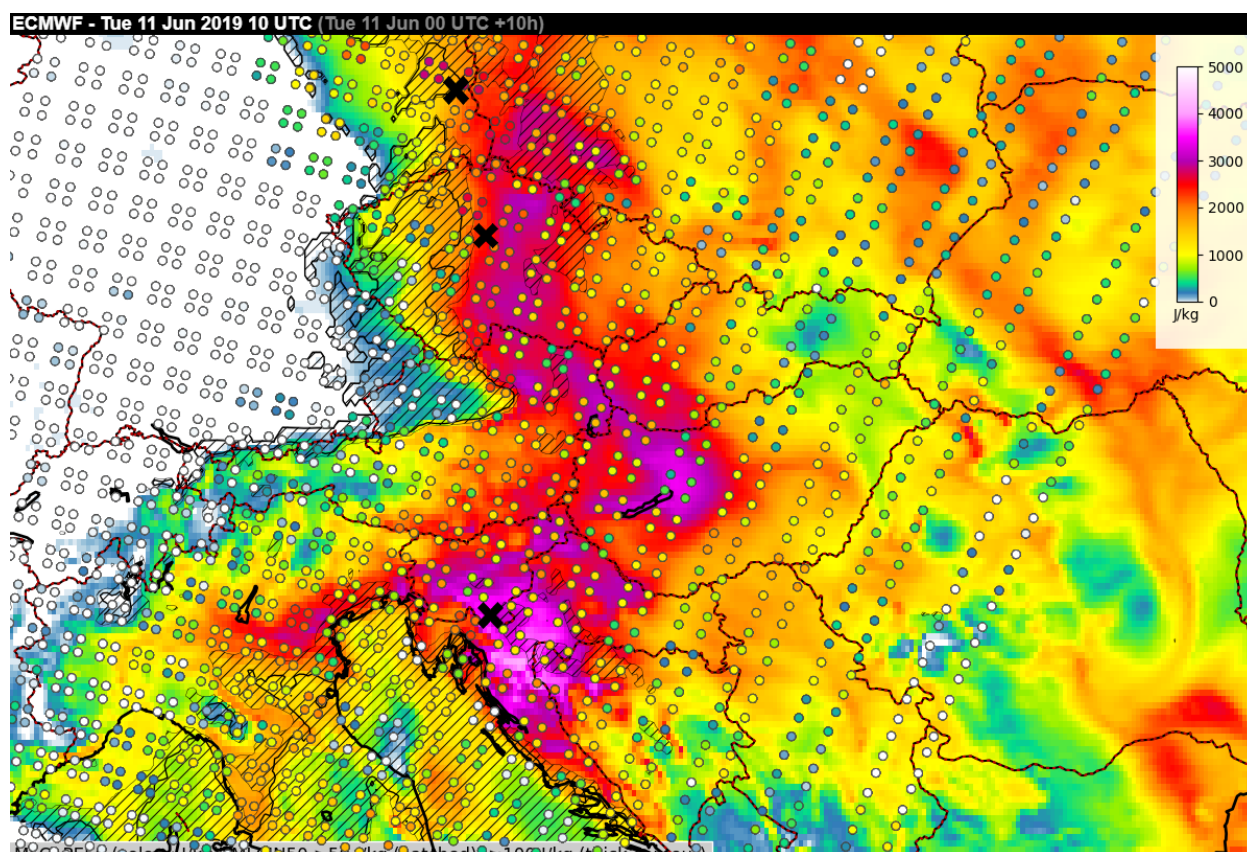


Fig. 4.24. As in Fig. 4.2, but for 11 June 2019 10 UTC. Vertical profiles, displayed below, are valid for the grid points marked by the black crosses.

Due to the differences in lower tropospheric moisture, there were large differences between the CAPE of the model and the IASI measurement. For the sample profile, the ECMWF model yielded 2915 J/kg of CAPE calculated using the mixed layer parcel of bottom 50 mb, while CAPE based on IASI was only 894 J/kg (Fig. 4.25). Large differences in model- and sounder-

based CAPE were present over much of the area of interest, including southern Slovenia and northern Croatia.

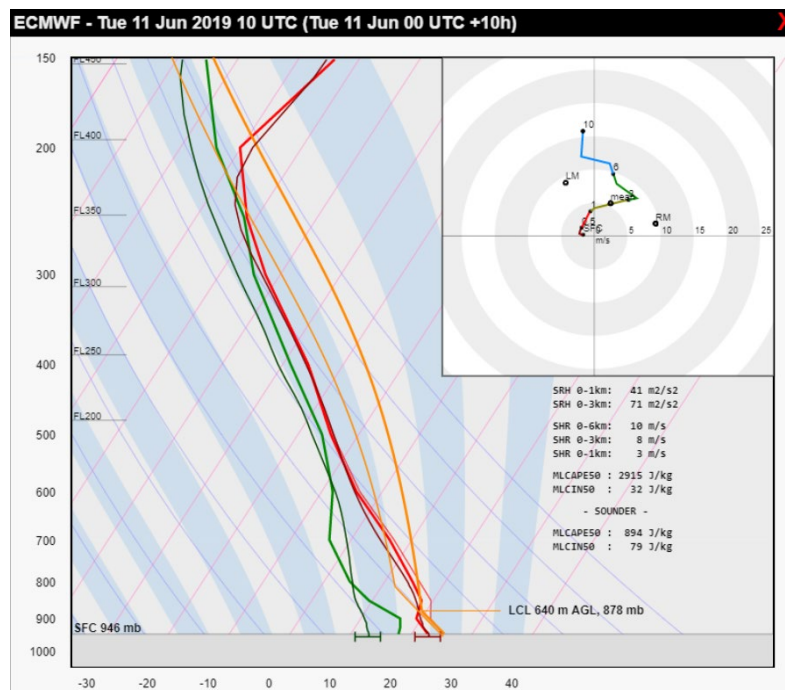


Fig. 4.25. As in Fig. 4.3 but for 11 June 2019 10 UTC over southern Slovenia, at the location indicated in Fig. 4.24.

Czech Republic

Over western parts of the Czech Republic, models also forecasted high values of CAPE, exceeding 2000 J/kg. Convective initiation was anticipated in the afternoon along the convergence zone. Due to the favourable overlap of high CAPE and moderate to strong vertical wind shear, thunderstorms were anticipated to become severe. However, except for the border mountain chain of Erzgebirge between Czechia and Germany, no storms formed over this area. Two possible reasons for the initiation failure are the stable layer at around 850 mb, contributing to high values of CIN, and the dry layer with low relative humidity above 800 mb, which increased the rate of dry air entrainment into the rising parcels.

The radiosounding from Prague taken at 12 UTC showed evidence for both (Fig. 4.26). The model-based profile from the same location also displayed the stable layer and dry air, but the CIN is lower than in the radiosounding (45 vs 117 J/kg). The IASI-based profile has a CIN of 57 J/kg, slightly higher than in the model, but does not clearly show the stable layer. The vertical profile of dewpoint misses the pronounced transition from abundant boundary-layer based moisture in the boundary layer to the dry layer just above it. Unlike over Slovenia, CAPE was quite similar between the sounder and the model, as the surface dewpoint in the sounder was lower by only 1 °C. Both the sounder and the model were close to the dewpoint observations (17 to 18 °C) of weather stations in Prague.

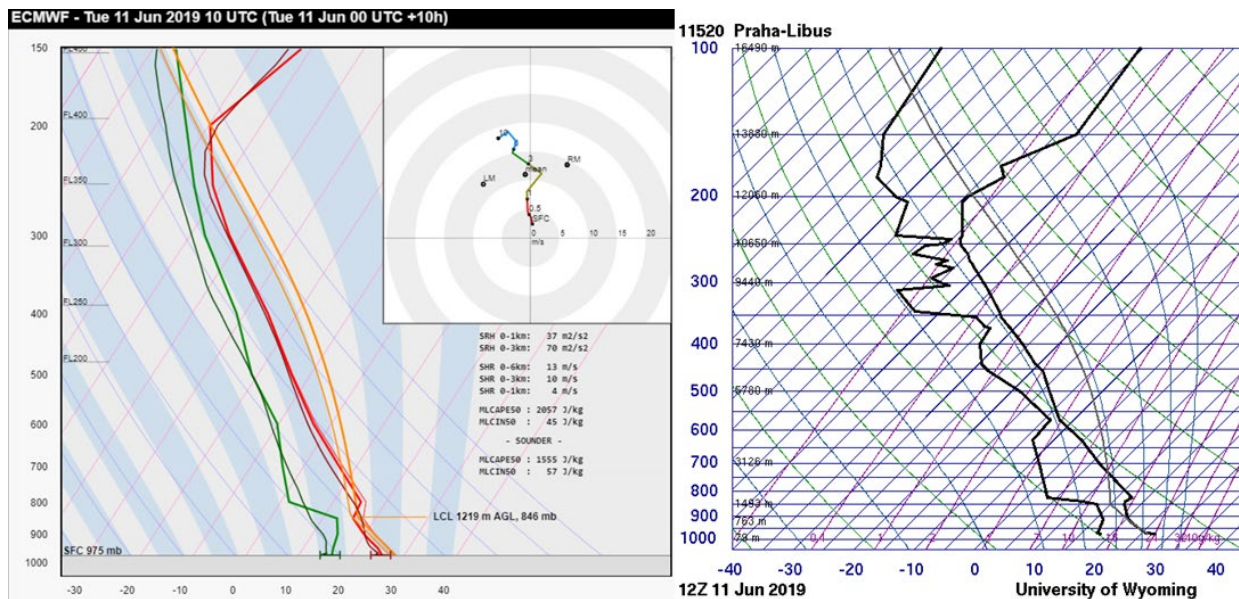


Fig. 4.26. As in Fig. 4.3, but for 11 June 2019 for Prague, Czech Republic (location indicated in Fig. 4.24). Left: Modelled and IASI-based profile at 10 UTC. Right: An observed profile of temperature and dewpoint based on radiosounding measurement from Prague at 12 UTC. Data source: University of Wyoming.

Eastern Germany

Two overpasses were available for the border area between eastern Germany and western Poland, where extremely severe storms developed in the afternoon and evening. Interestingly, the two overpasses yielded different information.

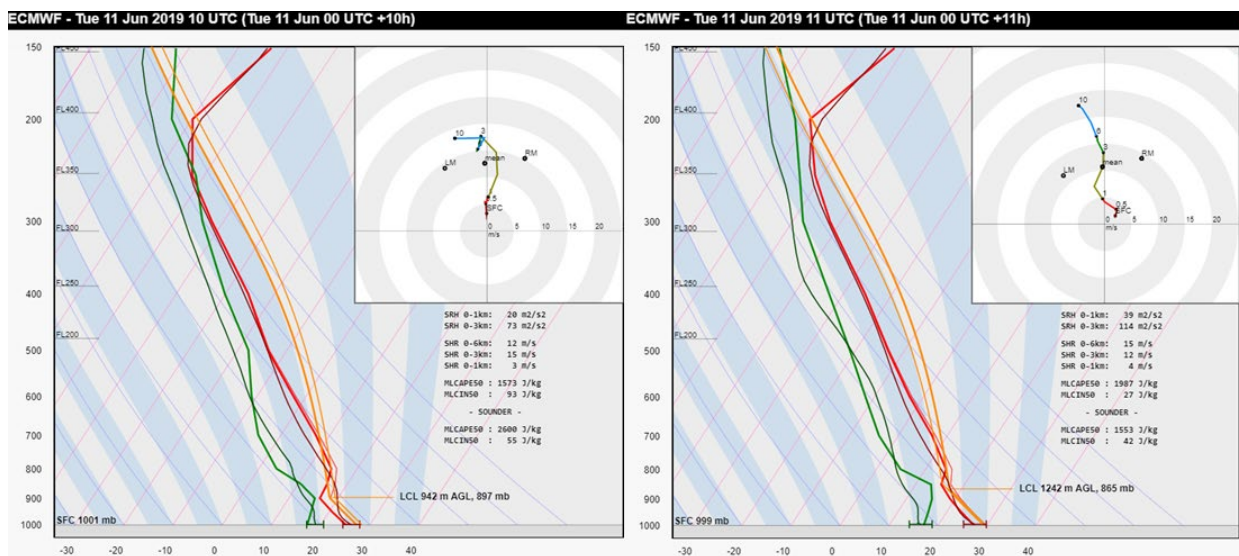


Fig. 4.27. Same as in Fig. 4.3, but for 11 June 2019, eastern Germany, for left/ 10 UTC IASI-based profile and 09 UTC ECMWF data and right/ 11 UTC IASI-based profile and 12 UTC ECMWF data.

For the first overpass at 10 UTC, the sounder data suggest that higher CAPE is present in the environment than simulated by model (Fig. 4.24). The difference in CAPE can be explained by the difference in the lower tropospheric moisture. The surface dewpoint was 2 °C higher in the IASI-based profile than in the model (Fig. 4.27). In this case, IASI was closer to reality as weather stations reported dewpoint readings of around 19 °C. The vertical profile acquired for the same

location from 11 UTC overpass, however, shows less lower-tropospheric moisture than from 10 UTC and also comparatively lower CAPE (Fig. 4.28). In the meantime, moisture was forecast to increase by the ECMWF model between 9 and 12 UTC. Dewpoint values as observed by the weather stations did not change between 10 and 11 UTC. Thus, the 10 UTC overpass likely represented the pre-storm environment better than that at 11 UTC. This may be because eastern Germany is on the edge of the 11 UTC overpass, yielding data of lower vertical resolution compared to the 10 UTC overpass. While large differences exist between the 10 and 11 UTC overpasses regarding the moisture content, the temperature profiles are similar.

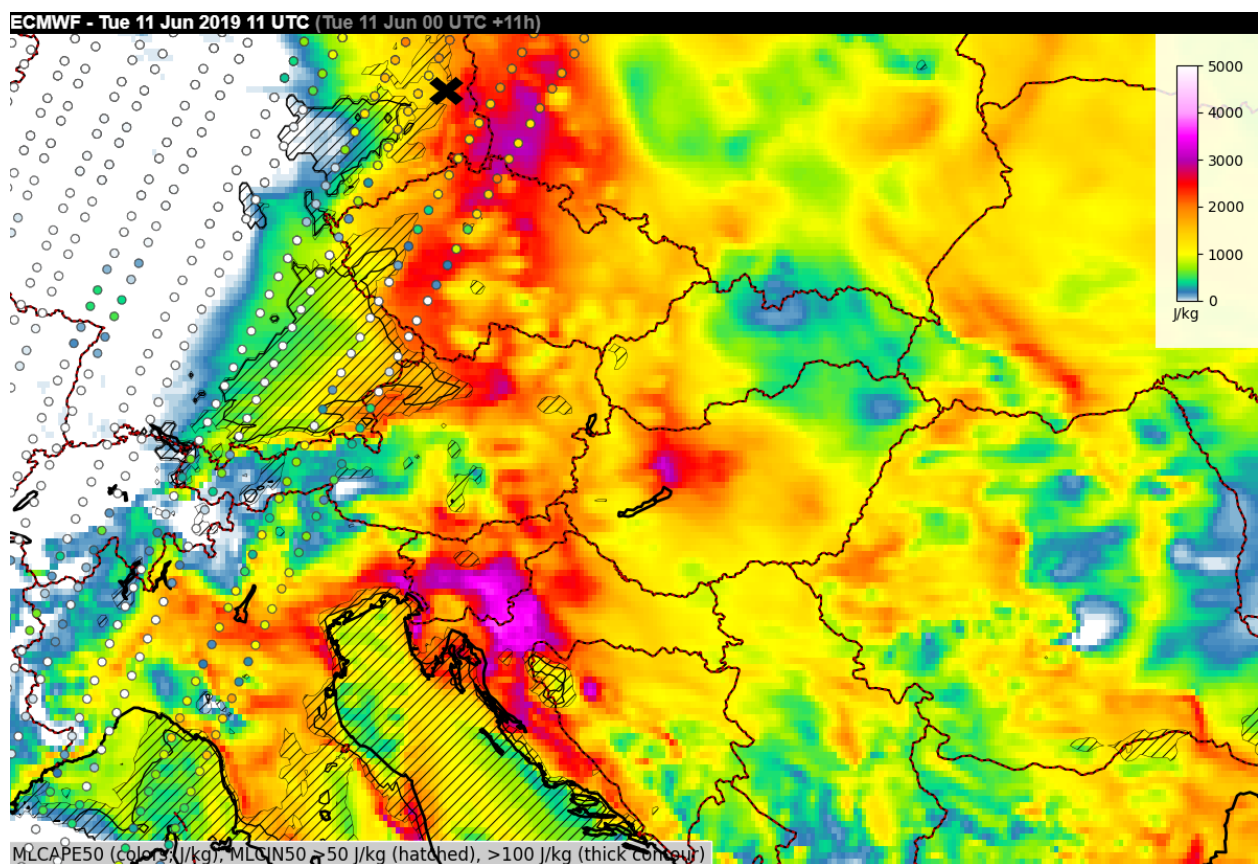


Fig. 4.28. Same as in Fig. 4.2 but for 11 June 2019 11 UTC.

Summary

On 11 June 2019, numerous severe thunderstorms formed over parts of central Europe with very large hail being the dominant threat. Sounder data were available for this region from 10 and 11 UTC overpasses. The largest discrepancies among the model, sounder and in-situ observations were noted for the moisture content in the lower troposphere. In some locations, the moisture was lower than the model simulation and in others it was higher. Shallow layers of abrupt changes in vertical temperature stratification were not well covered by the sounder, but, other than that, temperature profiles matched the modelled and observed ones well. Perhaps areas on the edge of the overpass domain are more prone to moisture errors than the areas in the centre of the overpass.

4.9 10 July 2019: Extremely severe storms over central Italy and northern Greece

This was the last of a multi-day outbreak of severe storms over parts of Italy and the Balkans. A short-wave trough in mid- to upper-troposphere was forecast to cross from the Balearic Sea towards Italy and Greece in the afternoon and evening. At the same time, a cold front was simulated across Italy and was forecast to move south-eastward during the day. South of the front, NWP models simulated abundant lower tropospheric moisture and steep mid-tropospheric lapse rates. In combination with strong mid-tropospheric flow, this resulted in an extremely favourable environment for severe convective storms, with CAPE exceeding 2000 J/kg and 0–6 km bulk wind shear values of 25 to 40 m/s. A major severe weather outbreak was anticipated during this day.

Severe thunderstorms already formed over Italy during the morning with two tornado and several severe wind gusts reports. By 10 UTC, another storm initiated near the eastern Italian coastline and quickly became severe. 15 minutes later, giant hail, up to 14 cm in diameter, was observed over Pescara. The hail, combined with severe wind gusts, injured 20 people. The relatively early timing of the storm provides us with an opportunity to look at the overpass data that were taken less than one hour before the major hailstorm and thus should be representative of the pre-convective environment.

More hail and severe wind gusts were reported later in the day across Italy. Some of the storms crossed the Adriatic Sea and affected Greece and Albania, also with damaging wind gusts and large hail (Fig. 4.29). One of the storms, having already travelled hundreds of kilometres, rapidly strengthened as it crossed the Aegean Sea and hit Chalcidice peninsula, where 6 people died and more than 120 were injured due to the severe wind gusts around 19 UTC. IASI-based profiles were available after 20 UTC, when the storm was already slowly weakening.

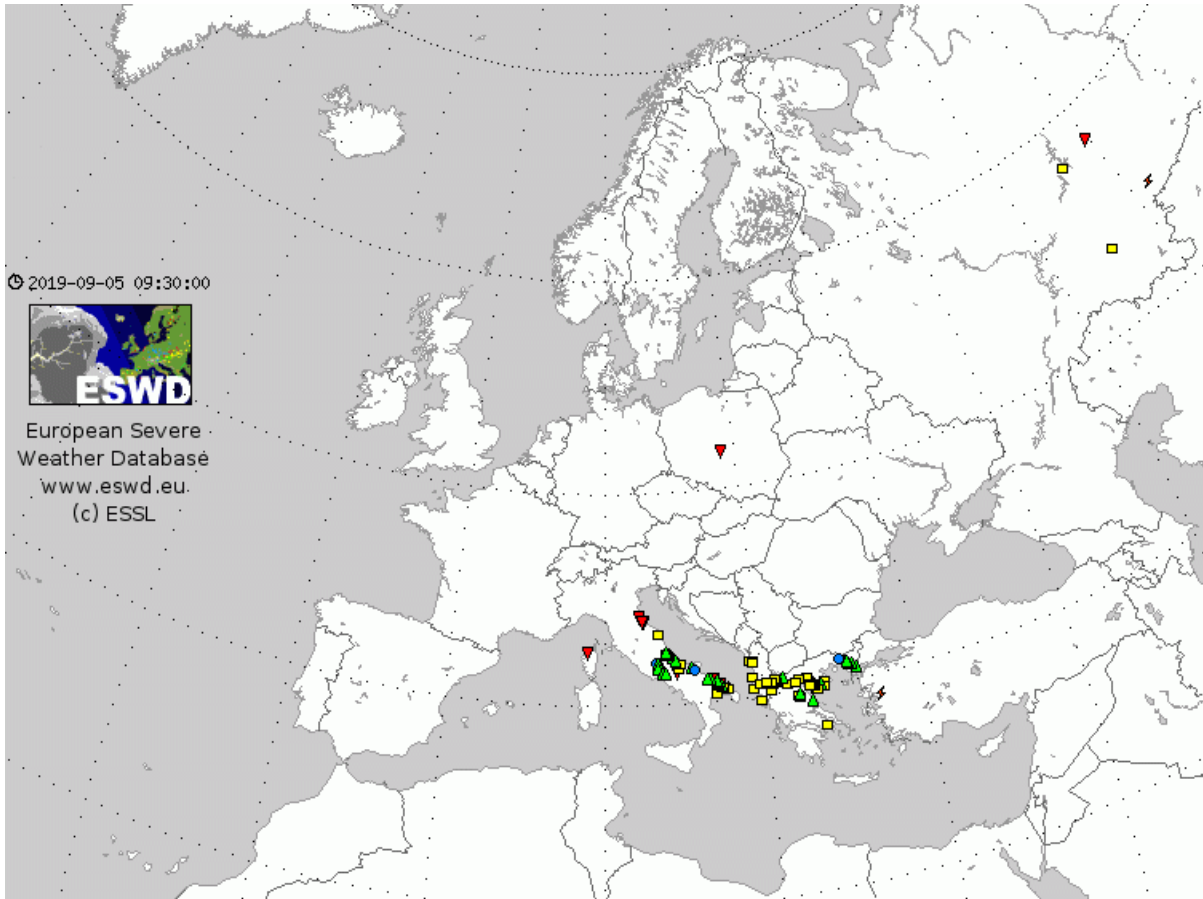


Fig. 4.29. Same as in Fig. 4.1 but for period of 10–11 July 2019 00 UTC.

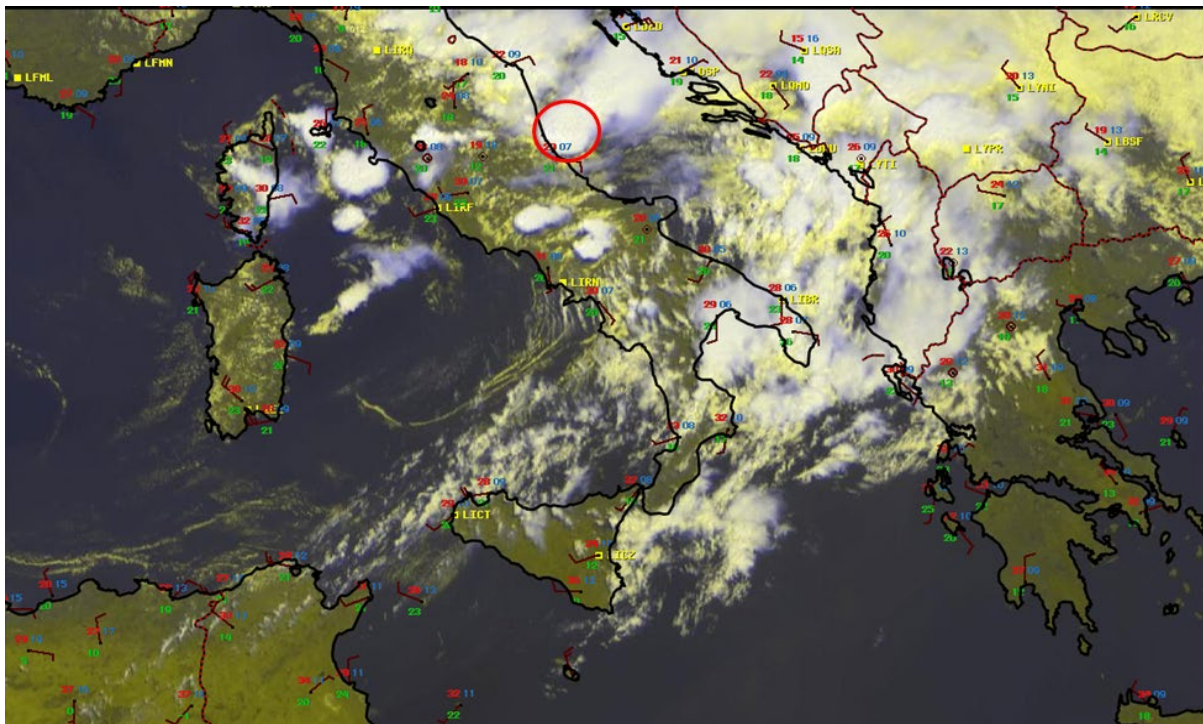


Fig. 4.30. Visible, infrared enhanced satellite imagery valid for 7 July 2019 09:55 UTC with surface stations data plotted (red numbers represent temperature, green numbers dew point temperature). Red circle indicates the location of the hailstorm.

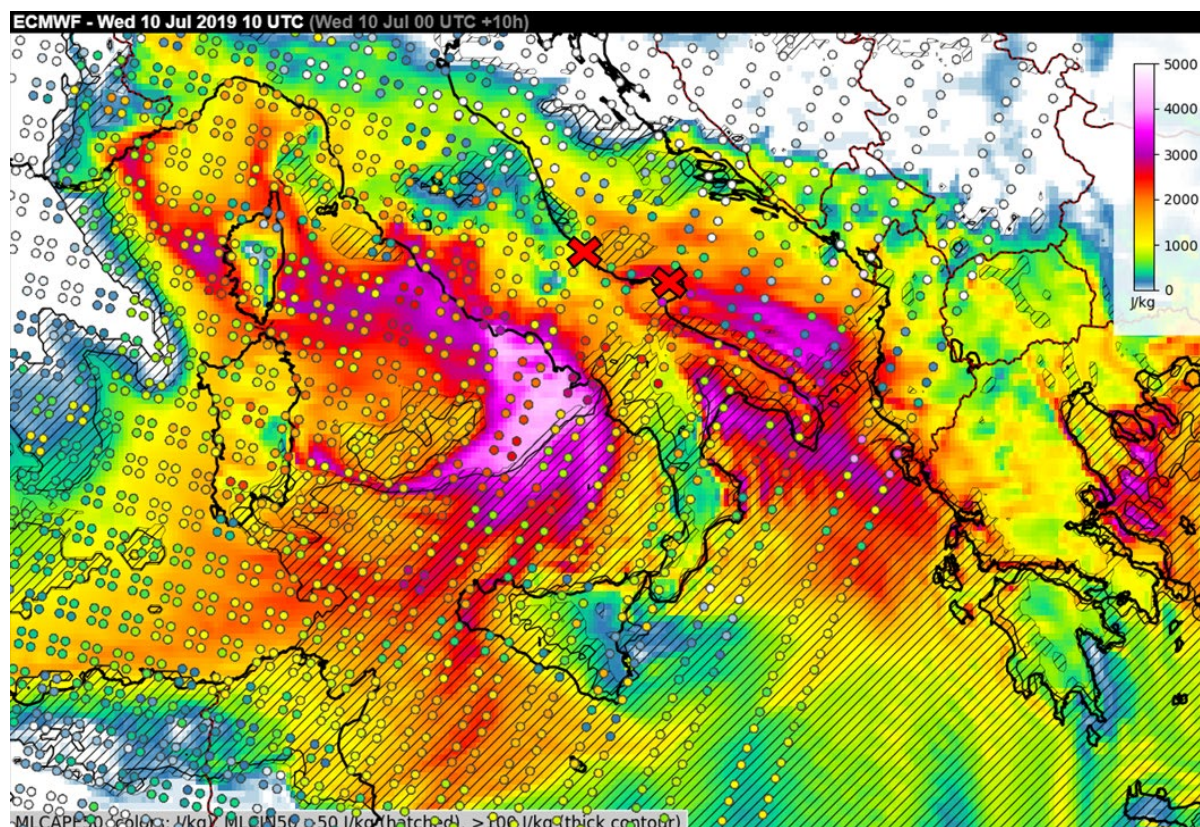


Fig. 4.31. As in Fig. 4.2., but for 10 July 2019 00 UTC ECMWF simulation of 10 UTC 50 mb mixed layer CAPE (filled contours) and the IASI-based MLCAPE (circles). Red crosses correspond to the locations of profiles displayed below.

Morning storms over Italy

Between 9:45 and 10:00 UTC, a large convective storm had developed along the eastern coastline of Italy (Fig. 4.30). The storm propagated south along the coastline with a swath of large hail and severe wind gusts. Because the storm reached extremely severe intensity soon after its formation, the conditions must have been favourable for severe weather in the zone of initiation.

The NWP model predicted CAPE between 1000 and 2000 J/kg over this area (Fig. 4.31). Sounder data from the 10 UTC overpass yielded lower CAPE near the area of initiation, but also show strongly increasing CAPE towards south. Over the Gargano Peninsula (the eastern cross), CAPE was already higher in the sounder data than in the model. Inspecting vertical profiles over both the point of storm initiation and also over the peninsula (Fig. 4.32) shows that for both profiles, the sounder detected a higher surface temperature than was simulated by the model. For example, at the location of initiation, the model simulates 21 °C, near the surface, compared to 24 °C in the sounder and 29 °C being observed in reality! Similar temperature differences can be seen over Gargano peninsula. Thus, the IASI data provided useful information that the lower troposphere was warmer than anticipated by the models.

At the same time, lower tropospheric moisture was locally underestimated by the sounder. Station measurements show dewpoint values of 20–21 °C along the whole eastern Italian coastline, while the sounder only detected around 16 °C in the area of storm initiation. Over the Gargano peninsula, the sounder-derived dewpoint matches both the model and observations. If we used the temperature profile of the sounder data and combine it with

humidity derived from the model with the real dewpoint measurement, we would attain CAPE of over 2000 J/kg.

Further south, storms did not develop until early afternoon because of a stable layer near 850 mb, which resulted in high values of CIN. This layer is reflected in the sounding data from Brindisi (Fig. 4.33 right). The IASI data represent the environment 2 hours before the actual sounding, not allowing for an exact comparison. Nevertheless, IASI data show the presence of this stable layer, not as significant as in the Brindisi sounding. IASI data were closer to reality than the model regarding the lower tropospheric moisture but did not capture the dry layer near 800 mb. Due to mid-level cloudiness over the area, there was a large uncertainty regarding the conditions underneath, as suggested by the error bars. This could have contributed to the underestimation of the dry and stable layer near 800 mb.

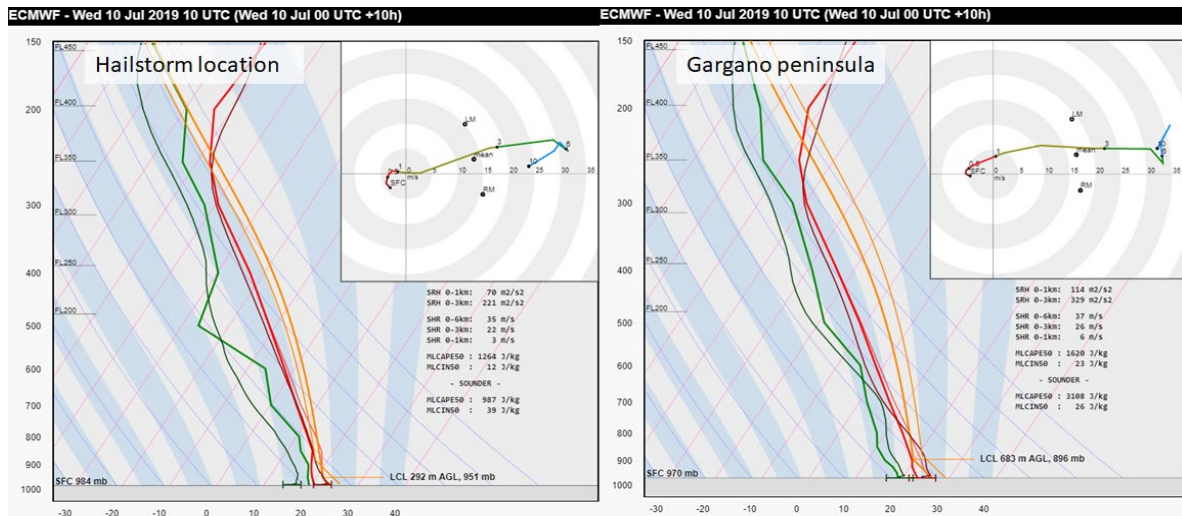


Fig. 4.32. Same as in Fig. 4.3, but for eastern Italy on 10 July 2019 10 UTC at the hailstorm location (left) and Gargano peninsula (right) indicated in the Fig. 4.31.

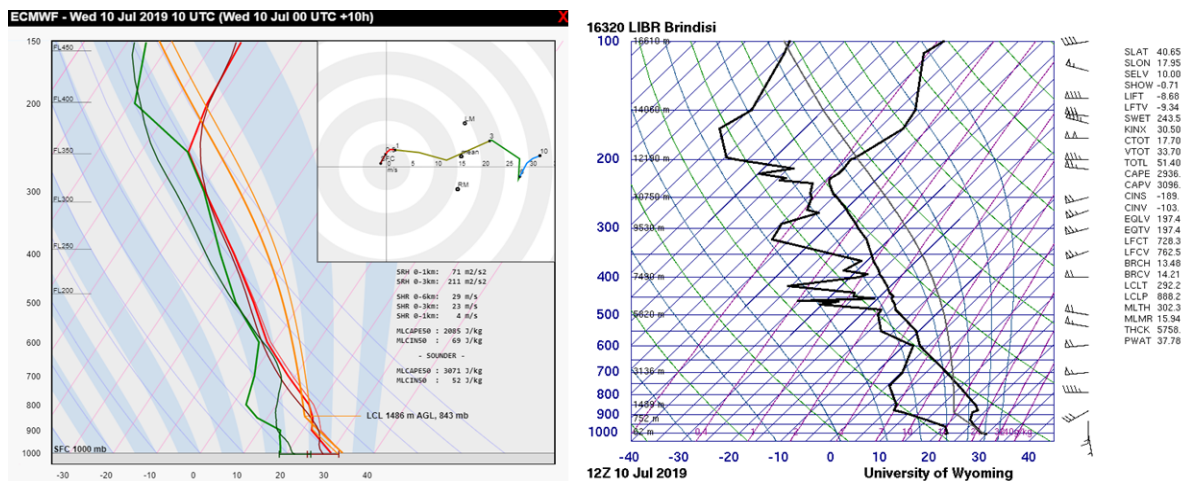


Fig. 4.33. As in Fig. 4.3, but for 10 July 2019 for Brindisi, Italy Left/ Modelled and IASI-based profile at 10 UTC. Right/ An observed profile of temperature and dewpoint based on radiosounding measurement from Prague at 12 UTC. Data source: University of Wyoming.

Evening storms over Greece and the Aegean Sea

4.10 An evening overpass sampled the environment just after the intense phase of the Chalkidiki

storm (Fig. 4.34), which brought damaging wind gusts and large hail to the area. Thus, we are not able to relate the most intense phase of the storm to the environmental conditions sampled by IASI. Instead, we look at the data from the perspective of subsequent development. At the peak of its intensity, the storm was propagating strongly to the south, but this propagation ceased after 19:30 UTC and storm travelled towards Turkey. While several other storms initiated over the northern Aegean Sea, none of them attained the intensity of the Chalkidiki storm and decayed quickly after moving further south. The reason for the rapid decay may have been a layer of dry air with stable temperature stratification near 900 mb. The layer was well sampled by the IASI and almost perfectly matches the model simulation (Fig. 4.34).

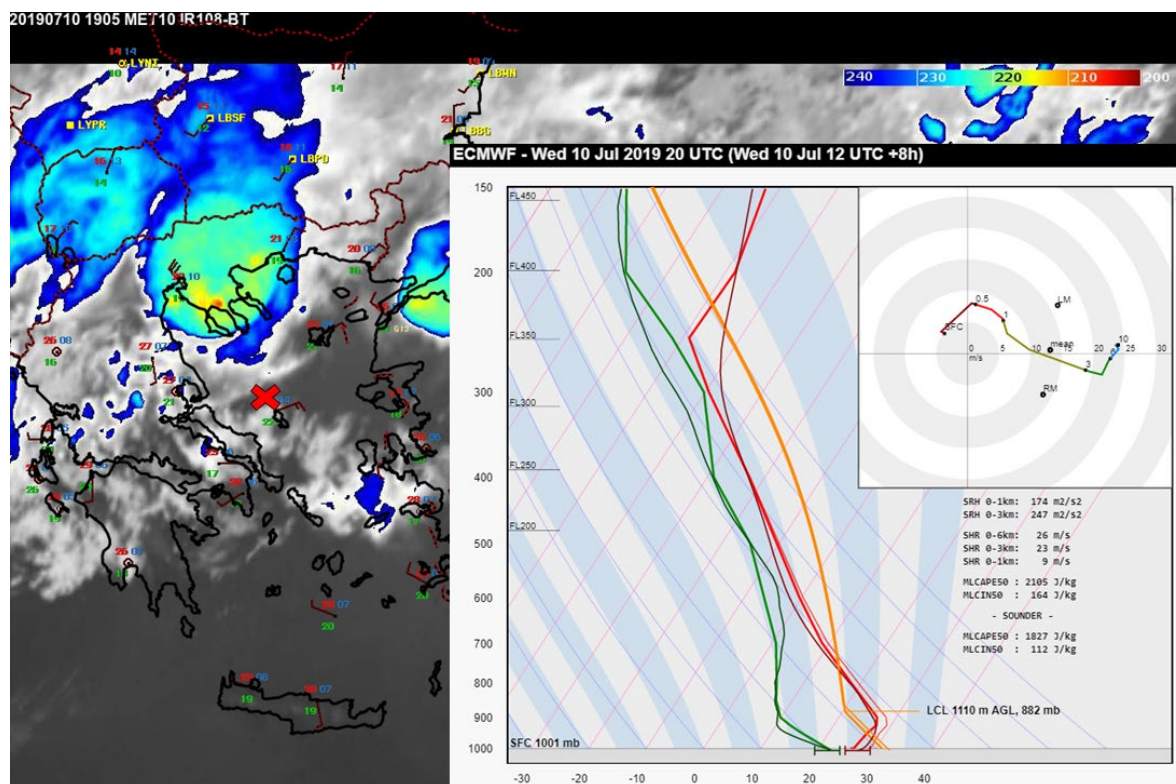


Fig. 4.34. An infrared brightness temperature enhanced satellite imagery valid for 19:05 UTC and a vertical profile, as in Fig. 4.3, valid for 20 UTC for the location indicated by the red cross.

Summary

On this day, numerous extremely severe storms with large societal impact were observed over Italy and Greece. IASI sampled the morning environment, in which a storm producing large hail formed over the eastern coastline of Italy. The evening overpass sampled an environment, in which storms were decaying over the northern Aegean Sea. For the morning storms, the sounder data provided additional information to the model, especially regarding the low-level temperature. Forecasters could be alerted to the fact that the surface is warmer than predicted

by the model and thus also more unstable. The low-level humidity information was not very helpful as it was underestimated.

There was a difference between how well the sounder could reproduce layers with significant changes in stability and humidity. While the sounder did not detect the presence of a significant stable layer over southern Italy in the morning overpass, the evening overpass yielded accurate information that such layer existed over the Aegean Sea. The difference may have been caused by the presence of significant cloudiness in the morning overpass over Italy, as suggested by the larger error bars compared to the Aegean Sea evening overpass.

4.11 9 August 2019: Severe wind and tornadoes across France, the Benelux and Germany

Between a deep cyclone over the Atlantic and a ridge over central Europe, a strong south-westerly flow with 500 mb wind speed up to 40 m/s, overspread France, the Benelux and western Germany. At the same time, a cold front was forecast to cross the area with 850 mb winds reaching 15–20 m/s ahead of the front. The strong flow created strong vertical wind shear both in the lower and mid-troposphere, overlapping with CAPE ranging from 200 to 1500 J/kg. While the highest CAPE was simulated over southern France, the strongest lower tropospheric shear was forecast over northern France and the Benelux.

During the day, numerous severe storms formed in a belt from southern France to northern Netherlands (Fig. 4.35). Severe weather began after 14 UTC with severe wind gusts and large hail over northern France. The most severe weather occurred between 15 and 17 UTC with isolated supercells producing swaths of wind damage, including an F2 tornado that crossed from France to Luxembourg and caused 19 injuries in the town of Pétange. Over eastern France, storms also caused considerable damage due to the severe wind gusts, with wind gust measurements of 35.8 and 42.7 m/s. Further severe storms occurred later in the day. Two tornadoes were reported in the Netherlands between 19 and 20 UTC, one of them causing some light damage in the centre of Amsterdam. Numerous severe wind gust reports also arrived from France after 17 UTC as a line of storms initiated along the advancing cold front.

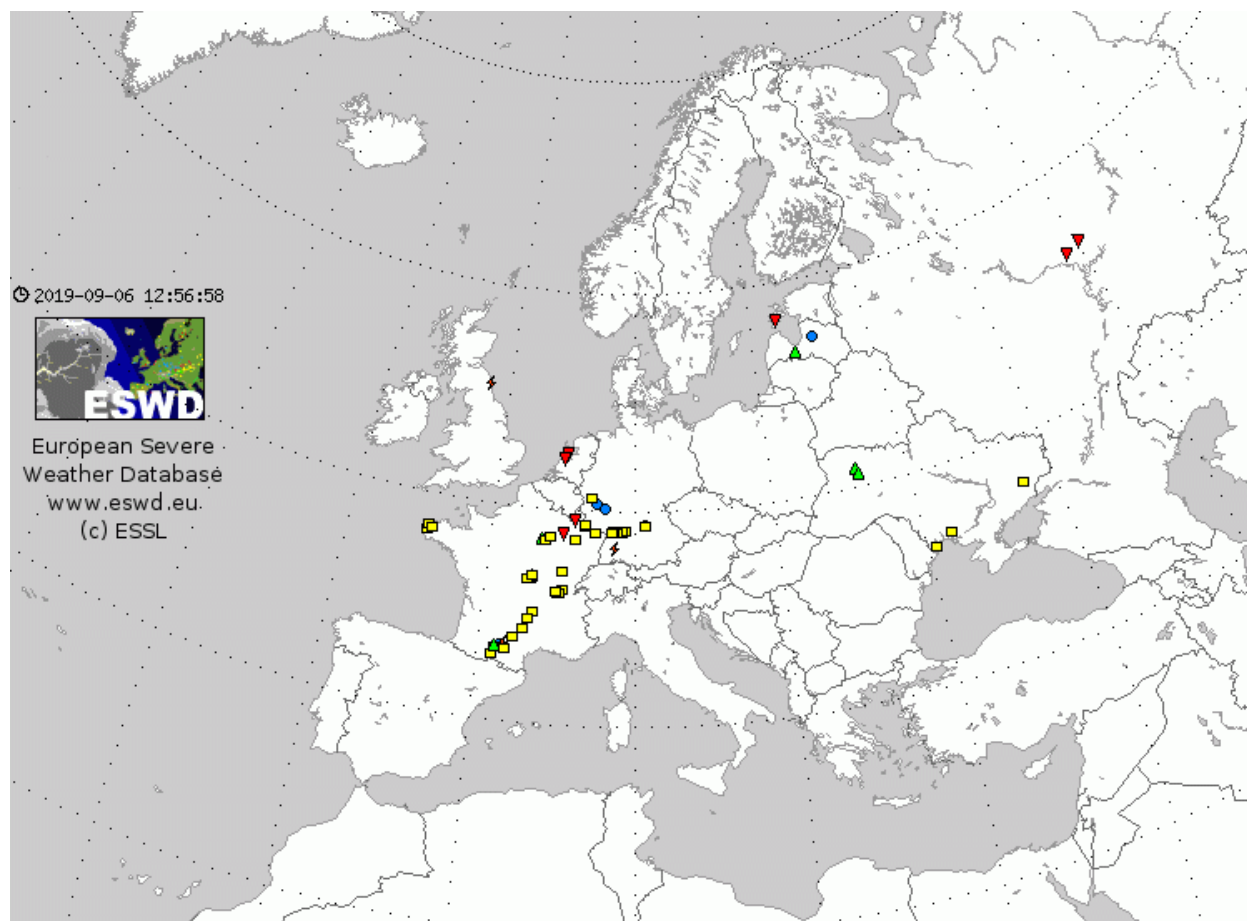


Fig. 4.35. Same as in Fig. 4.1. but for the period of 8 August 2019 00–24 UTC.

Morning overpass

While the 10 UTC overpass sampled the environment more than 4 hours before the first reports of severe weather, i.e. not very representative of the conditions just preceding convective initiation, there were still some interesting discrepancies between sounder and model data at this time. The sounder indicated higher CAPE than simulated by the NWP models over Belgium and northern France and lower CAPE over parts of southern France (Fig. 4.36). Vertical profiles of temperature and dewpoint show that the CAPE discrepancy is caused by the differences in lower tropospheric moisture (Fig. 4.37). Over northern France, the model simulated dewpoint values around 15 °C, while the IASI data showed 19–20 °C, which is close to the surface observations at 10 UTC with dewpoints of 18–20 °C in the area. Large CAPE differences can be seen over Belgium, where the sounder overestimates moisture, with surface observations (17–18 °C) in between of the model (15 °C) and the sounder (19–20 °C).

CAPE was likely underestimated by the sounder data over southern France, where the model was closer to reality regarding the moisture, with dew point temperature values around 20 °C. The vertical profile reveals that the high dewpoint values were confined to a shallow layer near the surface that was probably too shallow to be sampled by the sounder (Fig. 4.37). At the same time, a shallow stable layer near 500 mb was not captured by the IASI data. However, due to the lack of sounding data over the area it is not possible to verify whether this layer, as simulated by model, was also really present in the actual atmosphere.

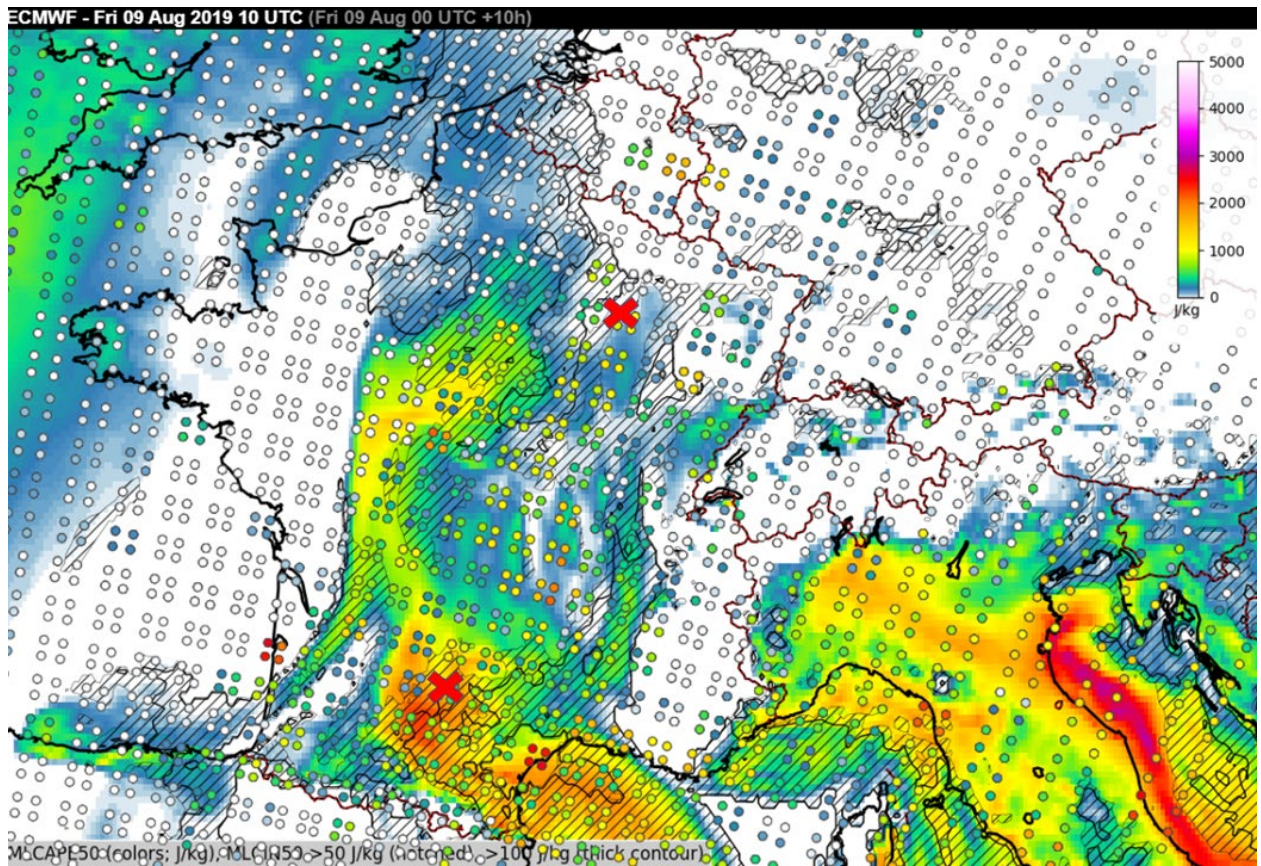


Fig. 4.36. As in Fig. 4.2, but for 9 August 2019 10 UTC. Vertical profiles, displayed below, are representative of the grid points marked by the red crosses.



Fig. 4.37. Same as in Fig. 4.X, but for France on 9 August 2019 10 UTC for northern (left) and southern France (right), precise locations indicated above in the Fig. 4.36.

Evening overpass

By 21 UTC, severe storm activity had already ceased over northern France and the Benelux, but an isolated severe storm had just formed near Toulouse, France (Fig. 4.38). The storm produced severe wind gusts, large hail and flash flooding shortly after 21 UTC and thus the 21 UTC overpass can be considered as a good proximity measurement for the conditions in which storm became severe. Compared to the model output, IASI data showed warmer conditions in the lower troposphere compared to the model. The weather station in Toulouse measured a temperature of 26 °C at 20 and 24 °C at 21 UTC (the 21 UTC measurement likely affected by approaching storm), more than the model simulation of 22 °C (Fig. 4.38). Overpass data suggested a surface temperature of 27 °C, higher than the reality. The likely reason for the discrepancy is an earlier passage of the cold front through the area in the model forecast compared to reality.

Both the model and sounder slightly underestimated the moisture (showing a 19 °C dewpoint) near the surface when actual dewpoint measurements were around 21 °C. If we adjust the sounder-derived vertical profile of temperature and humidity using the surface dewpoint station measurements, we would end up with more than 2000 J/kg of CAPE, which is more than shown by both the model (4 J/kg) and sounder (1200 J/kg) alone. Nevertheless, the sounder confirmed that there is more CAPE present in the environment than simulated by the model, which explains the rapid development of severe storms in the studied area.

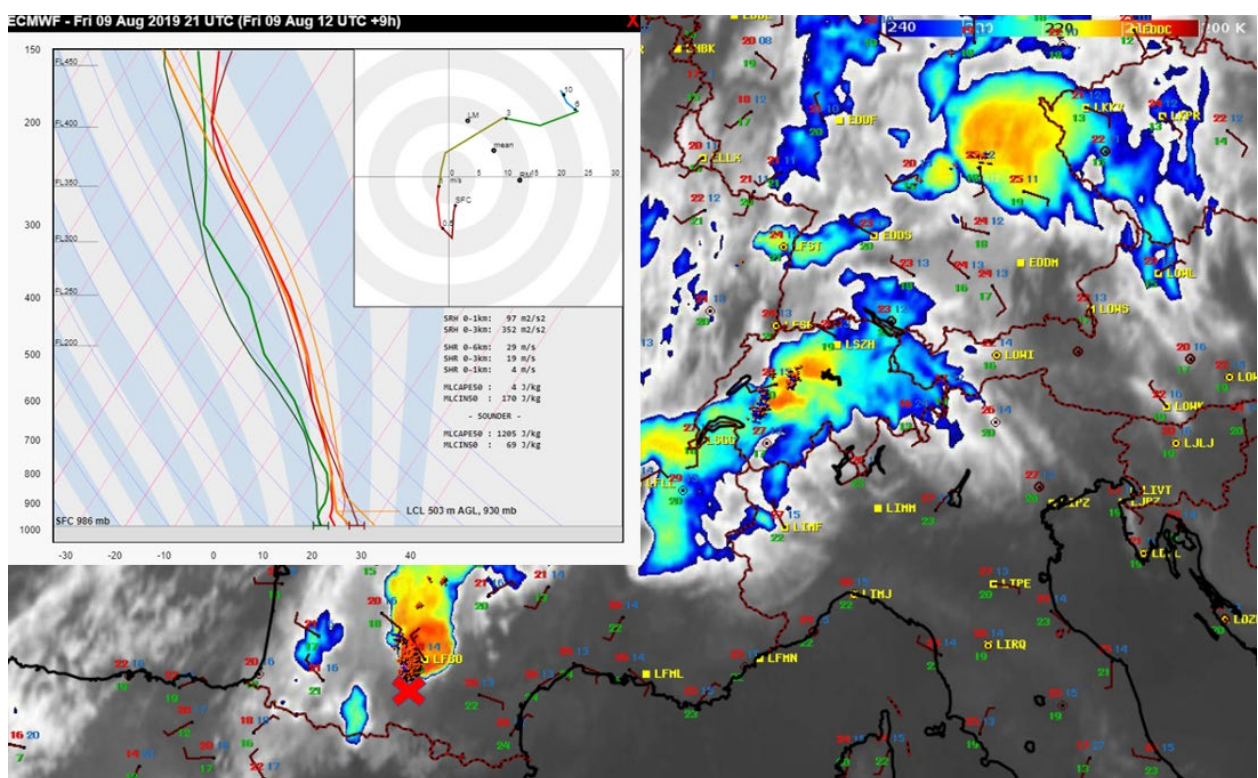


Fig. 4.38. An infrared brightness temperature enhanced satellite imagery valid for 9 August 2019 21 UTC, overlaid with surface station data (red and green values correspond to temperature and dewpoint values) and the EUCLID lightning detection network data (red and blue crosses). Vertical profile, displayed on the upper left, is valid for the location indicated by the red cross.

Summary

IASI sampled the late morning environment several hours before the occurrence of the first severe storms. The collected data could have been useful for the forecaster, revealing higher moisture over northern France than forecast in the models. Subsequently, the evening overpass sampled a warmer lower troposphere than expected in the Toulouse area, which helped to maintain higher CAPE than forecast by the model. While the sounder often underestimates moisture in the lower troposphere (such as over southern France both in the morning and evening overpasses), a signal in which the sounder has more moisture than simulated in the model may be an important hint to the forecaster.**

4.12 11–12 September 2019: Heavy rainfall over Spain in weak CAPE environment

A deep low-pressure area in the mid- to upper troposphere moved from the Balearic Sea towards north-western Algeria and Morocco. In the easterly flow north of the low, a tongue of moist airmass, characterized by mixing ratio above 14 g/kg, was advected towards the coastline of south-eastern Spain. With strong onshore flow bringing moisture rapidly inland, numerical models simulated high rainfall sums over south-eastern Spain and the situation resulted in widespread flash flooding over Valencia (Fig. 4.39). The most severe weather was anticipated in the afternoon of 12 September 2019, when models predicted the highest CAPE.

However, most severe flash flooding already occurred overnight between 11 and 12 September and during the morning of 12 September. The first storms already formed in the area before midnight. Between 00 and 03 UTC a narrow, quasi-stationary convective line formed over Valencia (Fig. 4.40). While the convection was rather shallow and only weakly electrified, it produced very heavy rainfall. By 03 UTC on 12 September, 359 mm of rain fell in Banniarés with a maximum 6 hourly sum of 191 mm. Station Ontinyent reported 296 mm of rain by 05 UTC, with 242 mm falling since midnight. 5 people perished during the flash floods, which brought widespread disruption to the region and several settlements were completely flooded. Besides heavy rain, an F1 tornado was reported shortly after 00 UTC.

Precipitation sums for the period of 12 September 00–06 UTC were underestimated by numerical models, as the highest sums were forecast not to fall during the night between 11 and 12 September, but rather in the afternoon of 12 September and further south, in the environment of higher CAPE. Two overpasses were available during the period of interest, on the evening of 11 September and in the morning of 12 September.



Fig. 4.39. Same as in Fig. 4.1. but for period of 11 September 2019 18 UTC–12 September 2019 18 UTC.

Evening of 11 September

Two overpasses, at 21 and 22 UTC, covered south-eastern Spain. For 22 UTC data, however, the area is on the edge of the domain and data have lower resolution, which is reflected in the worse reflection of lower tropospheric moisture than during the 21 UTC overpass (not shown). Thus, it is better to use the 21 UTC overpass to describe the pre-convective environment. This overpass coincides with the time of the occurrence of the first storms over Valencia. The most intense rainfall occurred several hours later, between 00 and 03 UTC of the following day.

IASI sampled a tongue of moist air over the Balearic Sea with surface mixing ratios of 12–14 g/kg (Fig. 4.41). Immediately inland the sounder shows less moisture than the model. Differences between the model and sounder decrease when looking at the deeper layer of moisture, such as the lowest 100 mb layer. Surface stations along the coastline experienced an increase of moisture during the evening, as the dew point rose from 15 °C to 17 °C between 20 and 22 UTC. These values are between the IASI-derived values (12–14 °C) and the model simulation (18 °C).

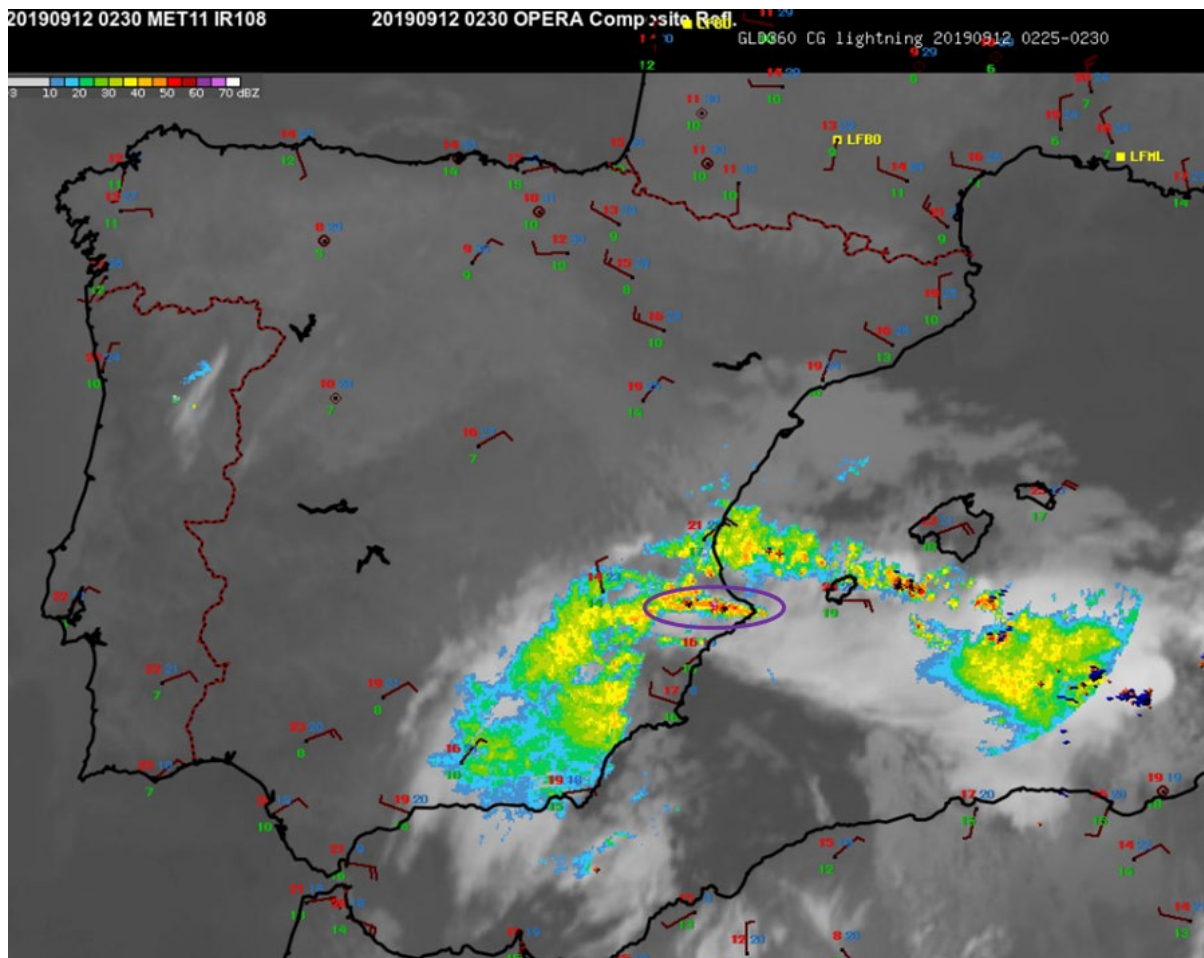


Fig. 4.40. 11 September 2019 02:30 UTC infrared satellite imagery, overlaid with OPERA radar data composite (colours), surface station data (red and green values correspond to temperature and dewpoint values) and the EUCLID lightning detection network data (red and blue crosses). Purple ellipse marks the location of the quasi-stationary convective system.

The IASI-derived vertical profile of dewpoint and temperature for a selected grid point shows less humidity compared to the model, both in terms of the absolute moisture content in the lower troposphere and relative humidity throughout the mid troposphere (Fig. 4.41). Low values of relative humidity (seen as a large spread between temperature and dewpoint at a given level) are surprising, given the fact that there were already storms ongoing at that time in the area and infrared satellite imagery showed overcast conditions. Due to the underestimation of the lower tropospheric moisture, the sounder-derived CAPE at the coastline was 0 J/kg, compared to the model which showed more than 600 J/kg of CAPE.

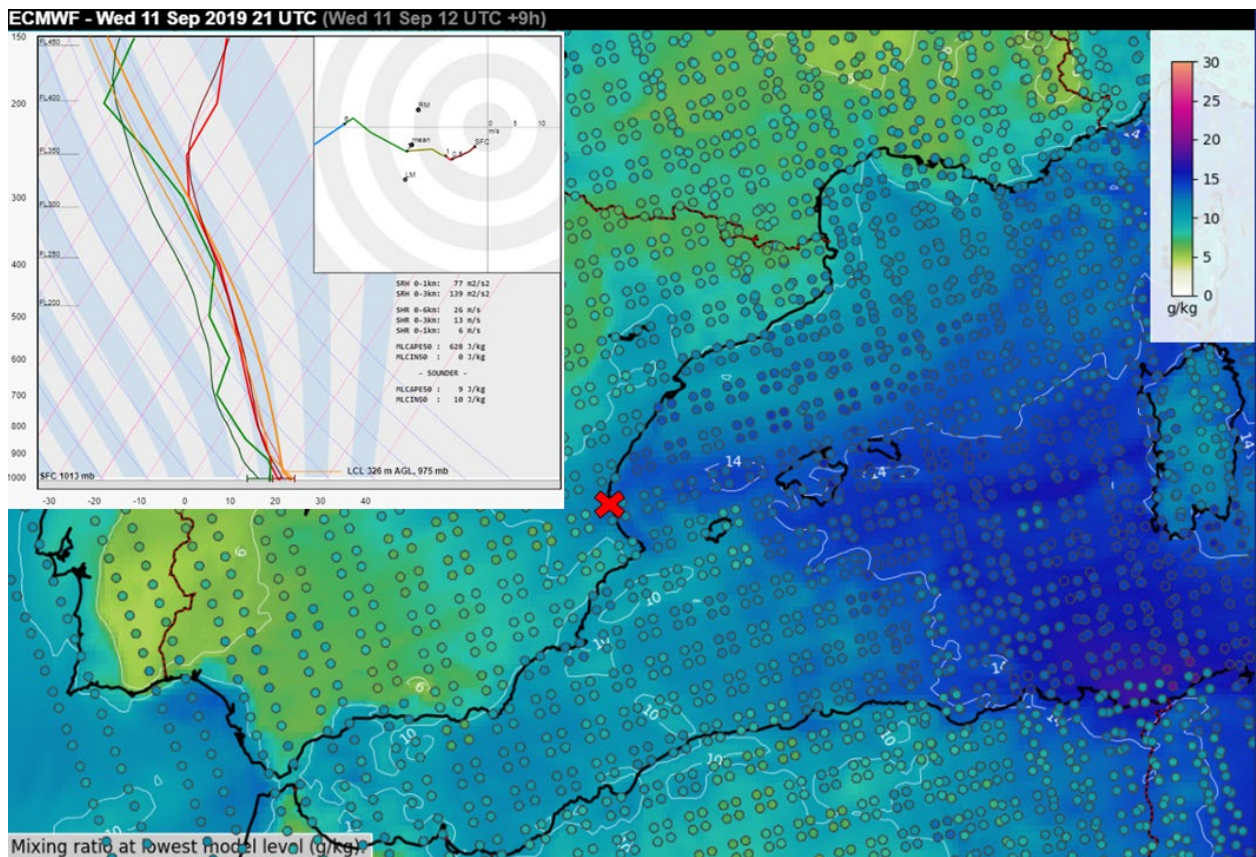


Fig. 4.41. As in Fig. 4.2, but for 11 September 2019 12 UTC ECMWF simulation of 21 UTC surface mixing ratio (filled contours) compared to the IASI-based MLCAPE (circles). Sounding is valid for the location marked by the red cross.

Morning of 12 September

The 10 UTC overpass data sampled the environment in which a convective line formed over the Balearic Sea and impacted south-eastern Spain during the late morning and afternoon. While these storms did not produce as much rainfall as the overnight storms, they were accompanied by more lightning. Model data showed higher CAPE along the coastline for this period, which explains the higher flash rates. However, vertical profiles based on IASI data from 10 UTC suggested that little to no CAPE was present inland and over the coastline (Fig. 4.42). This cannot be correct as there were storms ongoing at the time of the overpass and further storms formed in the subsequent hours. Similarly, to the other cases discussed, the sounder also underestimated the moisture in the lower troposphere. Weather stations near the coast measured dewpoint temperatures of 17 to 19 °C, which is more than the 12–15 °C measured by the sounder. The differences between the model and IASI were lower towards the east, i.e. over the Mediterranean Sea, where high CAPE over 2000 J/kg was simulated.

IASI also sampled an environment modified by the ongoing storm over south-eastern Spain (Fig. 4.42) where a cooler and drier airmass was present near the surface compared to the immediate surroundings. The selected profile shows a surface temperature of only 12 °C and a dewpoint of 9 °C, compared to the 19 and 17 °C respectively measured at the station close to the storm. While it is possible that both the surface temperature and dewpoint were lower than the station showed, 12 and 9 sound unrealistic given the high relative humidity in the

lower troposphere that would not allow for such degree of evaporative cooling within the downdrafts of the storm.

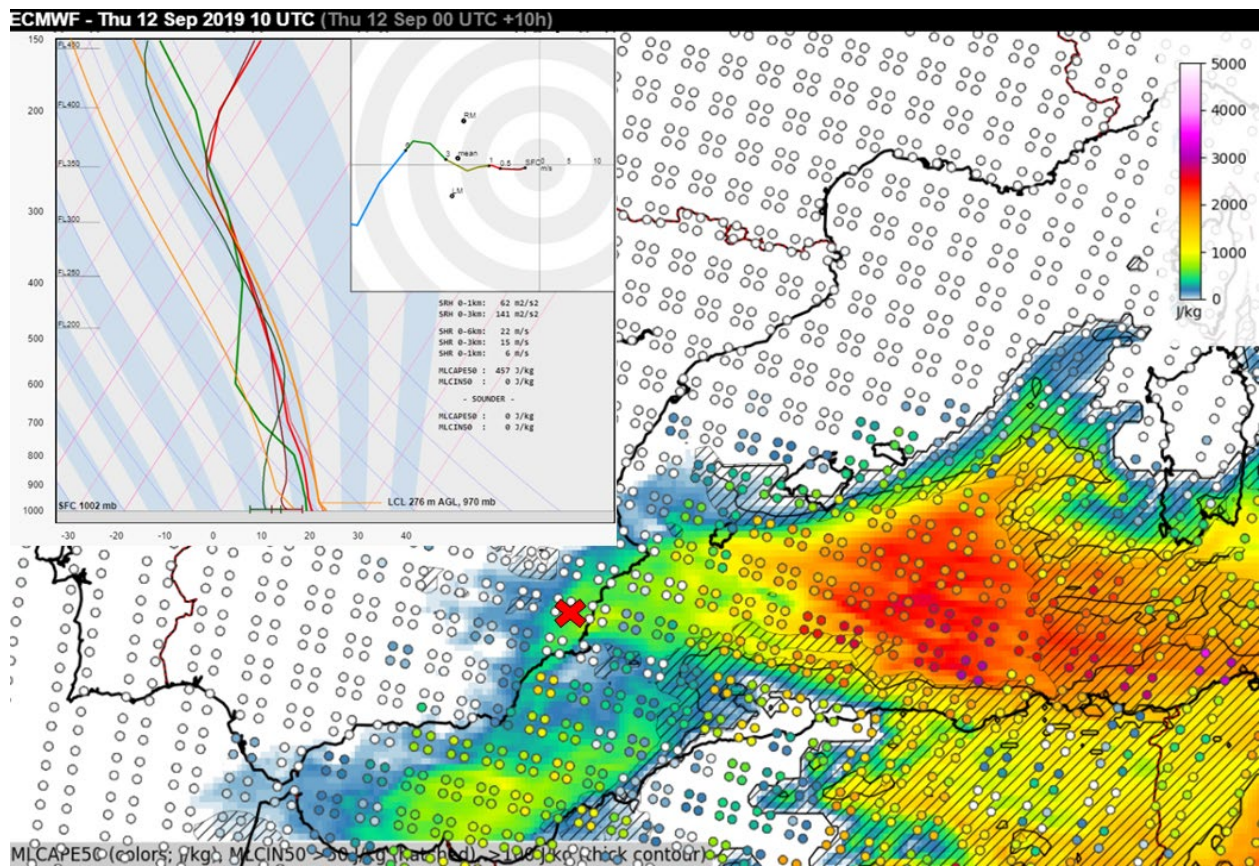


Fig. 4.42. As in Fig. 4.2, but for 12 September 2019 00 UTC ECMWF simulation of 10 UTC surface mixing ratio (filled contours) compared to the IASI-based MLCAPE (circles). Sounding is valid for the location marked by the red cross.

Summary

IASI sampled the environment resulting in development of long-lasting convective rainfall event, which caused serious flash flooding over south-eastern Spain. IASI resolved the tongue of moist air that was advected towards the coastline. The degree of moisture along the coastline was underestimated by the sounder, which in turn led to the failure to detect the CAPE. IASI also sampled the environment modified by a convective storm, showing cooling and drying near the surface. The degree of temperature and dewpoint decrease was overestimated, which may be caused by the sampling underneath a deep convective cloud, limiting the sounder accuracy.

5 Case catalogue

5.1 9 June 2014: Severe weather over Germany instead of the Benelux

Ahead of a low centred over the Atlantic at mid to upper troposphere, in a southerly flow, steep mid-tropospheric lapse rates were advected from northern Africa and Iberia over France, the Benelux and western Germany. Closer to the surface, a frontal boundary was forecast to cross France and the Benelux and initiate storms in an environment of high CAPE, between 2000 and 4000 J/kg, and strong vertical wind shear, exceeding 20 m/s in the 0–6 km layer. NWP Models simulated severe storms to impact France, Belgium and Netherlands.

Numerous severe thunderstorms developed over northern France and north-western Germany. A few isolated hailstorms with very large hail were observed near Paris. Further to the northeast, a devastating convective windstorm impacted Ruhrgebiet, Germany bringing traffic to a virtual standstill for the following days. A 40 m/s wind gust was measured at Dusseldorf airport. Compared to model expectations, storms formed more to the east than expected after morning convection stabilised the pre-convective environment over much of the Benelux.

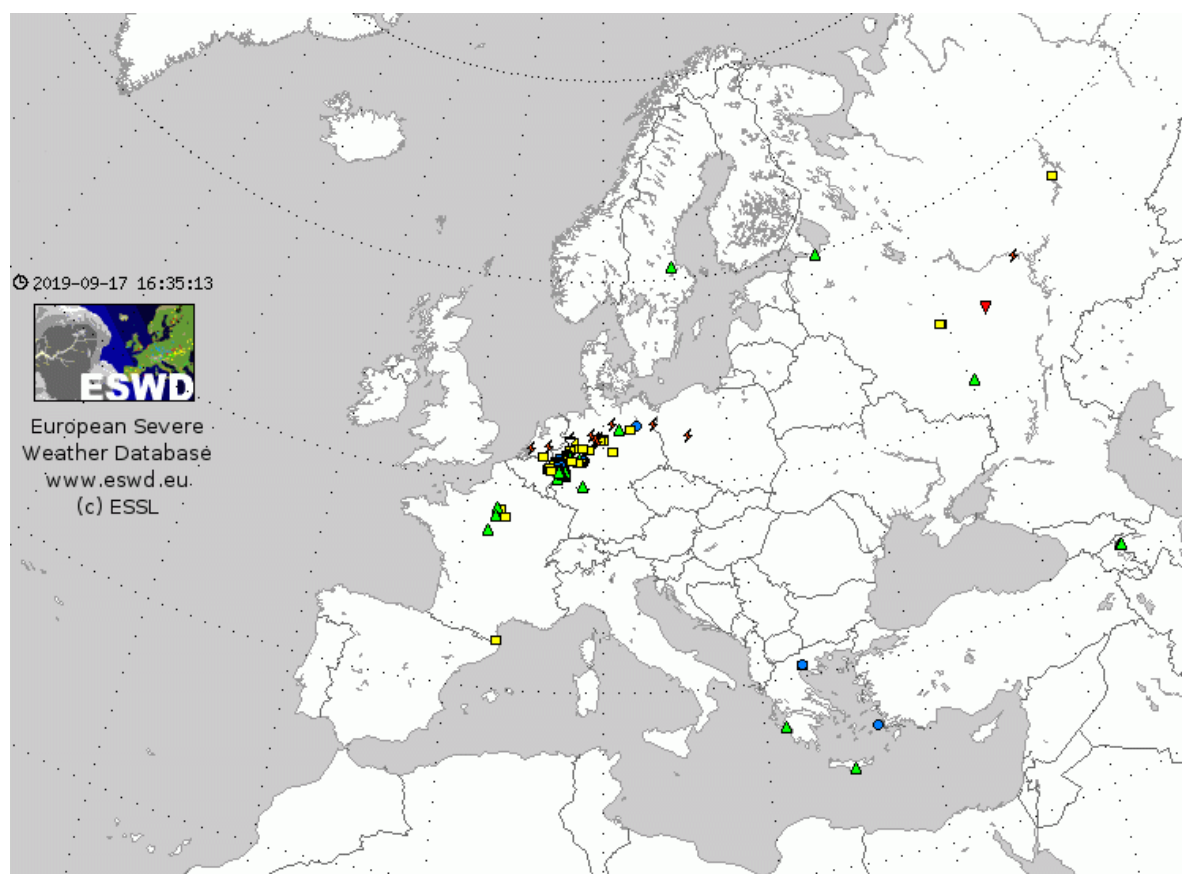


Fig. 4.43. Same as in Fig. 4.1. but for the period of 9 June 2014 00–24 UTC.

5.2 1 June 2016: Deadly flash flood in southeast Germany

A low-pressure system was centred over Austria. A tongue of moist air wrapped around the low towards southeast Germany, in an environment of marginal CAPE and weak vertical wind shear.

5 people perished in the devastating flash floods that affected the town of Simbach and other surrounding villages close to the Austrian border in south-eastern Germany. The flash flood followed after several cells trained over the same area in a quasi-stationary convective system.

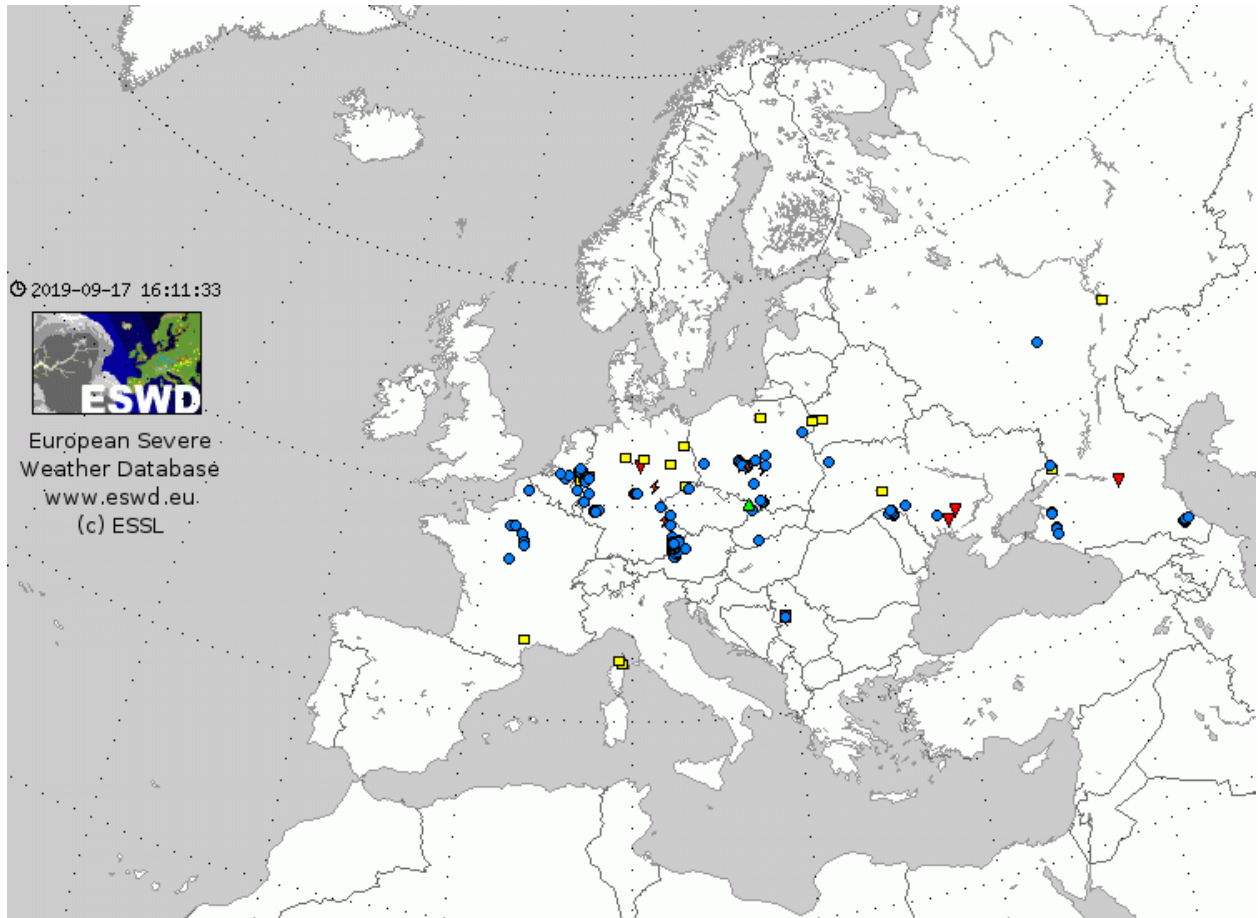


Fig. 4.44. Same as in Fig. 4.1. but for the period of 1 June 2016 00–24 UTC.

5.3 20 June 2016: Giant hail over Serbia, Romania and Hungary

On the forward flank of a deep trough located over the central Mediterranean a strong southerly flow advected air with steep lapse rates in the mid-troposphere from the Sahara over the Balkans. As these steep lapse rates overspread abundant lower tropospheric moisture, the environment was characterised by high CAPE, locally over 3000 J/kg. At the same time unseasonably strong vertical wind shear, reaching 20 to 30 m/s in the 0–6km layer, was present, culminating in a multi-day severe weather outbreak over Balkans, starting on 18 June 2016.

The first severe storms erupted over north-central Serbia and quickly spread into south-western Romania. A tornado was reported near Pancevo, Serbia, as well as hail up to 10 cm in diameter. Giant hell also fell near Timisoara, Romania, with hail up to 15 cm, the largest hail recorded in Europe since at least 1990. During the evening and overnight, severe hailstorms also impacted eastern Hungary and south-western Ukraine. Another swath of severe weather was observed with an isolated supercell that travelled across Poland with large hail, severe wind gusts and a tornado.

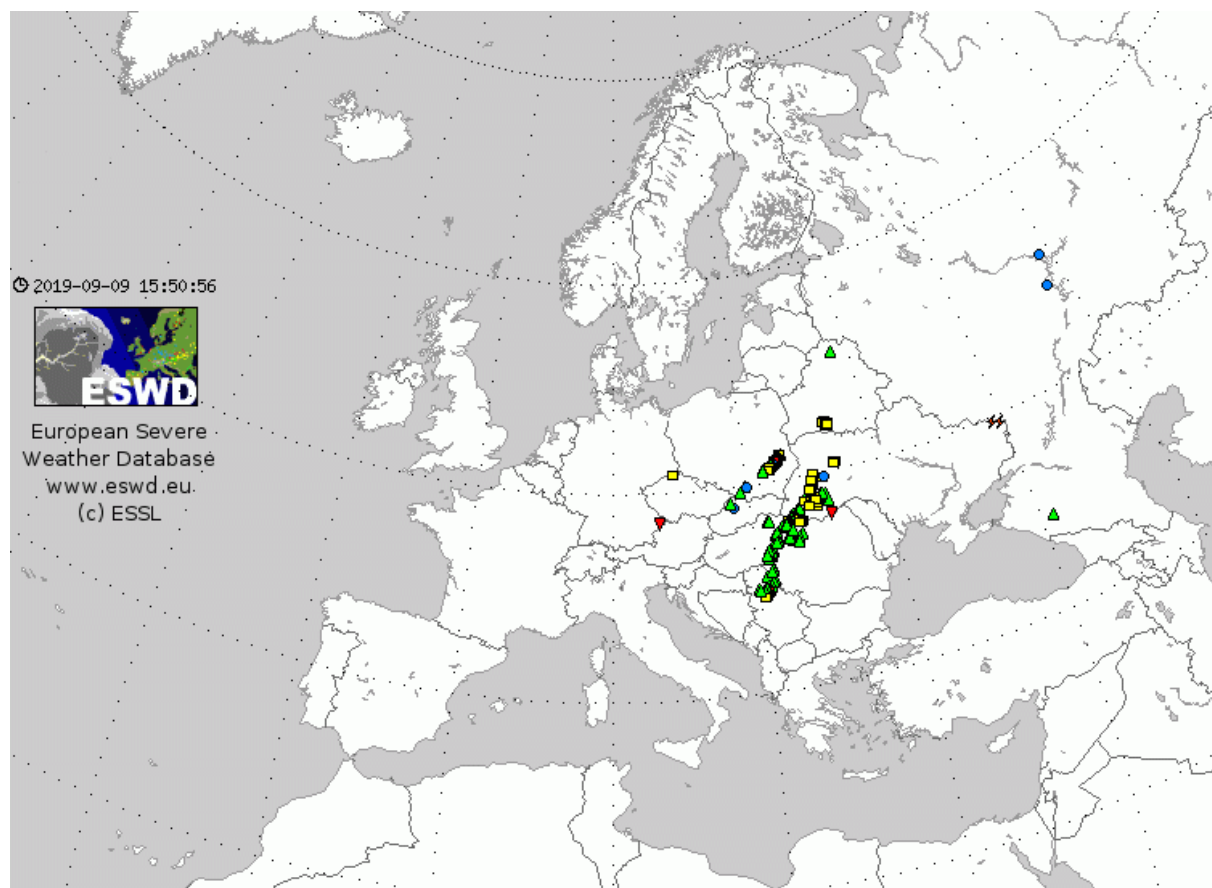


Fig. 4.45. Same as in Fig. 4.1. but for the period of 20 June 2016 00–24 UTC.

5.4 23 June 2016: Damaging hailstorms over Netherlands and Germany

A strong south-westerly flow in the mid-troposphere overlapped with warm and moist airmass ahead of a wavy frontal boundary that was crossing the Benelux and northern France during the afternoon and evening. Ahead of the front, models simulated a belt of CAPE between 1000 and 3000 J/kg, as well as strong vertical wind shear, around 20 m/s in the 0–6 km layer.

Severe thunderstorms occurred in an area from northern France to north-western Germany with damaging hail, severe wind gusts and heavy rainfall. The most severe storm occurred over the south-eastern Netherlands between 18 and 19 UTC as hail, 5 to 10 cm in diameter and often driven by strong winds, produced € 1.5 billion in damage to roofs, vehicles and greenhouses.

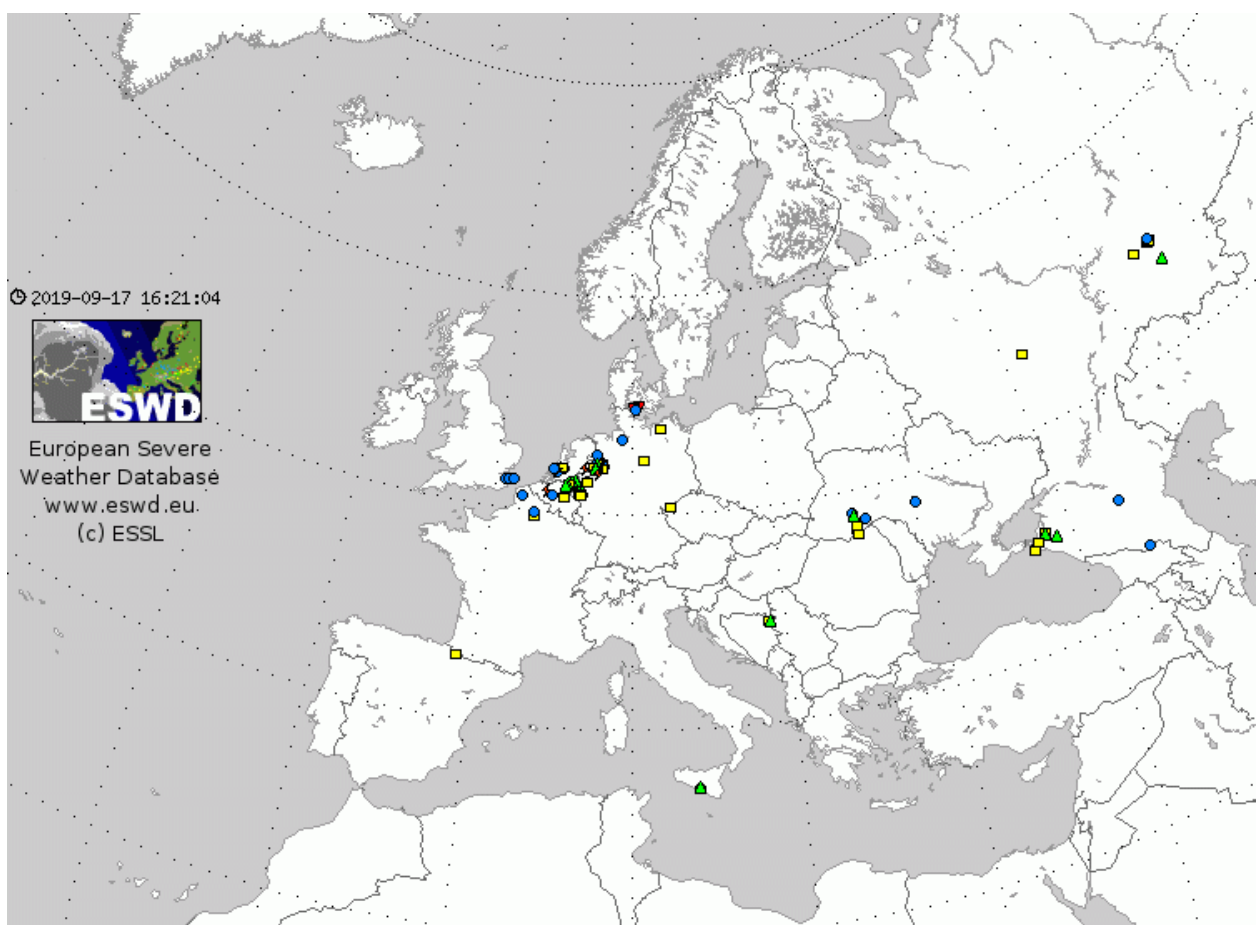


Fig. 4.46. Same as in Fig. 4.1. but for the period of 23 June 2016 00–24 UTC.

5.5 10 August 2017: Damaging convective windstorm occurs more east than forecast

A deep cyclonic vortex resided over France with deep and strong southerly flow observed in a belt from northern Italy through Austria into Czechia and Poland. In the hot airmass ahead of a cold front stretching from northern Austria through eastern Germany into northern Poland, models simulated CAPE between 1500 to 3000 J/kg, overlapping with strong vertical wind shear, reaching 15 to 25 m/s in the 0–6 km layer. Widespread severe storms were forecast from northern Italy through central Austria into Czechia and Poland.

Numerous severe storms occurred in reality with multiple swaths of damaging wind gusts, locally exceeding 32 m/s. The most severe complex of storms formed in the afternoon over north-eastern Italy and continued through Slovenia, eastern Austria into south-western Slovakia and eastern Czech Republic. In comparison to the model expectations the convective system tracked more to the east. For example, models simulated almost no storms over eastern Austria and south-western Slovakia.

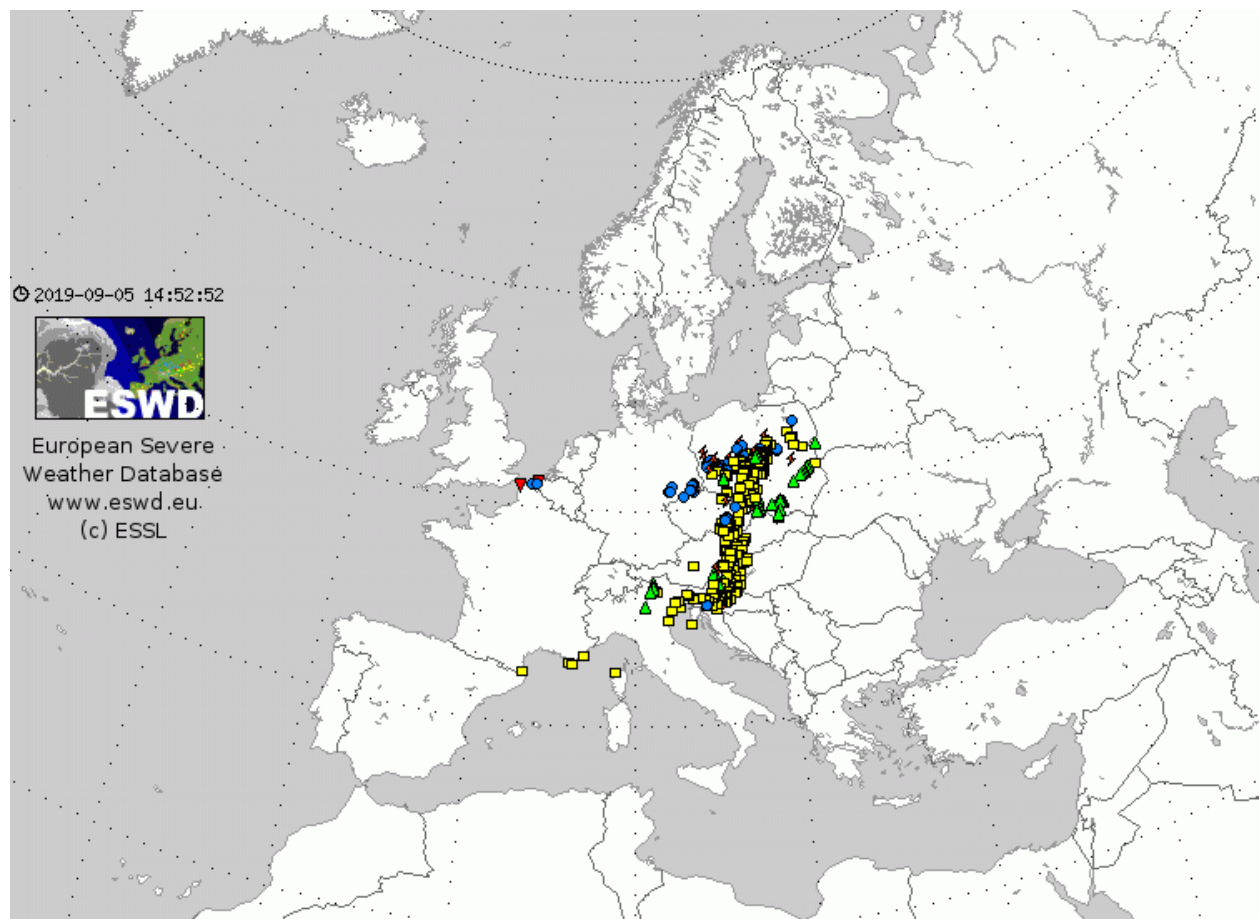


Fig. 4.47. Same as in Fig. 4.1. but for the period of 10 August 2017 00–24 UTC.

5.6 8 June 2018: Severe storms over Croatia and Slovenia with surprisingly large hail

On this day, a low-pressure area in the mid- and upper troposphere was centred over Italy, moving eastwards during the afternoon and evening. At the same time, a tropical airmass was advected over northern Balkans with substantial moisture in the lower troposphere, resulting in CAPE between 1000 and 2000 J/kg that overlapped with vertical wind shear between 15 and 20 m/s in the 0–6 km layer.

Numerous severe storms formed over Croatia and Slovenia, producing large hail and severe wind gusts. In Hungary, 4 people were killed as a tree crushed a car, but the most severe storm occurred on the boundary of Croatia and Slovenia at 14 UTC. The storm produced giant hail, up to 12 cm across, that destroyed hundreds of roofs in the town of Crnomelj in Slovenia. The intensity of the storm was unexpected given “only” moderate values of CAPE and vertical wind shear.

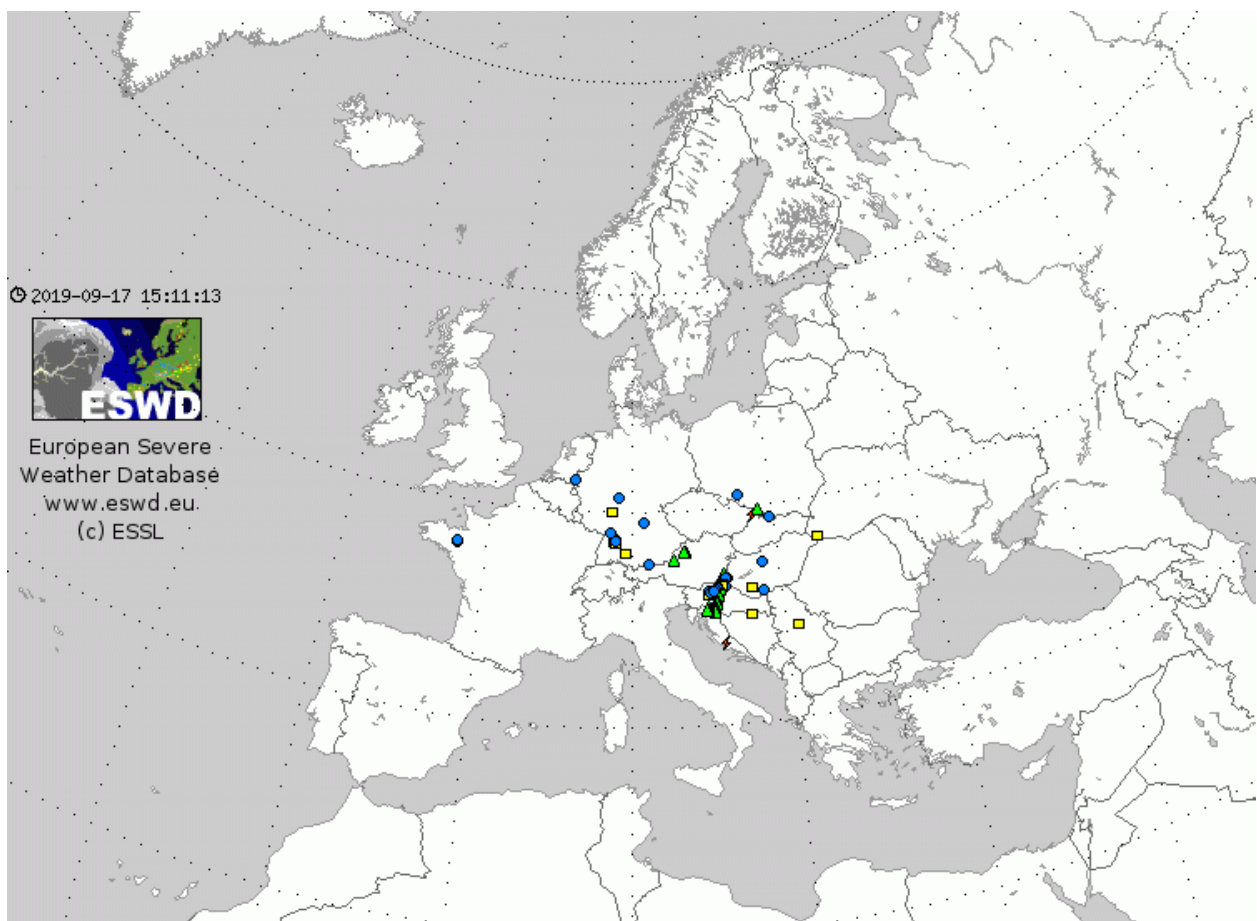


Fig. 4.48. Same as in Fig. 4.1. but for the period of 8 June 2018 00–24 UTC.

5.7 9 October 2018: Deadly flash floods over Mallorca

On the forward flank of a cut-off low over Iberia, moist airmass has been advected from southeast over the western Mediterranean towards the coastlines of Spain and southern France. NWP models simulated CAPE increasing from the Spanish coastline towards Sardinia, ranging from 500 to 3000 J/kg. The highest precipitation sums were forecast by models over the coastline of north-eastern Spain and southern France.

A pattern of training thunderstorms developed over the Balearic Islands, resulting in more than 200 mm of precipitation falling in 2 hours by 17 UTC across northern Mallorca. 12 people died in the subsequent flash floods. While NWP models indicated precipitation over the islands, the forecast rainfall sums were much less than reality and models also indicated the highest rainfall sums incorrectly over the coastal areas of Spain and France.

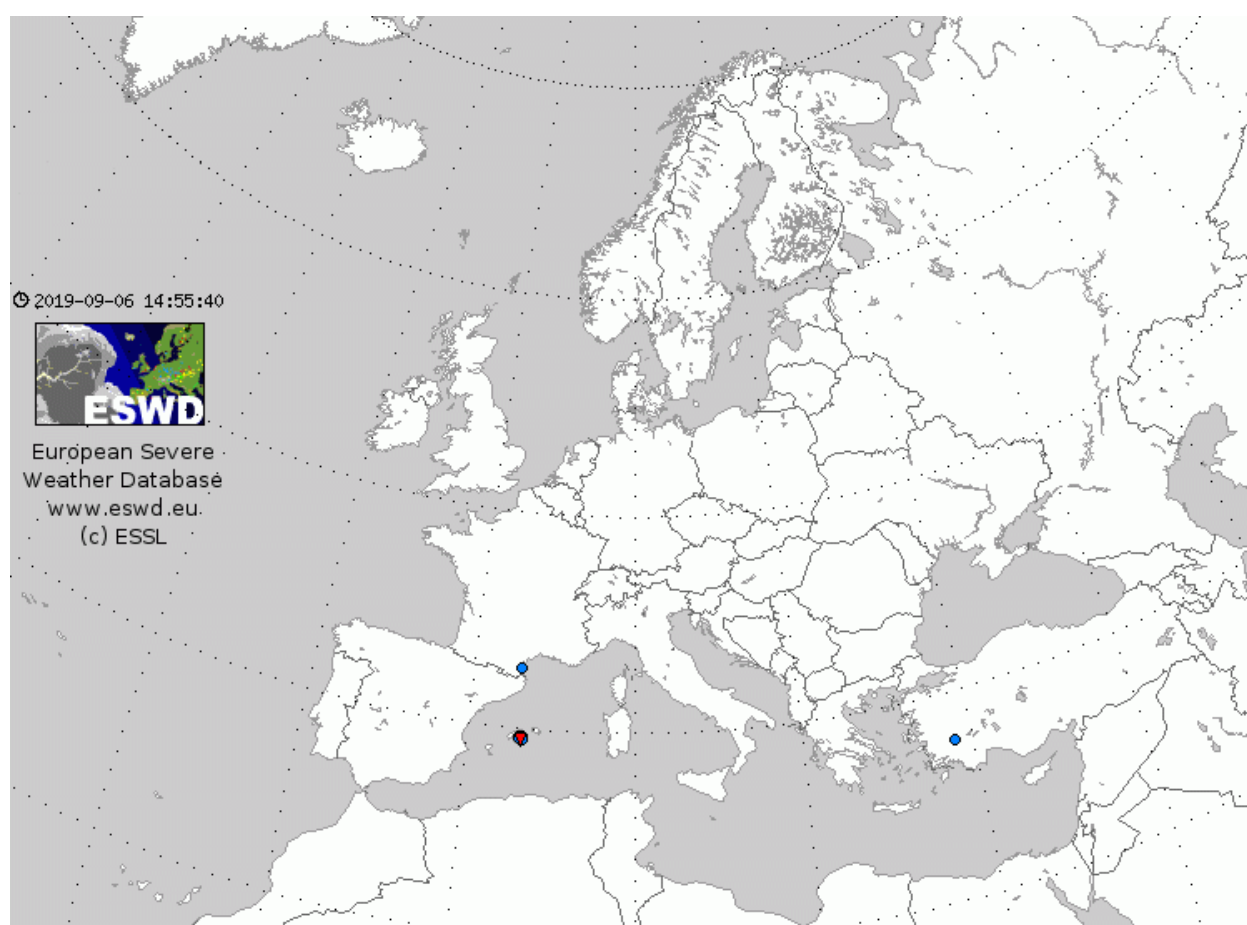


Fig. 4.49. Same as in Fig. 4.1. but for the period of 9 October 2018 00–24 UTC.

5.8 13 October 2018: Landfalling tropical storm Leslie in Portugal with severe wind gusts

A tropical storm Leslie was forecast to make landfall on the coastline of Portugal in the evening to night of 13 October. Models did not agree on the depth of the low (strength of the wind gusts) and also on its exact track. ECMWF produced the deepest low from the suite of global models.

Leslie impacted Portugal between 21 and 24 UTC with the most severe winds observed just to the south of the storm centre. The highest measured wind gust was 49.4 m/s in Figueira da Foz. 2 people died and 28 were injured as a result of the storm.

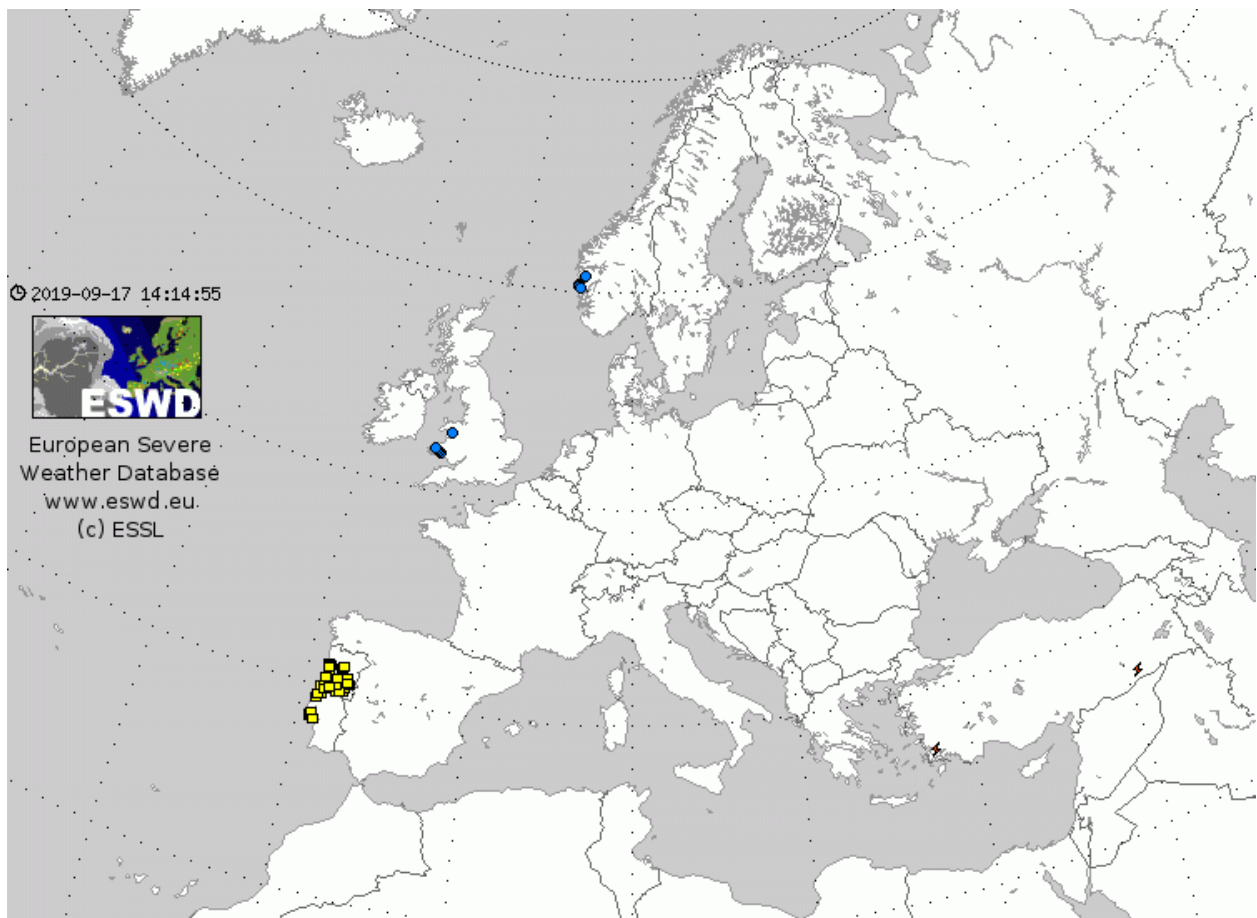


Fig. 4.50. Same as in Fig. 4.1. but for the period of 13 October 2018 00–24 UTC.

5.9 29 October 2018: Widespread severe weather over the Mediterranean

An unseasonably deep low at mid to upper troposphere was centred over the Balearic Sea and the associated short-wave trough rapidly progressed from northern Africa towards the Gulf of Genoa. On its forward flank, the southerly wind reached up to 50 m/s at 500 mb and 40 m/s at 850 mb level. Widespread storms were forecast over Italian coastline during the day ahead of the advancing cold front, in an environment of strong vertical wind shear and CAPE exceeding 2000 J/kg over the sea.

Widespread wind and flash flood damage was reported from central and northern Italy from a combination of both convective and non-convective severe weather, claiming 16 lives and multiple injuries. Several tornadoes, two of them strong, and large hail were reported from Corsica and Sardinia.

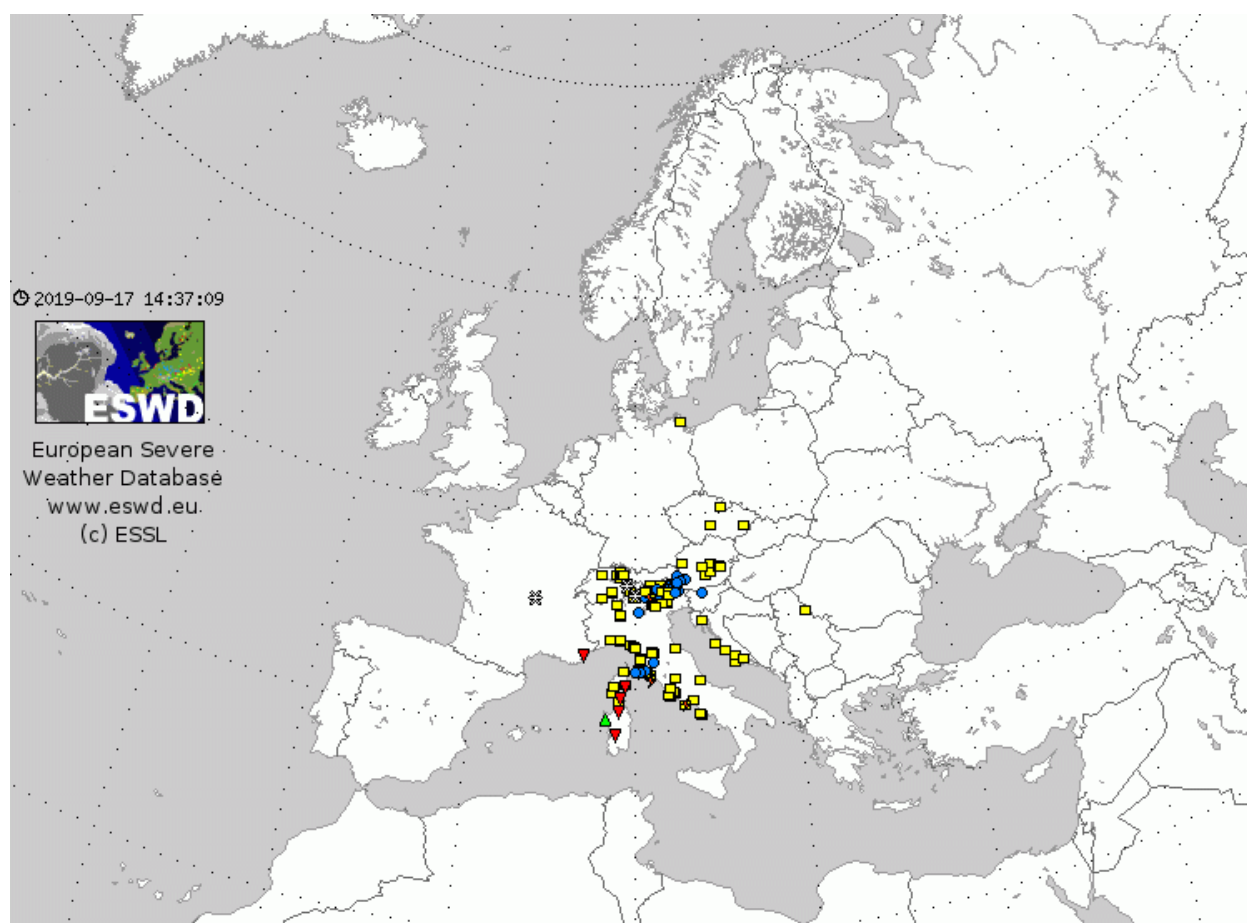


Fig. 4.51. Same as in Fig. 4.1. but for the period of 29 October 2018 00–24 UTC.

5.10 28 May 2019: Damaging hailstorm over Northwest Romania

A deep trough at 500 mb stretched from the Atlantic and western Scandinavia towards northern Africa with deep southerly flow at its forward flank over eastern Europe. In the lower troposphere, a wavy frontal boundary ran from eastern Poland to Hungary and Serbia. Ahead of it, in the warm and moist airmass, models forecast an overlap of 500 to 1500 J/kg of CAPE with 15 to 20 m/s of 0–6 km shear. The highest risk of storms was forecast over western Romania and south-western Ukraine.

The most severe storm of the day developed around 12 UTC over north-western Ukraine and produced a swath of large to large hail (up to 6 cm in diameter) and severe wind gusts. While a high risk of severe convection was also anticipated all the way to south-western Romania, almost no severe weather was reported there.

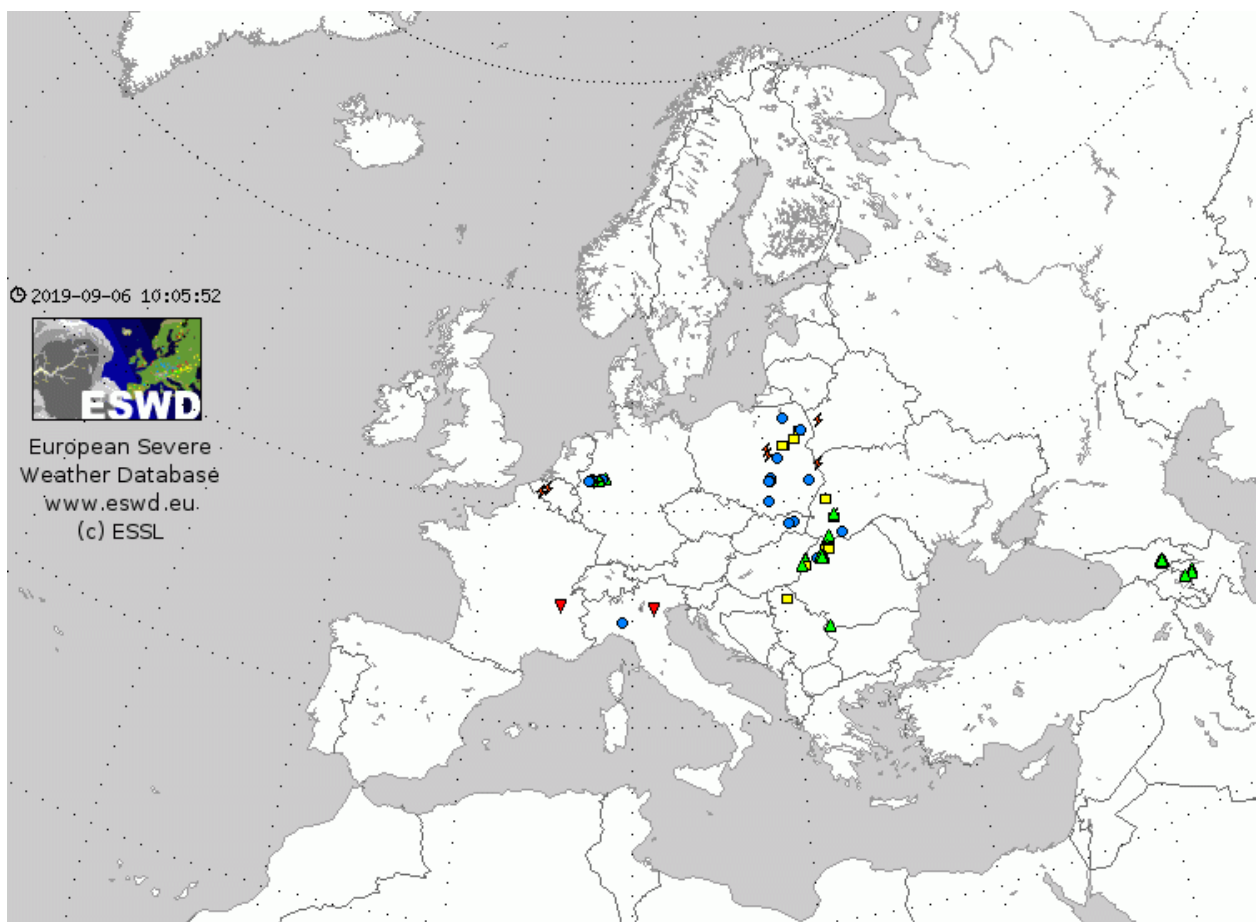


Fig. 4.52. Same as in Fig. 4.1. but for the period of 28 May 2019 00–24 UTC.

5.11 4 June 2019: Severe thunderstorms across north-western Europe

A deep trough resided over the Atlantic with a strong, 20–25 m/s, south-westerly flow at 500 mb in a belt from northern Spain towards the Benelux, Denmark and southern Scandinavia. Ahead of the trough, a cold front slowly moved eastwards across Spain and western France. Ahead of the front, models simulated a collocation of CAPE ranging from 500 to 2000 J/kg and strong vertical wind shear over northern France and the Benelux.

The first thunderstorms formed over northern France in the late afternoon and quickly moved northwest. Swath of severe wind gusts was reported over the Benelux with the highest measured gust of 30 m/s, as well as two strong, F2 tornadoes, one in Holland and one in Germany, close to the border. Most of the severe weather occurred in late evening.

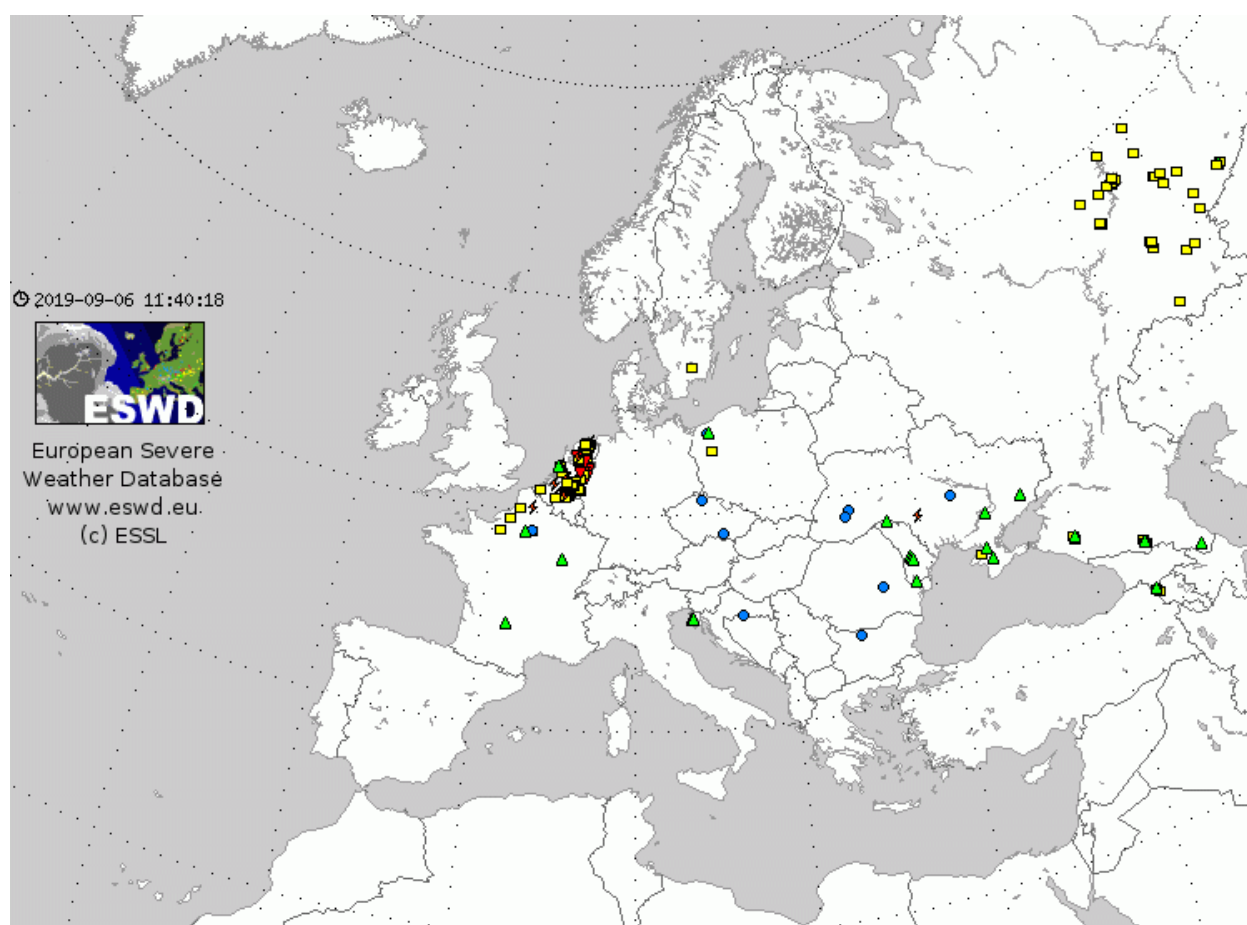


Fig. 4.53. Same as in Fig. 4.1. but for the period of 4 June 2019 00–24 UTC.

5.12 10 June 2019: Severe hailstorm hit Munich area

A deep cyclonic vortex situated over the British Isles was moving towards France with strong southerly flow at its forward flank. Severe storms were forecast along the cold front, stretching from Italy to Germany and southern Sweden, in an environment of high CAPE exceeding 1000 J/kg and strong vertical wind shear.

Numerous severe storms were reported from the region, with swaths of large to large hail and damaging wind gusts. Particularly costly was a supercell that hit Munich metropolitan area with wind-driven hail up to 6 cm in diameter. Most models did not forecast the storms to hit Munich, but simulated storms to the west and north of the area.

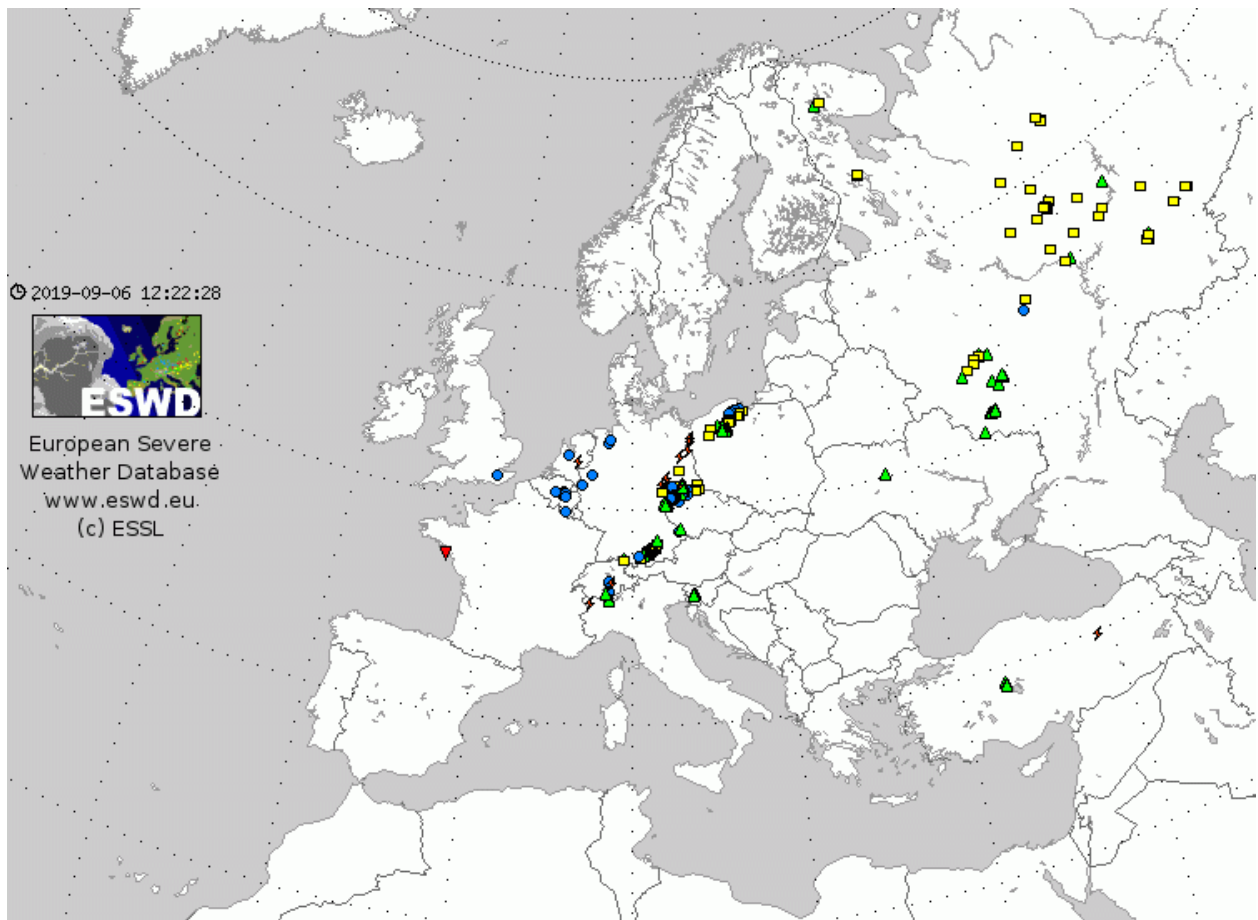


Fig. 4.54. Same as in Fig. 4.1. but for the period of 10 June 2019 00–24 UTC.

5.13 13 June 2019: Widespread severe storms over Czechia, Poland and Baltic states

Severe storms were forecast in a belt from northern Austria through Poland in the Baltic states ahead of the weak frontal boundary. Environment was characterised by moist boundary layer, CAPE around 2000 J/kg and 0–6 km vertical wind shear between 15 and 20 m/s.

Widespread severe weather was reported from eastern Czechia, Poland and the Baltic countries. Large hail, up to 6 cm, was observed over Czechia, Poland and Lithuania and numerous severe wind gusts were reported as well. Flash flooding occurred in south-eastern Czechia. Storm activity over the Baltic States was in general underestimated by numerical models.

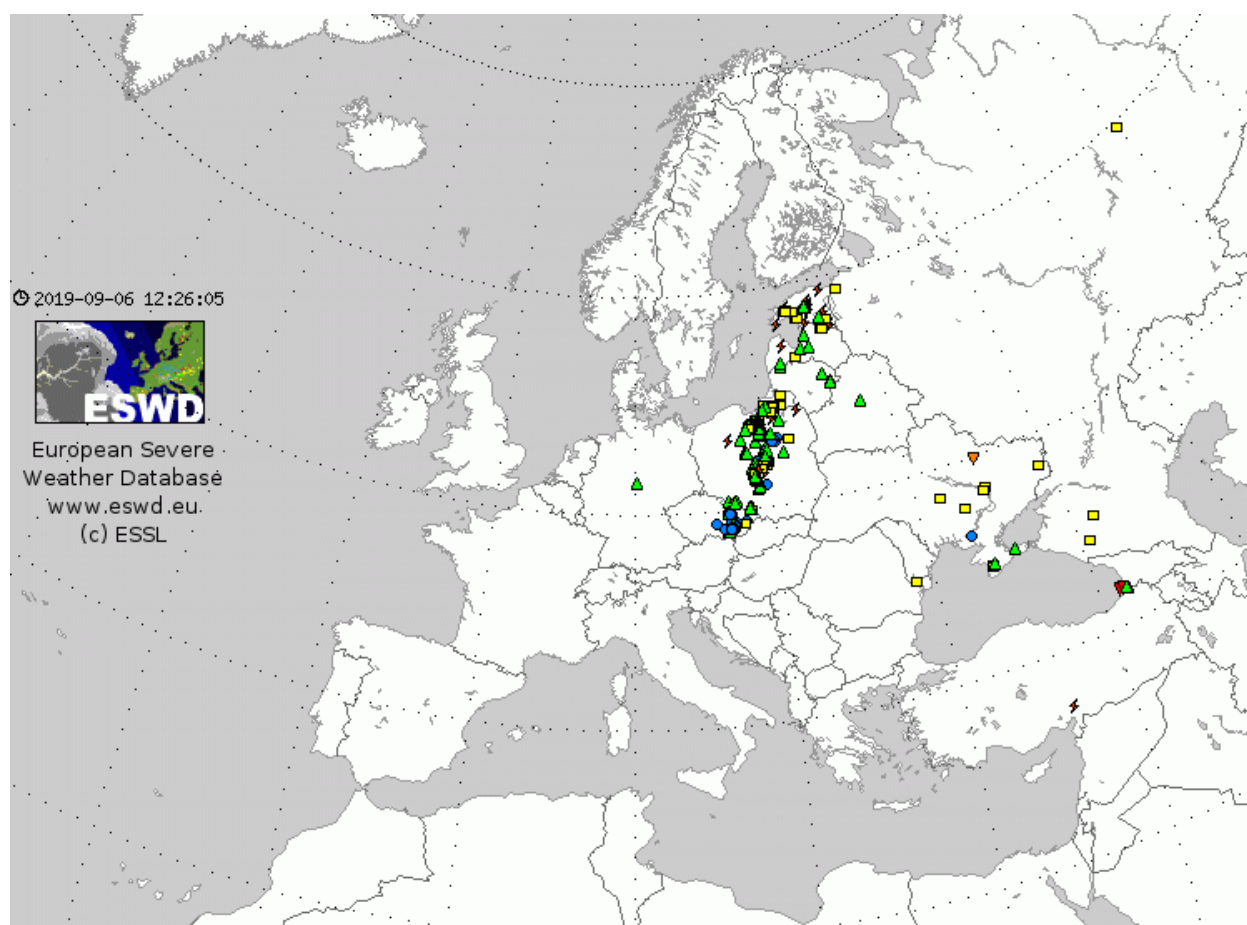


Fig. 4.55. Same as in Fig. 4.1. but for the period of 13 June 2019 00–24 UTC.

5.14 15 June 2019: Severe storms in central Europe; French storms more severe than expected

A deep cyclonic vortex resided over the Atlantic with south-westerly flow over much of western and central Europe. A short-wave trough was simulated to move from northern Spain, through France towards Germany. Severe storms were forecast ahead of an advancing cold front, in a belt from eastern France, through Germany into Poland. The most severe conditions were anticipated over eastern Czech Republic, Germany and Poland due to high CAPE, reaching up to 3000 J/kg.

The first severe storms occurred at night and during the early morning over northern Germany with large hail and heavy rainfall. During the day, further severe storms developed over parts of Germany, Poland and Czech Republic. Over northern Poland, a wind gust of 38 m/s was measured. Although lower CAPE was simulated by models over eastern France and western Switzerland, similarly severe storms occurred there, with hail up to 8 cm in diameter and severe wind gusts. 2 fatalities and numerous injuries were reported from this region.

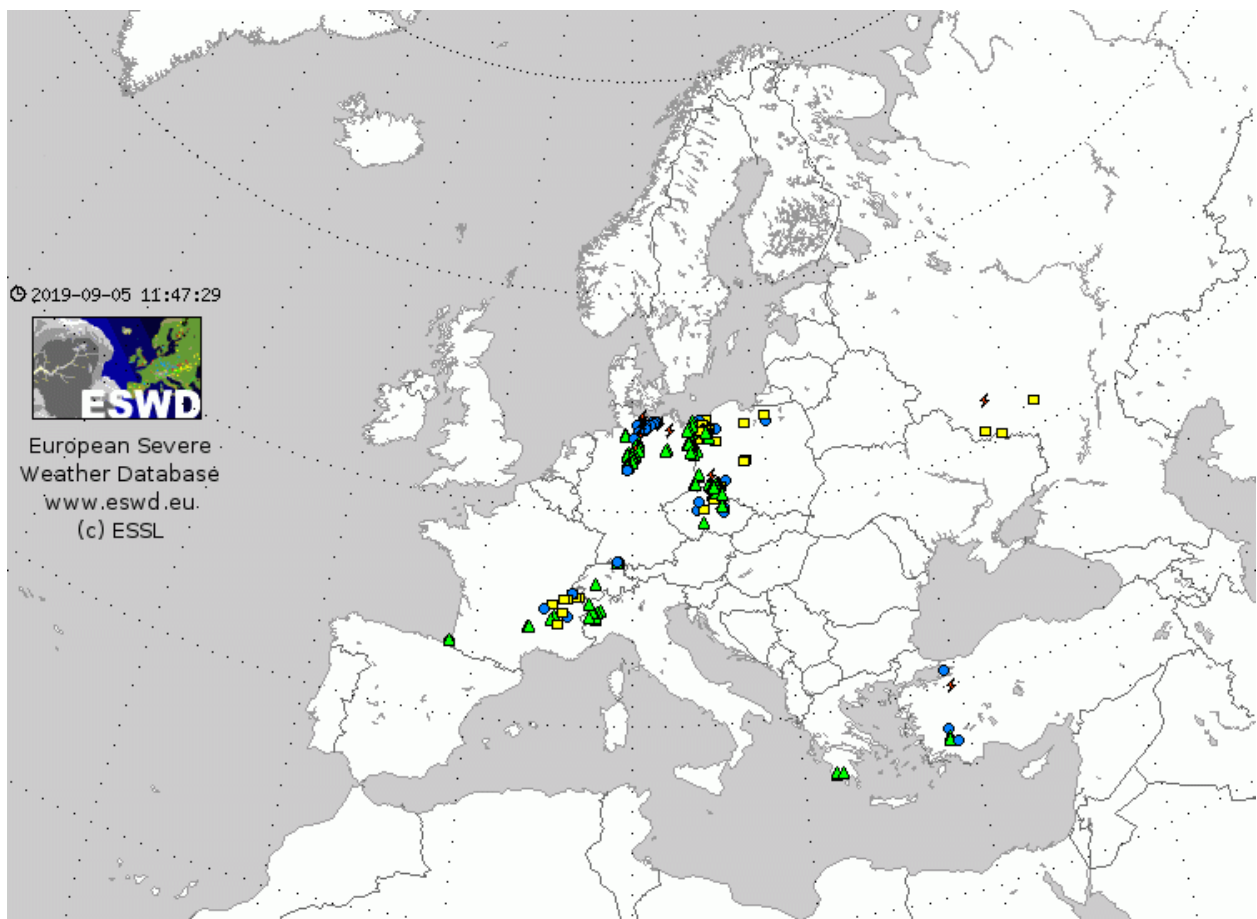


Fig. 4.56. Same as in Fig. 4.1. but for the period of 15 June 2019 00–24 UTC.

5.15 18 June 2019: Large hail in northern France and uncertain initiation across the Benelux

In a broad belt of south-westerly flow over western Europe, a short-wave trough was simulated to pass across northern France and the Benelux during the day. Another trough was anticipated to cross from Bay of Biscay to France in the evening to overnight. CAPE around 1000 J/kg and 0–6 km vertical wind shear around 15 m/s was simulated from northern France to Belgium.

Severe hailstorms eventually formed over north-western France by 19 UTC, but no convective initiation occurred further north and northeast, towards Belgium. Models were inconsistent regarding the exact location of storm formation for this day.

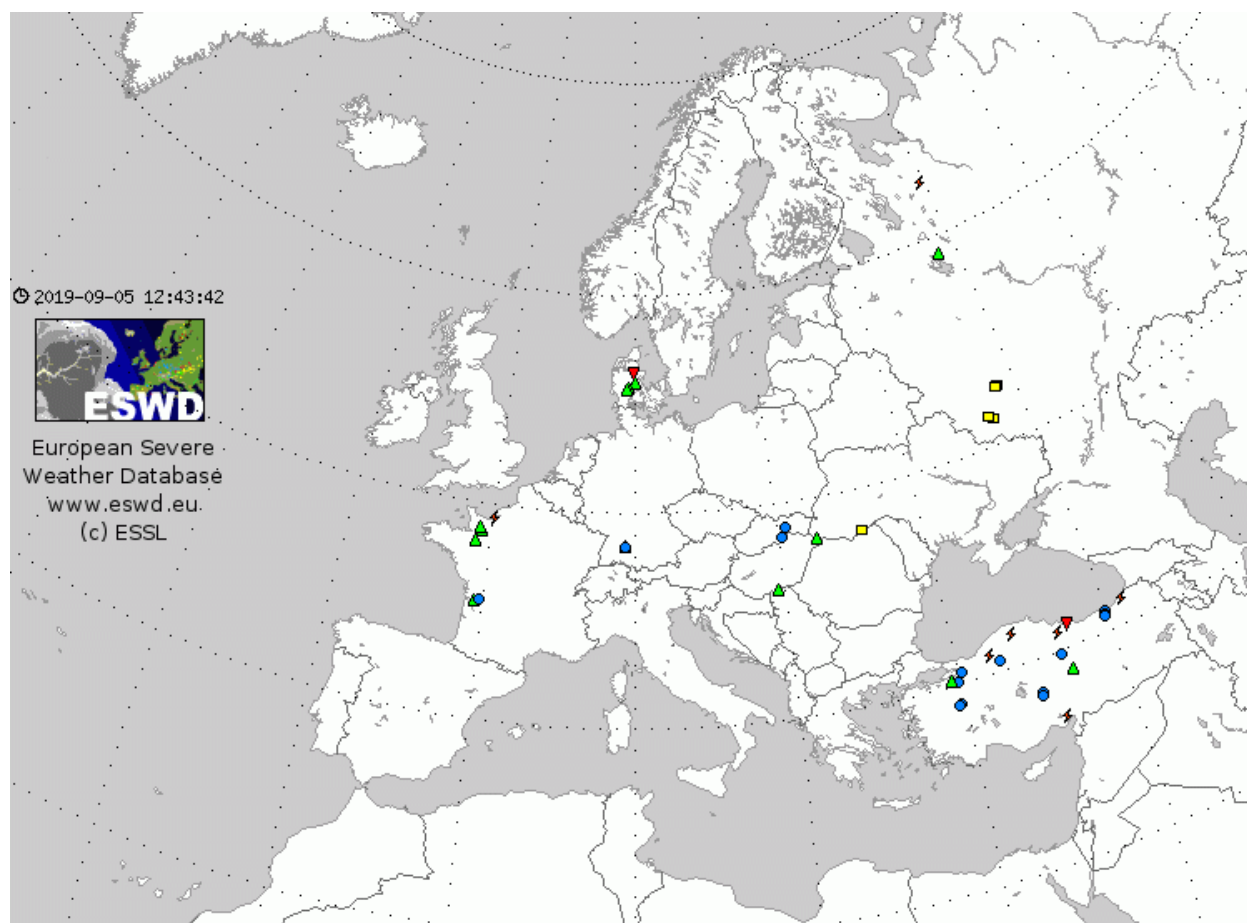


Fig. 4.57. Same as in Fig. 4.1. but for the period of 18 June 2019 00–24 UTC.

5.16 19 June 2019: Unexpected severe storm over Toulouse

Multiple rounds of severe storms were forecast over Europe on this day. Slow-moving storms with flash flood potential were forecast over parts of central and south-eastern Europe and more organised convective storms were forecast over parts of France, the Benelux and western Germany under moderate vertical wind shear, reaching 15 m/s in 0–6 km layer.

Severe storms indeed materialised over these regions. The most severe storm hit Toulouse, France as an isolated supercell passed over the city after 21 UTC with wind gusts up to 38 m/s. While isolated storms were forecast over the region, the intensity of the storm was higher than expected, given simulated CAPE of only 500 to 1000 J/kg. Furthermore, models gave only weak precipitation signals across southern France.

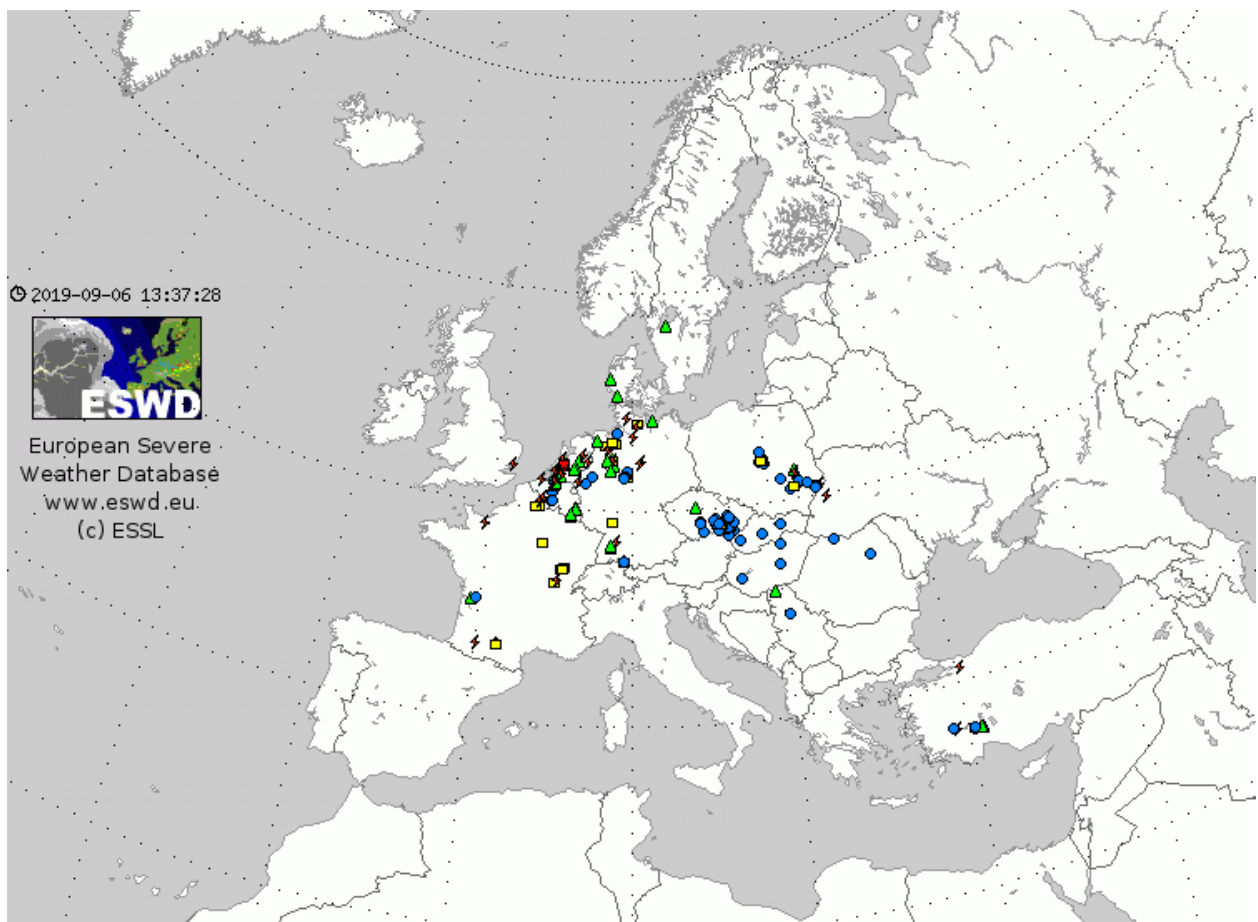


Fig. 4.58. Same as in Fig. 4.1. but for the period of 19 June 2019 00–24 UTC.

5.17 27 June 2019: Storms across Slovakia, Hungary and Romania; few storms over Germany

In strong mid-tropospheric flow, reaching 20 to 25 m/s at 500 mb, a short-wave trough travelled from the Balkans towards Poland, Belarus and Ukraine. At the same time, a powerful cold front surged across Poland and Germany towards southeast. Ahead of the advancing front, models simulated storms developing in an environment of CAPE between 1000 and 2500 J/kg and vertical wind shear reaching 15 to 20 m/s in the 0–6 km layer.

Severe thunderstorms formed in the late morning over eastern Slovakia and quickly spread south towards Hungary and Romania. large hail, up to 8 cm in diameter, and widespread severe wind gusts were reported from this region. On the other hand, little activity occurred over northern Austria and south-western Germany, where both the front and high CAPE were present as well.

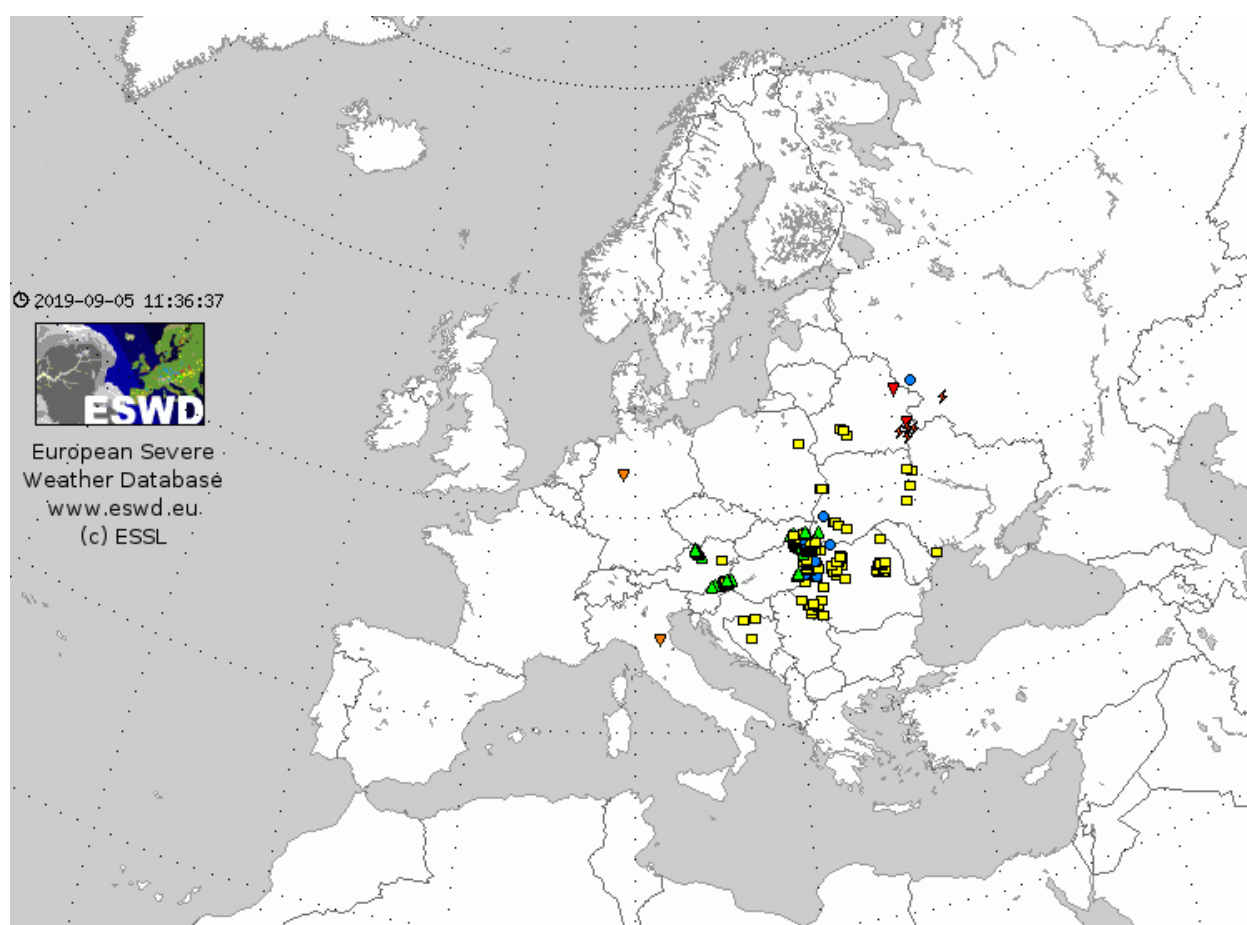


Fig. 4.59. Same as in Fig. 4.1. but for the period of 27 June 2019 00–24 UTC.

5.18 1 July 2019: Widespread severe storms across Europe: storms occurred further east than forecast

South of a deep cyclonic vortex over the northern Atlantic, a strong zonal flow was forecast across northern France, Germany, and Poland towards the Baltic Sea. In the lower troposphere, a cold front was moving from Germany and northern Poland towards the southeast. Ahead of the front, a belt of CAPE ranging from 1000 to 2000 J/kg overlapping with strong vertical wind shear (15 to 25 m/s in the 0–6 km layer) was forecast. In such conditions, models simulated the initiation of storms along the frontal zone.

Widespread severe storms occurred in the given day with multiple reports of large hail, up to 7 cm in diameter and severe wind gusts. The highest measured wind gust came from eastern France, at 35 m/s. While storms of such intensity were expected, some of them occurred more to the east than simulated by models, e.g. over eastern Czech Republic.

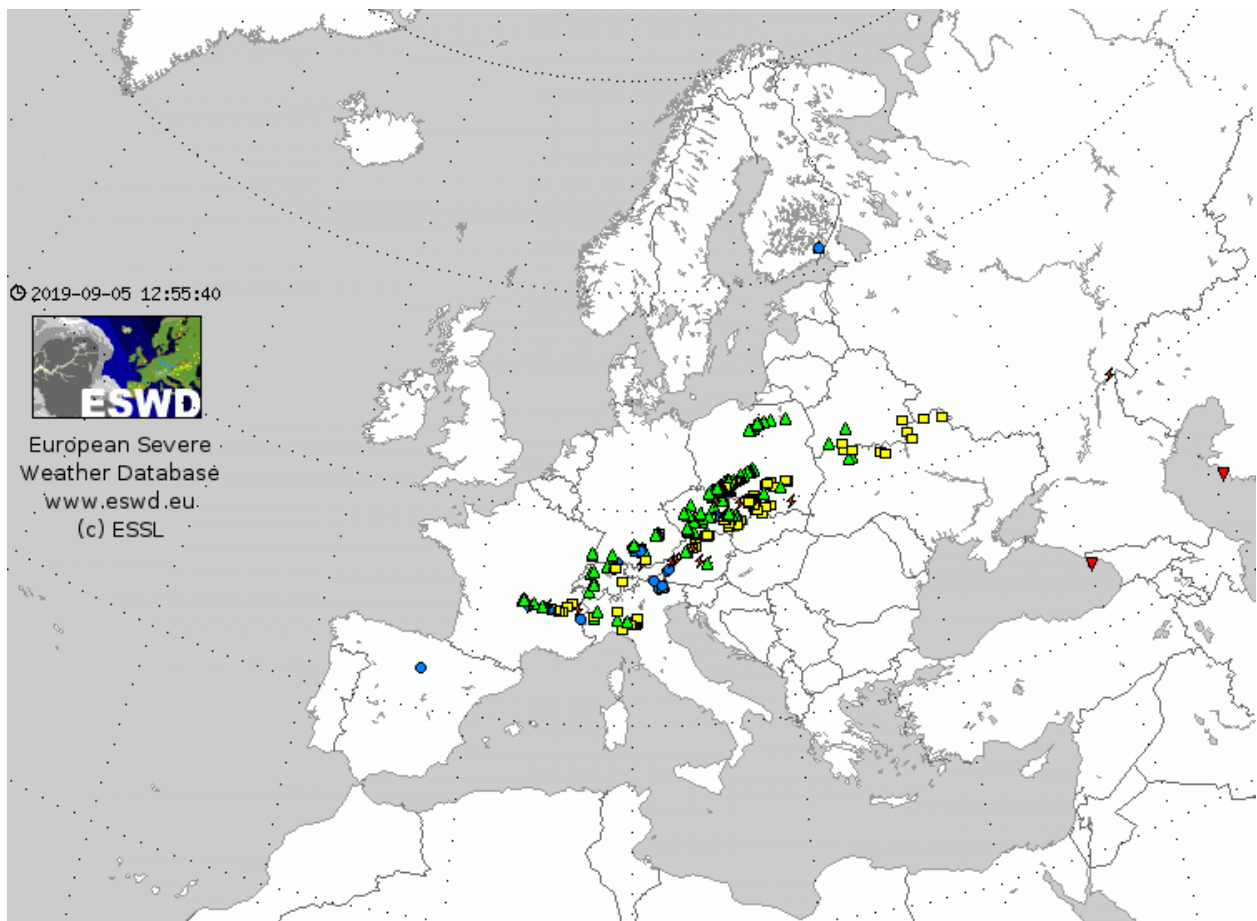


Fig. 4.60. Same as in Fig. 4.1. but for the period of 1 July 2019 00–24 UTC.

5.19 6 July 2019: Severe storms over France and Italy: coverage underestimated by models

Between a ridge over the Mediterranean and a cyclone crossing Denmark, a strong zonal flow has established over much of western and central Europe at the mid to upper troposphere. Models simulated an overlap of steep mid-tropospheric lapse rates and abundant lower tropospheric moisture in a wide belt from France across Italy into Slovenia and Hungary, resulting in CAPE between 1000 and 3000 J/kg. At the same time, strong vertical wind shear was forecast.

Extremely severe thunderstorms occurred in the afternoon and evening over France, Italy and Switzerland. Large hail up to 8 cm was observed in France and Piemonte, Italy. Over the latter part, hail caused extreme damage to roofs and vehicles in Vercellese area. A 38 m/s wind gust was measured in Lucerne, Switzerland. Models underestimated the coverage of storms over these areas. At the same time, a strong tornado (F2 in intensity) and severe wind gusts occurred over Latvia around 12 UTC. Models showed a band of strong vertical wind shear in the 0–1 km layer but disagreed on the extent of the CAPE over the country.

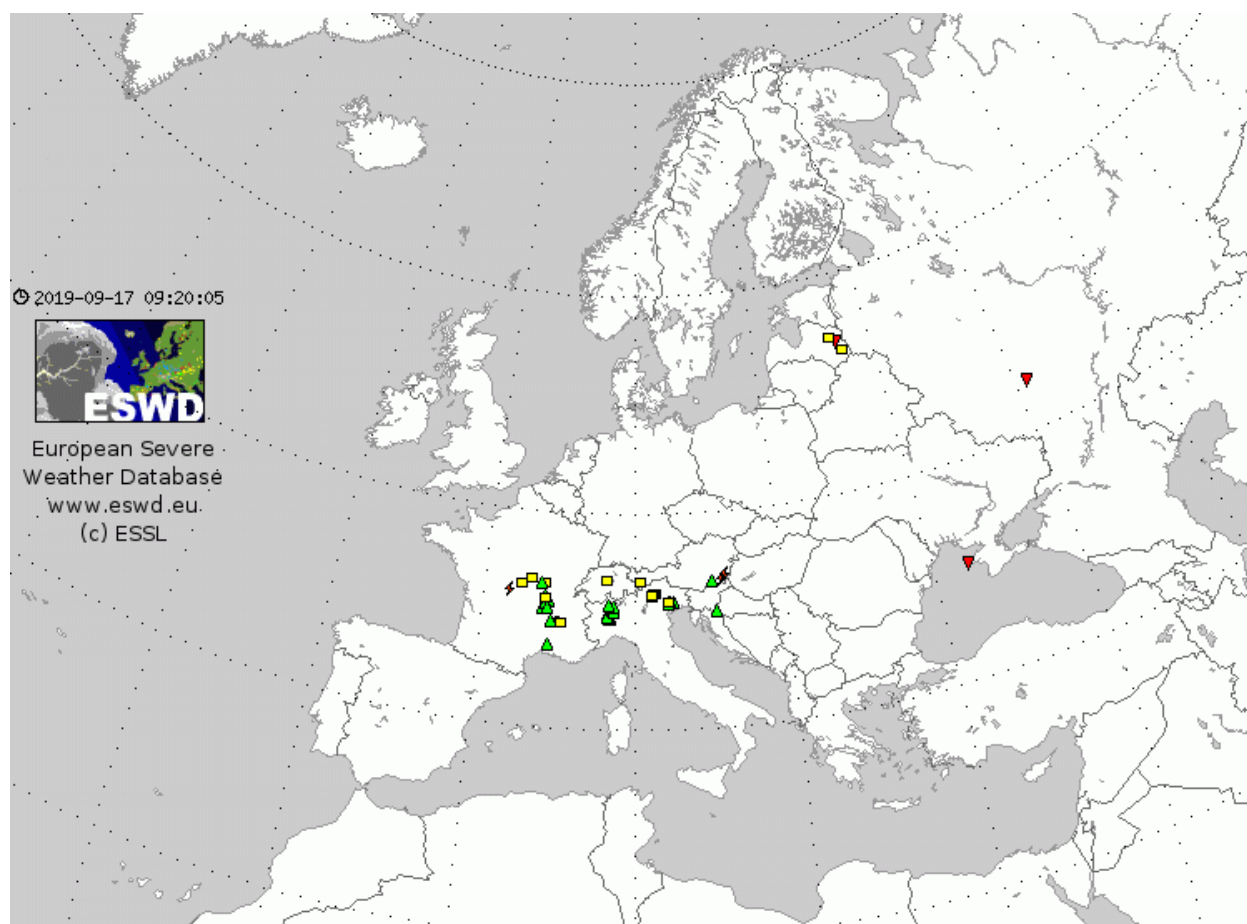


Fig. 4.61. Same as in Fig. 4.1. but for the period of 6 July 2019 00–24 UTC.

5.20 7 July 2019: Widespread severe storms: model underestimation of extent of convection

A severe weather outbreak was forecast for this day across a belt from northern Italy through Slovenia, Croatia, Serbia into western Romania and also from south-eastern Slovakia to the Ukraine. The environment was characterised by both high CAPE (locally exceeding 2000 J/kg) and strong vertical wind shear (15–25 m/s in the 0–6 km layer).

Widespread severe weather, mostly in the form of severe wind gusts and damaging hail indeed occurred over the mentioned regions. While most severe weather was predicted over the northern part of the Adriatic Sea, the storms reached more to the south than simulated by models, producing a swath of severe wind gusts that also affecting Zadar, Croatia, where a 30 m/s gust was measured.

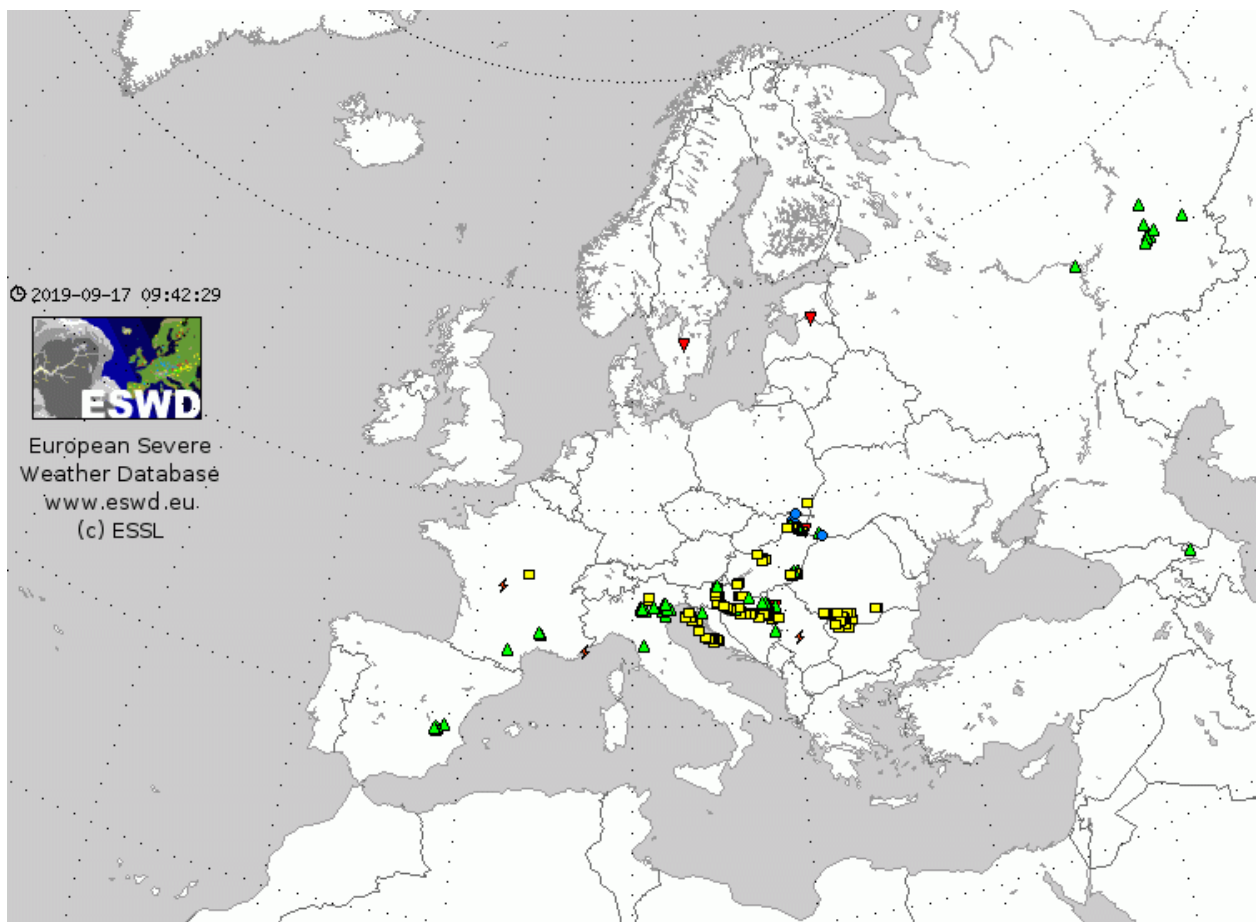


Fig. 4.62. Same as in Fig. 4.1. but for the period of 7 July 2019 00–24 UTC.

5.21 8 July 2019: Severe storms over Spain and Italy: Initiation failure over eastern Spain

During this day, two corridors of severe weather were forecast. The first one was over Spain, in conjunction with a cut-off low at mid- to upper troposphere. The second one was over northern Italy and the northern Adriatic Sea, underneath strong north-westerly flow. Both areas also experienced severe thunderstorms, with large hail up to 8 cm in diameter and severe wind gusts. Spain also experienced serious flash flooding with 1 fatality reported. For Spain, the corridor of most severe weather was forecast more east than eventually materialised. This was because storms did not or had trouble initiating in the corridor with the strongest vertical wind shear over eastern Spain, where the NWP-models showed substantial convective precipitation.

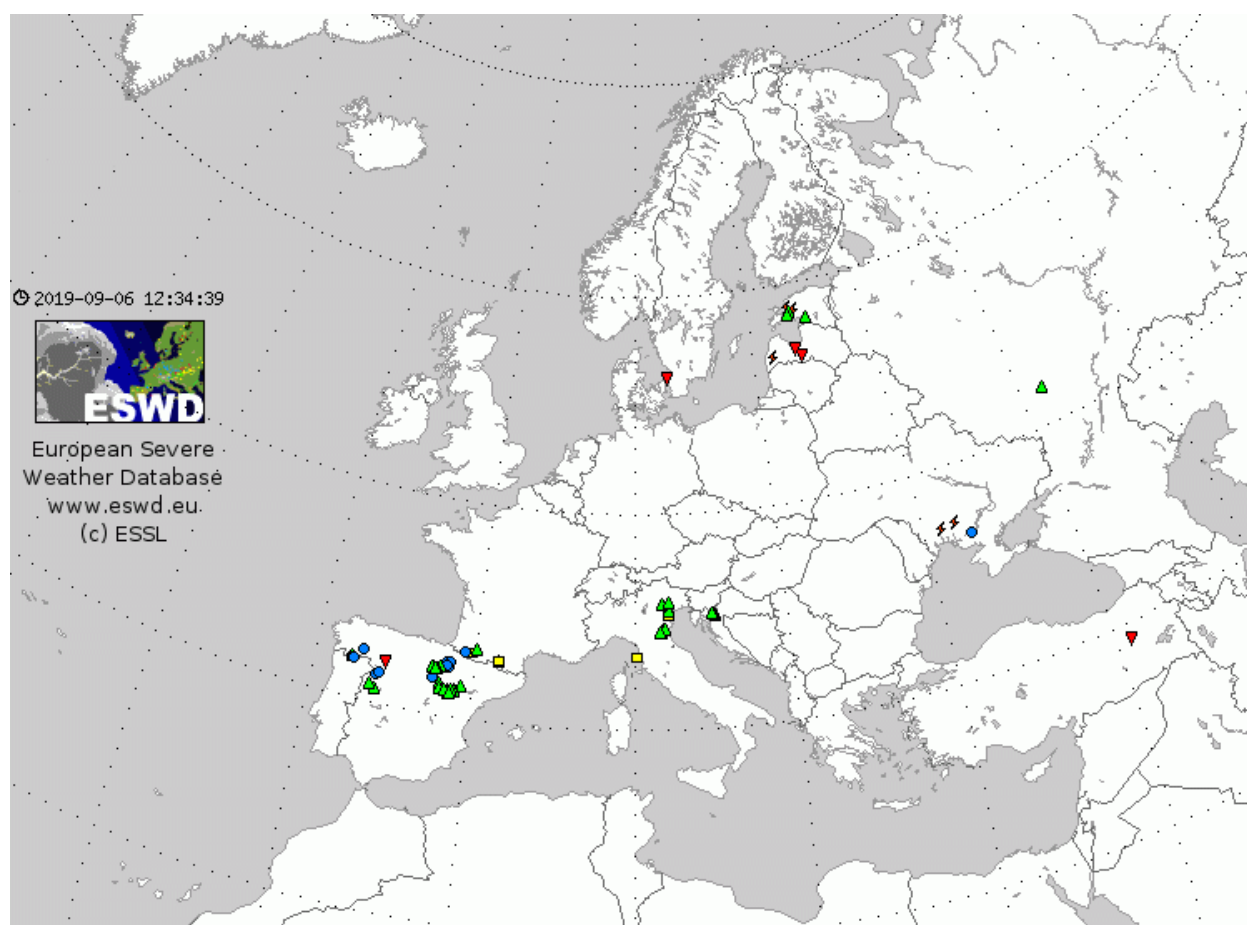


Fig. 4.63. Same as in Fig. 4.1. but for the period of 8 July 2019 00–24 UTC.

5.22 9 July 2019: Severe convective system over the Adriatic Sea further south than expected

Compared to the previous days, the highest severe weather threat shifted more to the south. The NWP models simulated a belt of high CAPE and strong vertical wind shear in a belt from the Balearic Sea through Corsica, Sardinia into Italy, the Adriatic Sea and western Balkans. Convective storms were simulated over northern Italy, the northern Adriatic Sea, Croatia, Bosnia and Montenegro.

A swath of severe wind gusts and large hail up to 8 cm in diameter occurred over north-Central Italy between 12 and 16 UTC. Severe wind gusts also occurred over southern Croatia and Albania in the evening. Models underestimated the storm activity over the Adriatic Sea. None of them simulated a significant storm that crossed from Central Italy to the coastline of Albania between 15 and 18 UTC. Models also failed to simulate a long-lived and large convective system crossing the Adriatic Sea from Italy towards southern Croatia, Montenegro and northern Albania between 16 and 23 UTC.

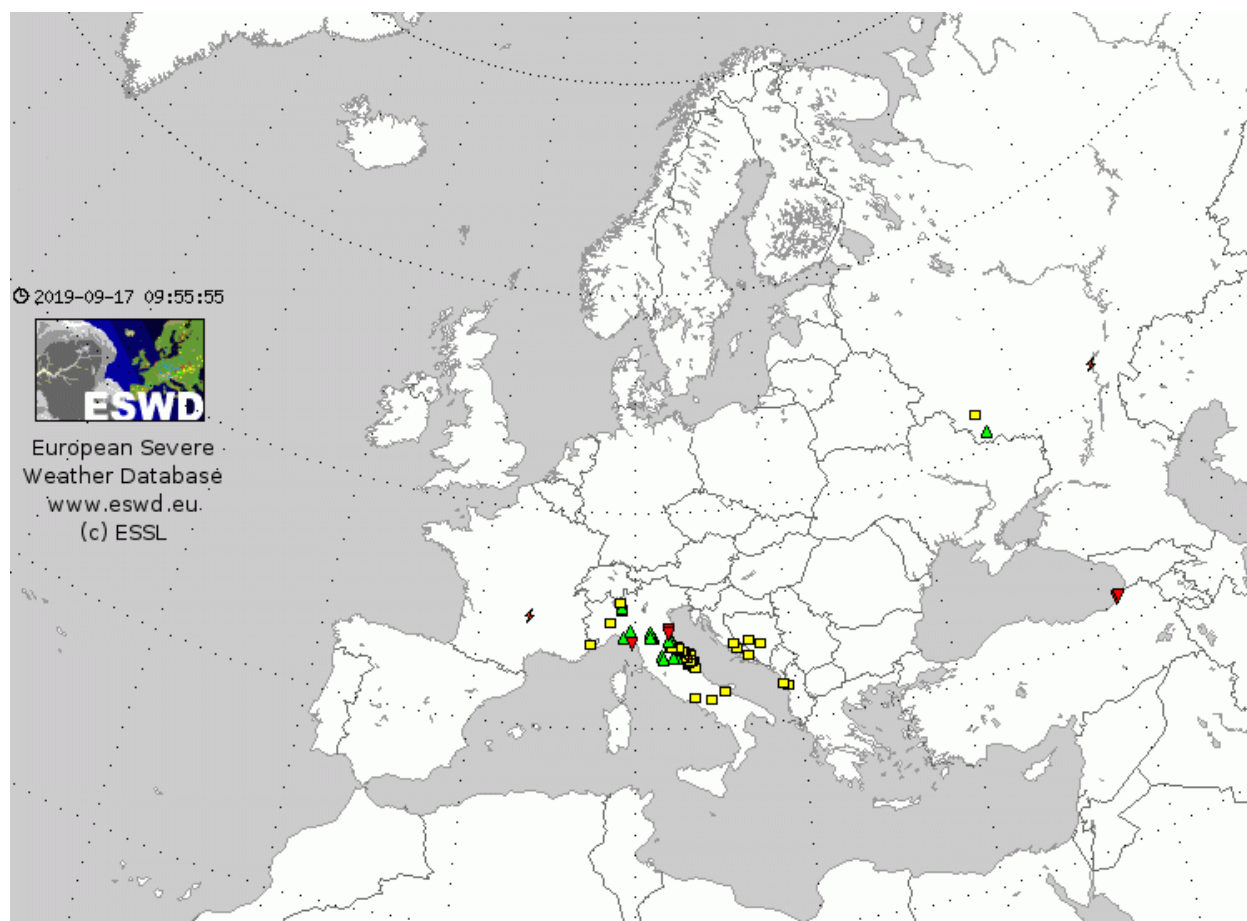


Fig. 4.64. Same as in Fig. 4.1. but for the period of 9 July 2019 00–24 UTC.

5.23 20 July 2019: Severe storms across the Benelux and Germany

A short-wave trough was moving from southern United Kingdom towards the Benelux and Denmark. At the same time, a cold front progressed across northern France, the Benelux and western Germany. Ahead of it, models simulated an overlap of CAPE between 500 and 1500 J/kg with strong vertical wind shear reaching around 20 m/s in the 0–6 km layer. Severe storms were forecast in a belt from the Benelux to Germany.

A swath of large hail and severe wind gusts was reported from the storms that formed over Belgium and the Netherlands and entered Germany. For the Benelux, models were inconsistent regarding CAPE. Some models only simulated up to 500 J/kg of CAPE, where hail up to 4 cm in diameter occurred, so it is possible that more CAPE was present in the environment.

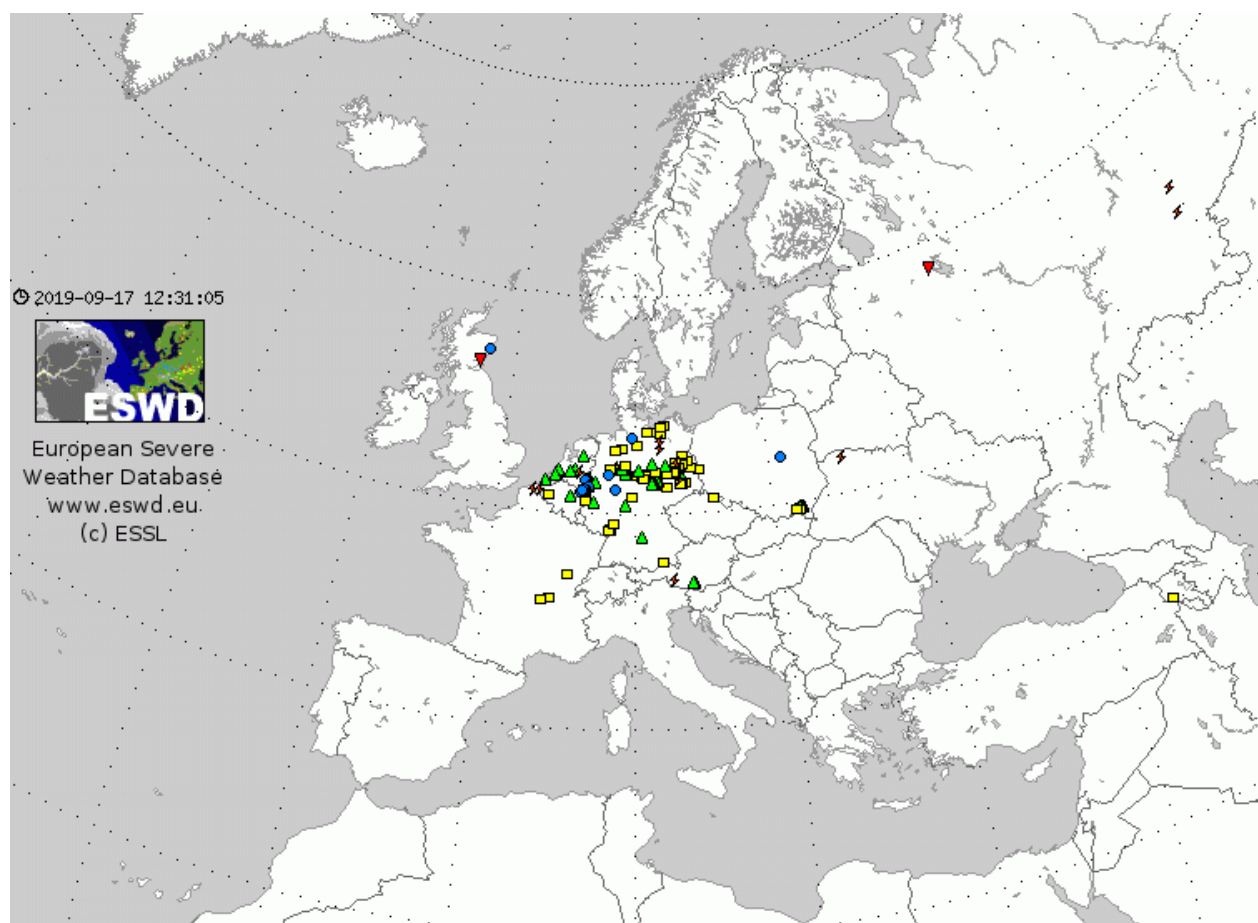


Fig. 4.65. Same as in Fig. 4.1. but for the period of 20 July 2019 00–24 UTC.

5.24 27 July 2019: Severe weather in Italy and central Europe; a night-time tornado near Rome

Synoptic-scale situation was characterised by a trough moving from the Bay of Biscay through France towards northern Italy and a cut-off low moving from Poland to northern Germany. Large part of Europe was under a threat of severe thunderstorms, but the highest threat was forecast for the late evening and overnight along the western coastline of northern to central Italy. Here, moist boundary layer over the sea yielded high CAPE, between 2000 and 3000 J/kg and a strong mid-tropospheric flow resulted in vertical wind shear exceeding 20 m/s in the 0–6 km layer.

Over Germany, Austria, Czech Republic and Poland, numerous thunderstorms resulted in reports of flash flooding. Towards the south, over south-eastern Austria and Hungary, storms caused flash flooding and large hail up to 7 cm in diameter. Further large hail and severe wind gusts were reported from northern Italy. Shortly after midnight, a strong tornado was reported near Leonardo da Vinci airport near Rome, claiming one fatality.

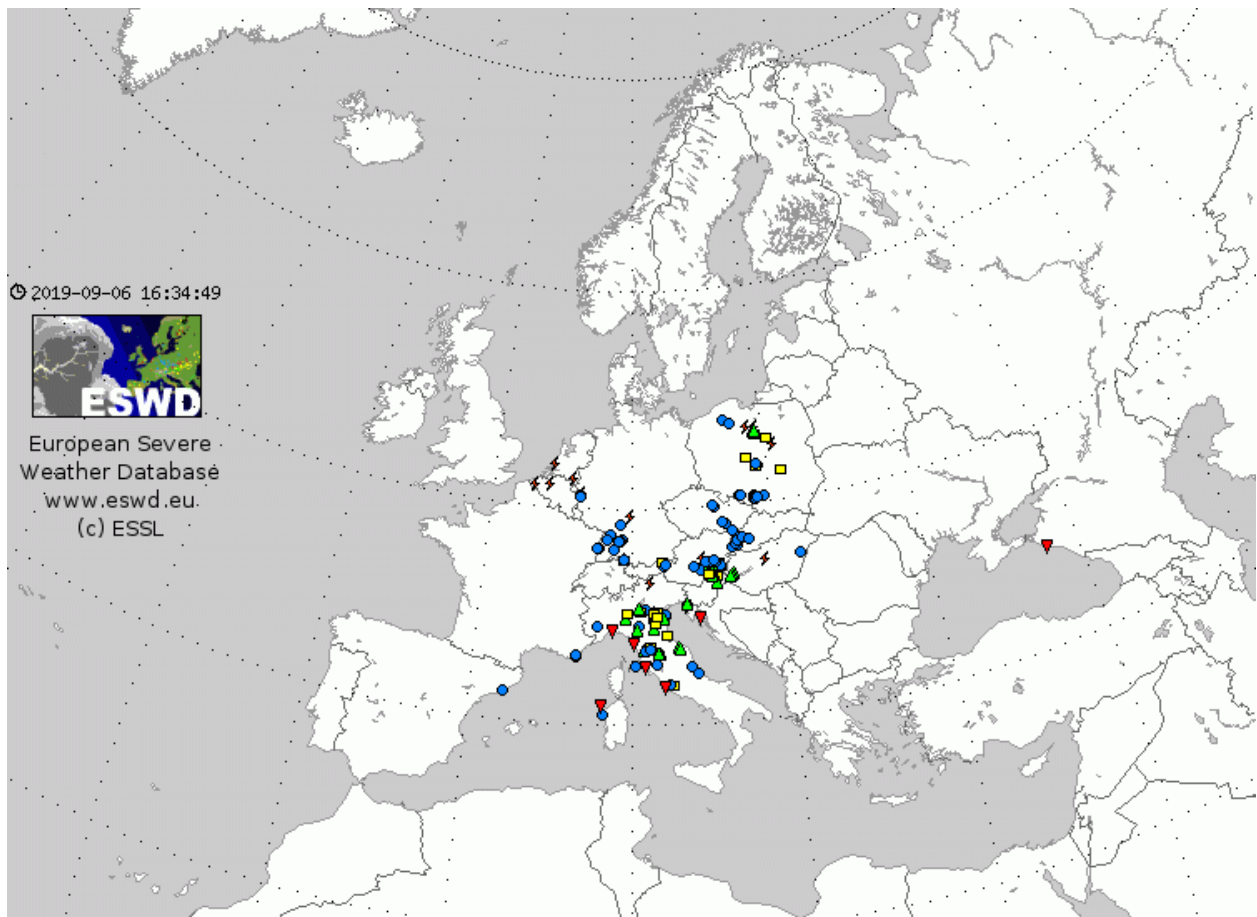


Fig. 4.66. Same as in Fig. 4.1. but for the period of 27 July 2019 00–28 July 06 UTC.

5.25 7 August 2019: Severe storms in Italy, central Europe; storms in Czechia weaker than forecast

In the mid- to upper-troposphere, a cyclonic vortex was centred over the Northern Sea, with a broad belt of 15 to 20 m/s westerly to south-westerly flow stretching from France across Poland to the Baltic states. A fast-moving short-wave trough quickly moved eastwards from France. In conjunction with a cold front, severe storms were forecast across northern Italy, eastern Czech Republic, western Slovakia and Poland. The modelled environment was characterised by moderately strong vertical wind shear (15 to 20 m/s in the 0–6 km layer) and CAPE around 1000 J/kg.

Severe storms formed over northern Italy, southern Poland and Slovakia with swaths of large hail, severe wind gusts, as well as locally heavy precipitation. Evening and overnight storms occurred further east than predicted by models, while storms over eastern Czech Republic remained quite weak. This was likely due to the presence of stable layer near the mid-troposphere that was not resolved well by numerical models.

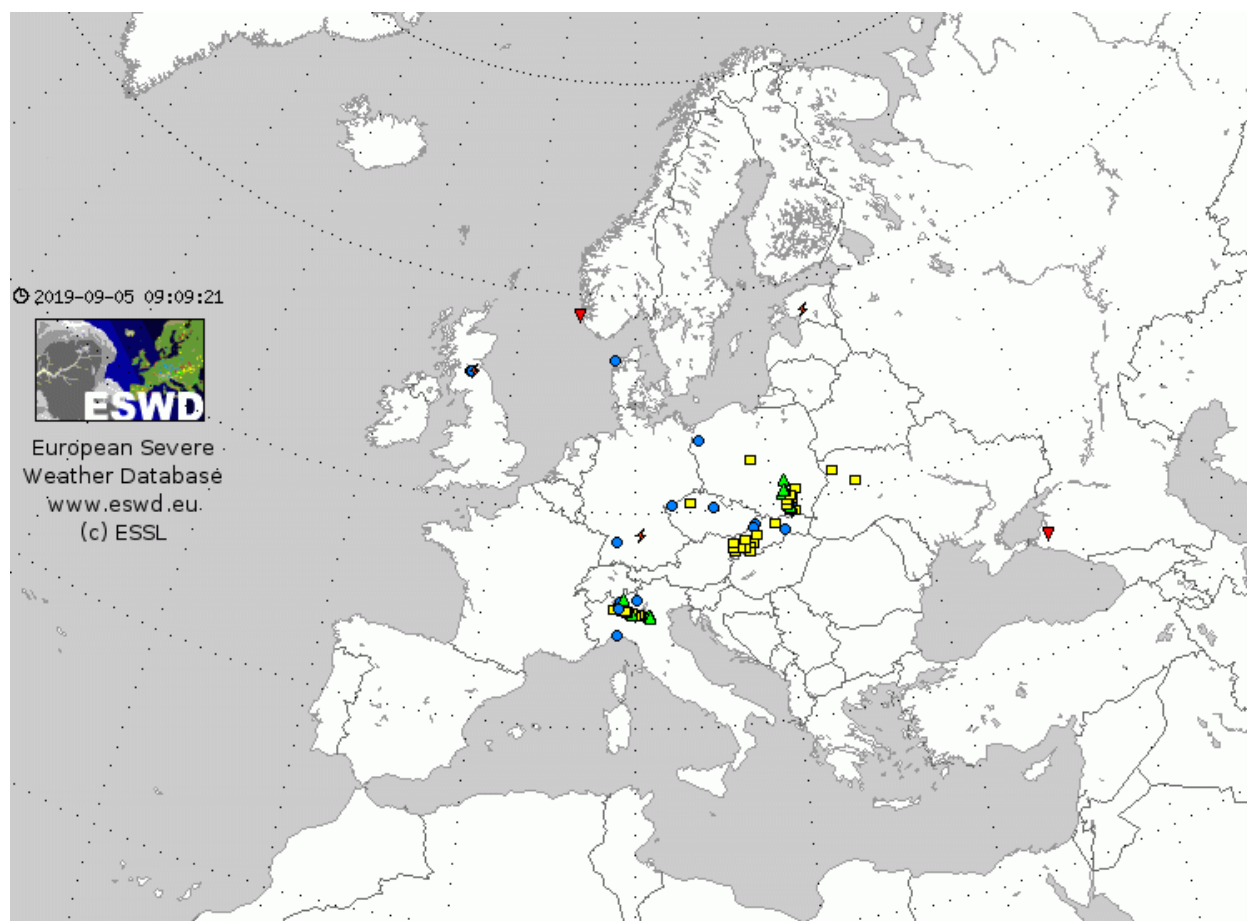


Fig. 4.67. Same as in Fig. 4.1. but for the period of 7 August 2019 00–24 UTC.

5.26 11 August 2019: Unexpected damaging hailstorm over Piemonte, Italy

A deep trough was located over the Atlantic with a strong south-westerly at the mid-troposphere flow simulated in a belt from Spain through France into Germany. A wavy frontal boundary stretched from Spain into southern France, Switzerland and Germany. Ahead of it, CAPE above 1500 J/kg was forecast to overlap with strong vertical wind shear over northern Italy. NWP models only simulated storms over the Alps, with no precipitation over the lowlands.

A swath of severe weather was observed over the Alps, but the most severe storm of the day occurred over the Piemonte region with a swath of large hail. Initiation over the lowlands was not forecast by any model.

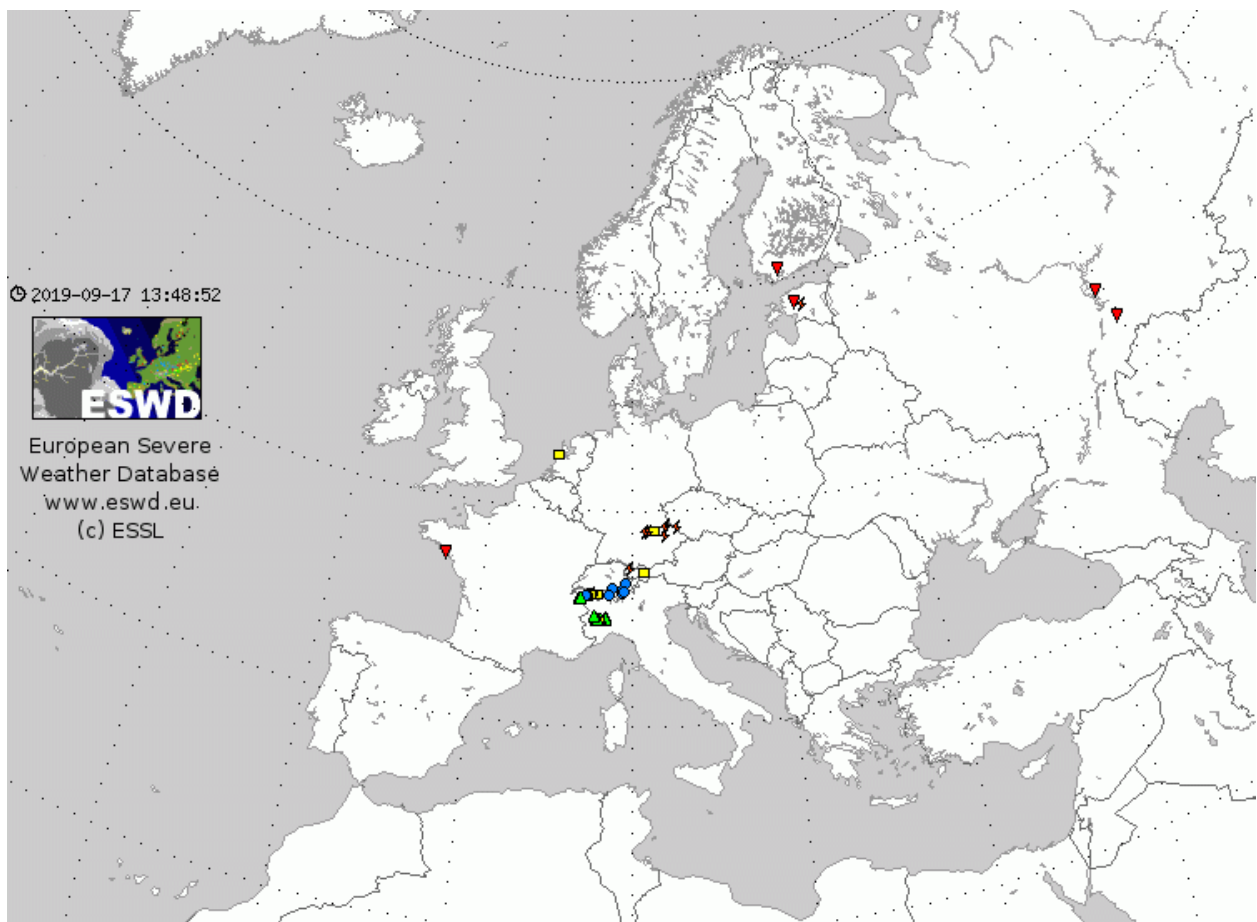


Fig. 4.68. Same as in Fig. 4.1. but for the period of 11 August 2019 00–24 UTC.

5.27 12 August 2019: Severe storms over Central Europe and Italy

A deep trough moved eastwards from the Atlantic with a strong south-westerly flow on its forward flank. Closer to the surface, a wavy frontal boundary was forecast to stretch from the Alps, through Austria and the eastern Czech Republic into southern Poland. Along and ahead of the boundary, NWP models predicted high CAPE between 1000 and 2500 J/kg, overlapping with strong vertical wind shear. Severe storms were forecast across parts of northern Italy and in a belt from eastern Czechia to southern Poland.

A long-lived supercell produced a swath of large hail and damaging wind gusts over northern Italy and numerous severe storms occurred in the evening over southern Poland. A severe storm also hit Vienna, Austria. Over northern Austria and eastern Czechia, storms were weaker than anticipated.

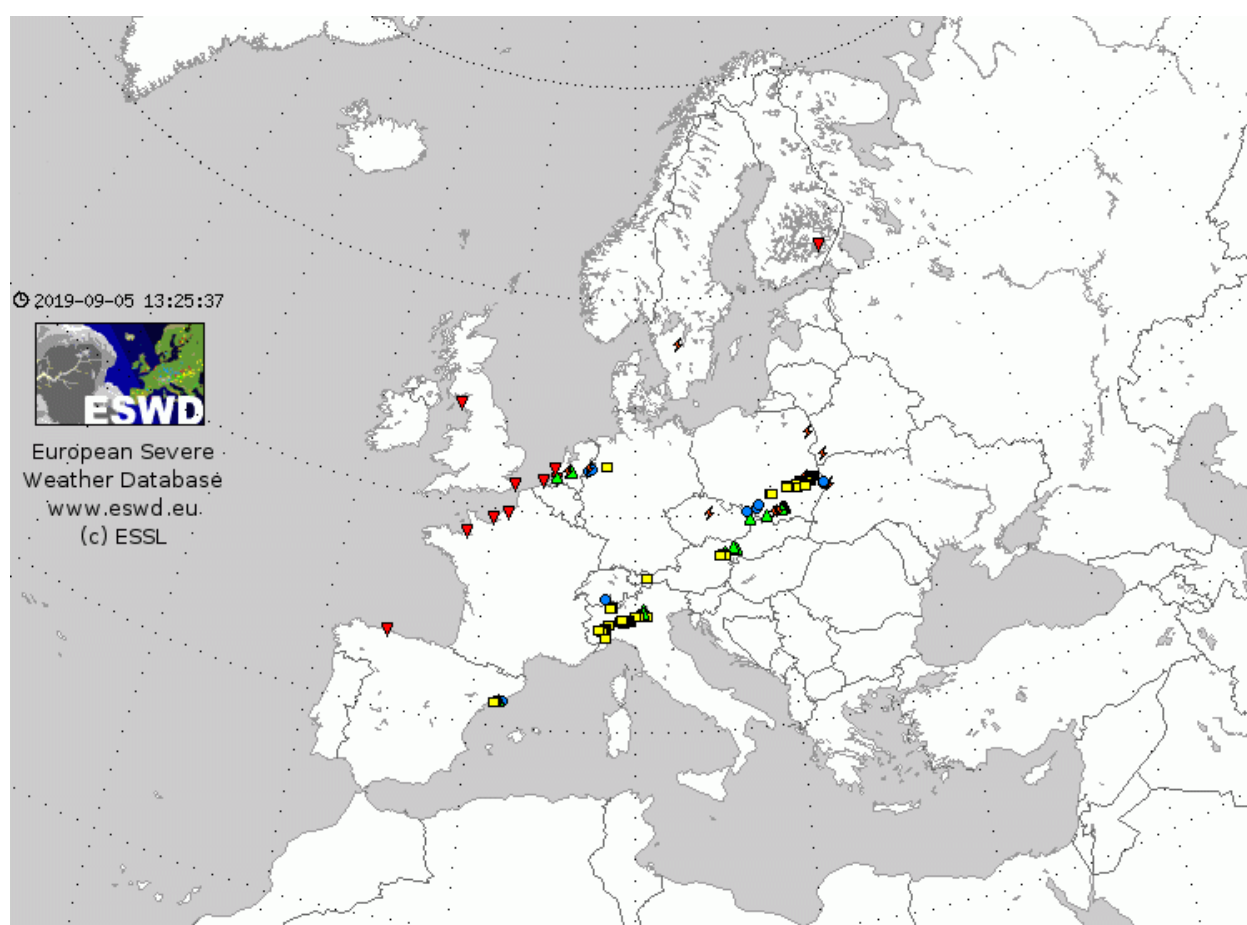


Fig. 4.69. Same as in Fig. 4.1. but for the period of 12 August 2019 00–24 UTC.

5.28 22 August 2019: Deadly lightning strikes in Poland and Slovakia with low CAPE

A quasi-stationary cold front was stretching across northern Alps, Austria into northern Slovakia and Ukraine during this day. In the mid to upper troposphere, a south-westerly flow was simulated ahead of the short-wave trough crossing from Germany to Poland. Along and south of the cold front, CAPE between 100 and 750 J/kg were forecast, increasing towards more abundant lower tropospheric moisture in the south.

Weak thunderstorms formed over central Slovakia during the morning and moved towards the Tatra mountains on the border between Slovakia and Poland. Hundreds of hikers were caught unprepared by the storm resulting in 5 fatalities and 159 injuries. The worst lightning strike was reported from Mt. Giewont in southern Poland with 4 fatalities and 156 injuries, as people were knocked down from the mountain or burnt as they held on the steel cable supporting them on the steep ascent to the mountain. Deadly lightning strikes occurred in a region, although little to no CAPE was simulated by NWP models.



Fig. 4.70. Same as in Fig. 4.1. but for the period of 22 August 2019 00–24 UTC.

5.29 26 August 2019: Severe weather over Spain, Czechia and Poland

During this day, there were two foci for possible severe storms: the first one over Spain, associated with a deep short-wave trough and the second one over parts of central Europe, under a subtle and shallow trough at mid-troposphere. Storms over Spain were forecast to form in an environment of around 1000 J/kg and 15 to 20 m/s of 0–6 km shear. Storms over central Europe were forecast to form in similar CAPE, but weaker vertical wind shear.

Both areas experienced severe weather. Over Spain, flash flooding and large hail, up to 5 cm was observed in Madrid area. Over central Europe, a swath of excessive rainfall and severe wind gust reports, as well as isolated large hail, was reported from western Slovakia, southern Poland and eastern Czech Republic. Many of the models did not correctly anticipate the initiation and severity of storms over this region.

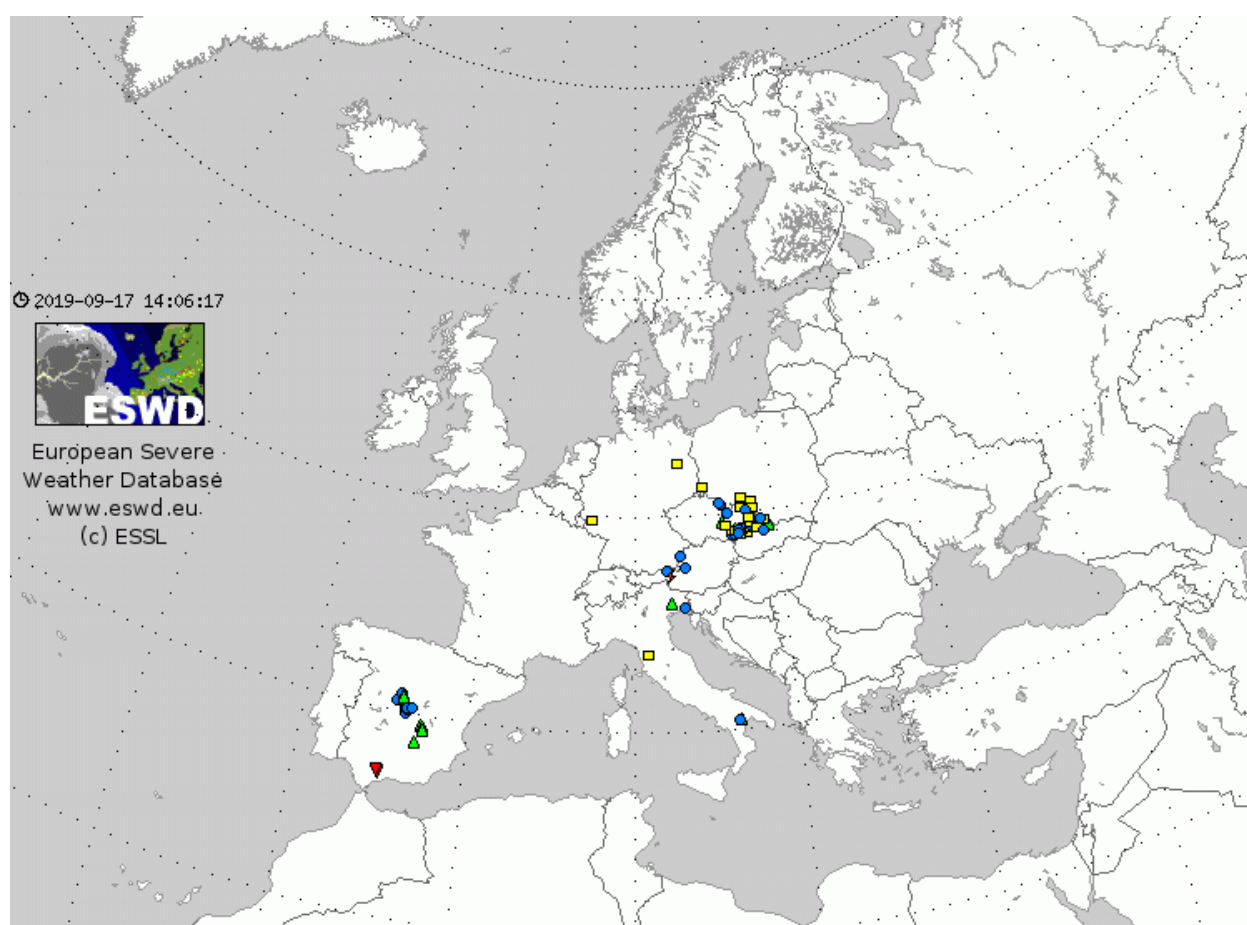


Fig. 4.71. Same as in Fig. 4.1. but for the period of 26 August 2019 00–24 UTC.

5.30 13 September 2019: Giant hail over Algeria

A strong southerly flow was simulated on the forward flank of a deep low centred over southern Spain at the mid-troposphere. With abundant lower tropospheric moisture along the coastline of Algeria, an environment of CAPE above 1000 J/kg and strong vertical wind shear was anticipated over the area. In contrast to the previous day, NWP models forecast only isolated initiation of storms.

An isolated storm erupted over Algeria around 15 UTC, that quickly became severe and produced giant hail reaching 10 cm in diameter over the Ain Delfa region. Roofs and vehicles were damaged, and birds were killed by the hail. While models showed around 1000 J/kg present over the location of the storm, giant hail suggests that perhaps higher CAPE were available to the storm.



Fig. 4.72. Same as in Fig. 4.1. but for the period of 13 September 2019 00–24 UTC.

6 Conclusions and recommendations

The study has revealed that the vast majority of forecasters (13 out of 15 respondent groups) is interested in using retrieved temperature and humidity profiles based on IASI-data for the purpose of short-term forecasting or nowcasting of (severe) thunderstorms.

The forecasters used IASI data visualized in interactively adapting thermodynamic diagrams (the 'roaming sounding') displayed alongside NWP predictions. In addition, key parameters relevant to thunderstorm forecasting such as CAPE and CIN were calculated. The same visualizations were used for the case studies by ESSL.

The case studies confirmed that the data in some cases provide additional information, such as when the forecast temperature in NWP models was incorrect and the sounder provided a better estimate. Such differences that IASI can detect are reflected in CAPE and CIN and have important implications for the probability of convective storm development and their intensity. An important characteristic of the IASI data is their independence from NWP models. Because of it, forecasters can consider the IASI data an observational data set that can be used to validate NWP predictions.

The feedback from forecasters and the case studies also identified a number of limitations of the data. Two limitations appear to be the most important. First, the limited temporal availability, i.e. twice a day a number of overpasses in quick sequence, means that it is not possible to follow the evolution of the profiles during the day. The MTG-IRS, with an availability every 30 minutes, will solve this problem.

The second main limitation is the lower accuracy of the humidity retrievals in the lower troposphere to which convective storms are very sensitive. This has large impacts on some of the derived parameters used for thunderstorm forecasting, like CAPE and CIN. Any mitigation of this inaccuracy will be valuable. Therefore, we recommend investigating whether any improvements of this quantity are possible using existing techniques. In addition, it may be possible to improve the estimates by complementing the IASI data with other measurements, such as traditional station measurements, as well as LIDAR data or aircraft observations (AMDAR). Through a synergy of these different observations, a purely observation-based three-dimensional estimate of humidity and temperature can be created, that will likely have a higher accuracy than IASI alone.

Regarding the visualization of the data, a number of further developments are suggested. In order to simplify the comparison between IASI data and NWP models, gridded difference fields of key parameters can be computed and visualized. Additionally, forecasters expressed their interest in obtaining error estimates of the measurements throughout the retrieved vertical profiles. Finally, a number of minor improvements to the current visualizations can be implemented, including the display of dew point temperature and the shading of CAPE areas in the thermodynamical diagrams.

References

Buck, A. L., 1996: *Buck Research CR-1A User's Manual*, Appendix 1.

Craven, J.P., Jewell, R.E. and Brooks, H.E., 2002. Comparison between observed convective cloud-base heights and lifting condensation level for two different lifted parcels. *Wea. Forecasting*, **17**, 885-890.

Doswell III, C.A. and Markowski, P.M., 2004. Is buoyancy a relative quantity? *Mon. Wea. Rev.*, **132**, 853-863.

Doswell III, C.A. and Rasmussen, E.N., 1994. The effect of neglecting the virtual temperature correction on CAPE calculations. *Wea. Forecasting*, **9**, 625-629.

Emanuel, K.A., 1995. *Atmospheric convection*. Oxford University Press.

Haklander, A. J., and Van Delden, A. 2003. Thunderstorm predictors and their forecast skill for the Netherlands. *Atmos. Res.*, **67**, 273-299.

Kunz, M., 2007. The skill of convective parameters and indices to predict isolated and severe thunderstorms. *Natural Hazards and Earth System Science*, **7**, 327-342.

Appendix A:

Usage instructions of Python programme for the computation of convective indices

ESSL provides a Python script to compute a number of parameters used by forecasters to forecast convective storms. This script's name is **sounder_eumetsat.py** and it can be run from the command prompt. The input and output directories for the test data need to be specified in the script. The script is written and tested with Python 3.7. It requires only a few standard libraries that are imported at the beginning of the script. The parameters the script produces are:

- PW: Precipitable water, the vertical integral of watervapour in a column, in mm
- LR850500: The lapse rate of temperature between the 850 and 500 mb level, in K/km
- LRSFC500: The lapse rate of temperature between the surface and the 500 mb level, in K/km

And the following parameters in four different versions:

- CAPE: Convective available potential energy, in J/kg
- CIN: Convective inhibition, in J/kg
- Lifted Index: The buoyancy of a rising parcel as it reaches the 500 mb level, in K or °C

These three indices are calculated for:

1. a surface parcel, i.e. a parcel lifted from the lowest detected level (prefix SB)
2. a mixed-layer or mean-layer parcel, a parcel with the mean properties of either the lowest 50 or the lowest 100 mb of air above surface (prefix ML, suffix either 50 or 100)
3. the most unstable parcel, a parcel lifted from that level that yields the highest CAPE (prefix MU)

For all these parcel calculations, a pseudo-adiabatic process was assumed, which means that the liquid and solid condensate is assumed to leave the parcel immediately. No mixing between the parcel and its environment is assumed. See Emanuel (1995) for details. Furthermore the so-called virtual temperature correction was applied (Doswell and Rasmussen, 1994) to account for the lowering effect of water vapor on the density of a air/water-vapor mixture.

To run the code, enter **python sounder_eumetsat.py *yyyymmddhh*** at the prompt, where *yyyymmddhh* are the date and time for which data should be processed (with a 60-minute margin earlier or later). It scans for all IASI hdf files in the directory `~/input`, where `~` is the present working directory and will write the output csv files to `~/output`.

Appendix B: Responses to IASI evaluation at the ESSL Testbed 2019

Question 1

Could atmospheric soundings such as those provided from Metop/IASI (available within 30 minutes from sensing) be useful for your forecasting work? In what way?

Responses to Question 1:

1. *Yes. If in a larger area, there is a pronounced difference compared to NWP, which we can verify with sfc observations, it can help to interpret/correct the NWP output in terms of CAPE etc.*
2. *Yes, especially in the nowcasting. When the model has precipitation which is not happening in reality and the model soundings don't reflect the environment whereas the IASI sounding does. Provides information to have a chance to evaluate the model.*
3. *it can be useful, but also sometimes confusing. It forces you to check both with the real surface observations so in that way you also verify the accuracy of the model*
4. *Yes. Comparing the model with the satellite one is able to find the discrepancies in the model. Especially in situation when overnight convection is present that was not covered by the model. Then you get an idea how the environment was changed by that convection.*
5. *Yes, when it's available 24/7, especially around noon when the convection starts. So that we get every three hours a new sounding. But we have to rely on this sounding data, to be more precise than the model, especially inversions must be visible.*
6. *yes. The delay of the sounding isn't an issue. 1] better spacial and temporal (time) coverage 2] observation data vs. model data 3] it's not so good to use IASI like the only source of data*
7. *yes. Comparing the model output and find out which model pics up the situation best (not for nowcasting but more for current day)*
8. *Yes it can be, but then it needs to be more accurate in the lower troposphere. In the case of Slovenia 20190611 10Z, the IASI is underestimating the low level moisture (850 - 1000 mb) a lot. Therefore the CAPE calculation of the IASI is completely off. A second remark on this case is that the error bars provided to the IASI are smaller than the actual error on the ground level.*
9. *It could be, mainly nowcasting, compare the actual state or past 3 hours (for example) with the model and see how well it is doing.*
10. *It will be very usefull in situations when we are expecting , for example, thunderstorms few hours after the passage of satellite, so it is possible to verify / compare model and the reality.*

11. *Metop/IASI data seem to be not so useful. For example, we tried to assimilate IASI observations in the Data Assimilation system developed in Italian Met Service based on LETKF algorithm, but these observations had 0 impact on the analysis, and consequently on the forecast. Maybe the problem is related to the fact that these profiles are not accurated in the lowest atmospheric levels.*
12. *in Theory yes, practice would decide. needs a robust verification of the quality of the soundings , in respect to observation soundings, not to the model soundings....*
13. *It is another valuable information with advantages and disadvantages. Under the limited time we had to evaluate we have not reached a concrete conclusion.*
14. *Yes, in general way it could be useful. Especially to get a sense about the trustworthiness of the model. It could also be helpful to see if the frontal movement/advection by the model is correct.*
15. *Yes, it could be very useful especially in places with difference between model data and sounding.*

Question 2

Which of the provided parameters based on the sounder data do you find most useful? Please mention the 3 to 5 most useful ones.

Responses to Question 2:

1. *Sfc mixing ratio (or dewpoint), ML/MUCAPE (especially also for elevated situations!). We would also like the 2m temperature (in a 2D map instead of having to check the soundings), because the surface parameters are the only parameters we can actually check with sfc observations. For example ML mixing ratios are of less interest, because you lose information by mixing (then we'd rather look at the profile itself).*
2. *lapse rates, moisture, CAPE*
3. *lapse rates, MLCAPE50, MUCAPE*
4. *ML50 mixr, 850-500 mb lapse rates*
5. *Total Precipitable Water, MLCAPE, CIN*
6. *CAPE and CIN, moisture profile and temperature profile*
7. *850-500 mb lapse rate (as temperature profiles are impressively precise); Total precip water (an integral variable); CAPE we think quite problematic because it is very sensitive to surface influence which has the biggest error in the measurement.*
8. *Temperature, lapse-rates, profile in the middle and upper levels.*
9. *CAPE and CIN parameters, Precipitable water, Mixing Ratio...*
10. *SFC - 500 mb lapse rate Total precipitable water CAPE parameters*
11. *850-500 mb lapse rate, Total precipitable water, CAPE*

12. TPW, CAPE, lapse rate, mixing ratio 50 mb
13. temperature, dew points, MLCAPE
14. At the moment we would prefer the parameters which are not so much influenced by moisture measurements in near-surface layers, like: Total precipitable water, ML CAPE, MU CAPE, ML CIN, 850/500 mb lapse rates
15. Cape, Hodograph, Dew Point Temperature

Question 3

We would like to know how interesting you think the current products are for operational forecasting, considering the limited spatial and temporal resolution in comparison to the planned Meteosat Third Generation - Infrared Sounder (MTG-IRS), that will deliver data every 30 minutes with contiguous pixels sampled at about 7 km over Europe. Please select the statement that best describes what you think:

- A. I think the IASI products with their limited temporal availability (twice a day) already provide important additional information that makes the data interesting to use.*
- B. I think the IASI products could be useful for forecasting, but first it is necessary that more observations become available throughout the day.*
- C. I think the IASI products as they are now have limited value for forecasting, but are interesting to prepare for the MTG-IRS data, that will have better resolution.*

Responses to Question 3, motivation:

- 1. B. Higher observation frequency would definitely be better. The current moment of availability is ok for forecasting for longer lead times, but for shorter-term forecasting and for nowcasting, more updates would be highly appreciated.*
- 2. B. Because the soundings come too early before the convection starts.*
- 3. B.*
- 4. B. It really can help to get an idea of the current situation but it would be nice to have it more often especially during the time when CI is most pronounced (during noon/early afternoon). So it may help to have available more frequent measurements.*
- 5. B. See Question 1*
- 6. A. same as 1. it seems to be good to verify model data in case of extreme CAPE values (Croatia 10th June).*
- 7. B. The limited number of obs now provides a sample of comparison, we would more like a continuous evaluation of difference between model output and obs in the continuous data flow to the forecaster, as fcsters are continuously adjusting their conceptual weather image.*
- 8. C.*

9. B. *The changes between the profiles at different times would be interesting. You can then look at the temporal development of the profiles.*

10. C. *They are often missing when you need them the most :)*

11. B. *To have information in every 30 min. it is very useful, especially for nowcasting purposes. It is like near-realtime information which could be important in convective situations.*

12. B. *used as a nowcasttool, therefore 30-60min time resolution necessary*

13. A. *it is additional information that it is useful in areas that models do not adequately represent the actual atmosphere (example: eastern Mediterranean has very few radiosondes to assimilate into operational runs)*

14. B. *Some information could already be valuable at the moment, but better spatial and temporary resolution would be huge help. Especially to have more data available through the different times of the day.*

15. B. *Because we found that there is big difference between real data and data from model or satellite in mountains stations.*

Question 4

In principle, NWP (forecast model) data could be used to improve the limited vertical resolution of hyperspectral sounder products, but this would introduce a dependence on them. In their present form the data are available in the form of smoother/less resolved profiles (than e.g. sondes) and as integrated-/lapse-/instability quantities, but they are fully independent of any NWP model. How important is it to your work that the products are independent of any NWP model?

Responses to Question 4:

1. *It is quite important, otherwise you don't know what the impact of either the model and the sounder is. On the other hand, it could definitely be useful to use the sfc observation data to improve the profiles; perhaps it would be interesting to have both options available.*
2. *It is very important to have the profiles independent of any NWP model, because it would be very hard to figure out what comes from the model and what from the satellite measurements.*
3. *It is important that we have information that is purely observed. In this way all observed data will improve the model accuracy.*
4. *We would prefer to have the SAT data independent to not getting biased by a wrong model information.*
5. *The independence of this two datasets is important when the model deviates from the actual weather situation/observations very much. Then you have another dataset which could explain the actual development.*

6. *at least for now is better to keep it independent.*
7. *Both products have a valuable information. If the model forecast is good then a merging of model data and profiler makes sense, BUT you need independent profiler data to find out model errors. What we think might be a promising approach is to add surface observations to adjust near surface measurements.*
8. *It is very dangerous to put in the model data. If a model forecast fails, the "observations" are also biased a lot by the model data. It is probably better to keep it independent. A forecaster is then able to compare different data sets to estimate the real state of the atmosphere best.*
9. *We think that it should be independent, so that observations are closer to reality and then we could compare them with model data. But of course it is a good thing that the IASI data are assimilated into the model to improve the performance of the model.*
10. *Model information should be kept independent from the soundings even if there is some errors in these soundings. So with time when these errors are reduced it will be better if the parameters stays independent and there is no model input in them.*
11. *We think that it is important to have a product without dependence from the model, because with the use of a model, we need to take into account not only the observational errors, but also the model ones.*
12. *if it is the aim to compare with model data, it should be independent. accuracy of the sounding should be tested against observation soundings*
13. *Our team believes that all information will be valuable: the information from the satellites is complementary to observations and another product using satellite and model output could improve in some cases the forecast.*
14. *Independence of any NWP model would be really important to have a better comparison against the models. If such considerations are made, a separated or additional product would be better served. Instead of model output maybe limited vertical resolution could be enhanced by using observation data from surface or ground based data.*
15. *It will be good to be independent of any NWP models if possible.*

Question 5

The vertical profiles are currently provided with a single error estimate, displayed with an error bar at the bottom of the profile. In principle, it is possible to display errors for any given level. How useful do you think this would be for your work? In practice, how would you use this quality-control information?

Responses to Question 5:

1. *Not very useful, we think that we already can picture the uncertainty in our head for inversions for example. The error bars at the surface are nice to have, although sometimes they seem to underestimate the actual error.*

2. *It would be useful to have more information about the quality but not for each level, more for different layers (for ~5-6 layers). It would give information how much and which extent the profile can be trusted.*
3. *Maybe you can provide both, but the display of information should not be overloaded. Perhaps a possibility of clickable selection is helpful.*
4. *It would be a help to have the uncertainties available for the whole profile. But in such a case it would be better to have them as shaded area and not as bars (like the visualization of the vertical profiles on the ECMWF website).*
5. *Error bars are useful. The best solution are three lines. One for the 'real' solution and one with error to the right and one to the left. This area could be shaded. We don't want "boxplots".*
6. *no error bars, just some (semi) shade/transparent range area along the profiles*
7. *Knowing the error and thus the reliability of the measurements is very important. Maybe there are better ways to show the errors than errorbars in order to keep the profiles clear (for example variation of line thickness proportional to the error). Also it would be nice to have the uncertainty information in the surface map to figure out the reliable areas.*
8. *It is useful to have the error estimate over the complete profile. A shady colour around the best estimate can give a nice indication of the error at different levels. Now it is not really clear from what level the single error estimate comes from. (copied from 1:) A second remark on this case is that the error bars provided to the IASI are smaller than the actual error on the ground level. However this looks strange. It looks already better if the error bar is then larger near the surface.*
9. *It would be good, maybe some shadowed area, or dashed lines...*
10. *In operational work it wouldn't be very useful, so it easy to read the information like it is now. But it could be nice to make like a "click" option to decide if need to display errors in any levels.*
11. *I think that it is very important, in particular in the lowest levels, because a small error can do the difference between having or not a storm.*
12. *KISS "Keep it simple stupid" ;-) Problem overkill of information as a first guess, one error level at the bottom*
13. *Proposal: shaded area around the line*
14. *Maybe error areas/paths could be used to gain better information about uncertainties in different height levels.*
15. *It will be good to have error bar for temperature and dew point at some high levels (1000m, 1500m, 2000m, 2500m) for weather forecast for mountains (example High Tatras).*

Question 6

Do you have any additional comments or suggestions regarding the data? Did something in particular catch your attention?

Responses to Question 6:

1. *In the case we studied (6th of July 2019, in France/Italy/Switzerland region), at a lot of places the NWP seemed to underestimate the surface dewpoint, which was more accurate in the sounder. (but locally, it was the other way around)*
2. *It would be nice to have the data in 3D visualization.*
3. *There are some places the data fit very well (6.7.2019. - Gulf of Lion), and at some places there was big differences due to surface values of T and Td and boundary layer profile.*
4. *It would be good to have surface dewpoints available as map to easily compare them to the surface measurements. Some work of overcoming deficiencies in CAPE from IASI due to lower vertical resolution would be very much appreciated.*
5. *Personally the data on the sea fits better to the model data. Especially on the highlands e.g. in Turkey there are differences in lapse rates which uses the surface observation. But we don't know the truth.*
6. *The temperature profiles are impressively good, so maybe it is a good idea to concentrate on products that make use of this (like lapse rate ...) The use of all sort of observations (ie aircraft, sfc based profilers, masts) will be usefull in calibration/verification*
7. *for moisture in low levels its not working so good. This also affects the CAPE values significantly. In our case 10th June 2019 over Munich it wasn't very useful because the profile lacked of CAPE. It would have been useful to have 15 Z profiles.*
8. *Interesting product. However for the best use, it needs improvement in scanning the low levels (especially the dew point). To make it better in the lower levels, would it be possible to merge surface observations in the product? This would be even more useful than merging model data in the product.*
9. *we noticed surface temperature differences - IASI data almost always higher above ground and lower above sea compared to the model. The IASI data maybe caught fog at costal area of netherland at around 20190626 09:15 UTC when the model showed nothing (dry layer near the surface).*
10. *There are bigger differencies in the moisture profile than in the temperature between the model and sounding profiles. Noticed that there is not that big differences in lapse rate parameters but at the same time there is reasonable differences in CAPE parameters which seems strange*
11. *An issue could be the time difference between the validity time of the model and the satellite time in a point. So it would be useful to know at what time the satellite is over a point.*
12. *good approach !*
13. *When ECMWF CAPE is in agreement with the satellite information the Temperature and TD of both sources are accurate.*

14. *Weather situation from Wednesday 05 June 21 UTC over Western Germany: Big differences in regard to dewpoints (around 5 K) between model and sounding. Model and observations matched much better. Bigger differences occurred in drier conditions.*
15. *It will be great if it is possible to add the name of station (localisation of observation data). If will be possible it will be great to highlight CAPE area.*